International Tables for Crystallography (2006). Vol. D, Chapter 3.1, pp. 338–376.

3.1. Structural phase transitions

By J.-C. Tolédano, V. Janovec, V. Kopský, J. F. Scott and P. Boček

This chapter contains six contributions describing aspects of phase transitions in crystals that are of interest to crystallographers. The first contribution (Section 3.1.1) is a brief introduction aimed at defining the field of *structural transitions*. This restricted field constitutes, at present, the background of the clearest set of experimental and theoretical considerations. In this section, the terminology is specified. The second section (Section 3.1.2) describes the ideas and methods of the *theory of structural phase transitions*. This theory relates the symmetry characteristics of the transitions to their physical characteristics. The application of the symmetry principles that derive from this theory is illustrated by the results contained in Tables 3.1.3.1 and 3.1.4.1. The first of these two tables concerns the simple but experimentally widespread situation in which a structural transition is not accompanied by a change in the number of atoms per *primitive* crystal cell. The second table concerns the general case, in which the number of atoms changes, and which corresponds to the onset of superlattice reflections at the phase transition. This table provides, for a set of hypothetical transformations, the various symmetry-based predictions of the theory. Section 3.1.5 is devoted to the important topic of *soft modes*, which is related to the microscopic mechanism of a structural transition. Finally, Section 3.1.6 is an introduction to the accompanying software package *Group Informatics*.

3.1.1. Introduction

By J.-C. Tolédano

Phase transformations (the term *transitions* can be considered as a synonym) are experimentally recognized to exist in a large variety of systems submitted to a change in temperature or pressure: fluids, solids or mesophases, crystalline or disordered solids, metals or insulators.

This recognition is sometimes based on very obvious effects. This is, for instance, the case for the boiling or the freezing of a liquid, because the different *phases*, vapour, liquid, solid, differ greatly in their physical properties (*e.g* the difference of density between the two fluids, or the difference of mechanical hardness between the liquid and the solid). In these cases, a phase transformation appears as an abrupt and major change of the physical properties.

In other systems, solids in particular, the existence of a phase transformation is generally revealed by more subtle effects only. The nature of these effects differs from one system to another: minor discontinuities in the lattice parameters of a crystalline phase; occurence over a narrow temperature range of anomalies in certain specific physical properties; onset of a definite pattern of crystal twins *etc.*

Systems undergoing phase transitions constitute an important field of interest for crystallographers. This is due to the fact that, at the microscopic level, a phase transformation is generally accompanied by a change of the global or local atomic configuration. The structural data, *i.e.* the specification of the differences in atomic configurations between the two phases, or the study of the local ordering precursor to a transition, are thus essential, or at least important, clues to the understanding of the mechanism of the transition considered.

Conversely, the investigation of phase transitions has stimulated new developments in the techniques and concepts used by crystallographers. For instance, it has been necessary to improve the precision of goniometric measurements and the control of temperature in order to detect accurately anomalies affecting the lattice parameters across a phase transition or to study the asymmetry of diffraction spots caused by the domain structure in a 'low-symmetry' phase. On the other hand, new methods of structural determination, relying on concepts of *n*-dimensional crystallography, had to be developed in order to study transitions to incommensurate phases.

Standard crystallographic considerations, based on the determination of the characteristics of a lattice and of a basis, appear to be most useful in the study of phase transformations between crystalline phases, due to the fact that, at a microscopic level, each phase is entirely described by its periodic crystal structure. There are a wide variety of such transformations and the task of classifying them has been attempted from several standpoints.

The most important distinction is that made between *reconstructive* and *non-reconstructive* transitions. This distinction stems from a comparison of the crystal structures of the two phases. In a *reconstructive transition*, the distances between certain atoms change by amounts similar to the dimension of the unit cell, and certain chemical bonds between neighbouring atoms are then necessarily broken (see Tolédano & Dmitriev, 1996, and references therein). The graphite–diamond transformation and many transformations in metals and alloys are examples of reconstructive transitions. If, instead, a transition preserves approximately the configuration of the chemical bonds between constituents, the transition is *non-reconstructive.*

Other classifications, which partly overlap with the preceding one, involve distinctions between *diffusionless* and *diffusion-assisted* transitions (*i.e* those that require random hopping of atoms to achieve the change of atomic configuration) or between *displacive* and *order–disorder* transitions. Likewise, a number of transformations in metals or alloys are assigned to the class of *martensitic* transformations that is defined by a set of specific experimental observations (twinning behaviour, mechanical properties *etc.*). Finally, the distinction between *ferroic* and *non-ferroic* transitions has been progressively adopted in the recent years.

Owing to an insufficient understanding of the observations, the relationships between these various classifications is not fully clear at present. It is not even clear whether the same definitions and concepts can be applied to the description of all phase transformations between solid phases. For instance, one observes in certain solids (*e.g.* mixed lead magnesium niobates with an average perovskite structure) very broad anomalies of the physical properties (*i.e.* extending over a wide range of temperatures). These systems, which have stimulated many studies in recent years, are known to be chemically and structurally heterogeneous *simultaneously at several length scales*. The relevance to these systems of standard concepts defined for phase transitions in homogeneous systems, in which the anomalies of the physical properties are sharp, is uncertain.

It is therefore reasonable to restrict a review of basic concepts and theories to the simple reference case of *structural phase transitions*. We consider this terminology, in its *restricted* meaning, as pertaining to the situation of only a fraction of the phase transitions that take place in solids and imply a modification of the crystal structure. These are part of *non-reconstructive* transitions between homogeneous crystalline phases. It is customary to specify that a structural transition only *slightly*

alters the chemical bond lengths (by less than *e.g.* 0.1 Å) and their relative orientations (by less than *e.g.* a few degrees).

Experimentally, such transitions are characterized by small values of the heat of transformation (less than a few calories per gram), weak discontinuities in the relevant physical quantities (*e.g.* lattice parameters) and *the occurrence of a symmetry relationship between the two phases surrounding the transition*.

In the simplest case, this relationship consists of the fact that the space group of one of the phases is a *subgroup* of the space group of the other phase, and that there is specific correspondence between the symmetry elements of the two phases. For example, for the phase transition occurring at 322 K in triglycine sulfate (Lines & Glass, 1977), the same binary axis can be found in the two phases. Likewise, the vector defining one of the primitive translations in one phase can be a multiple of the vector defining a primitive translation in the other phase.

In a more general way, the crystal structures of the two phases considered are both slight distortions of a *reference* structure, termed the *prototype* (or *parent*) structure. In this case, the space groups of the two phases are both subgroups of the space group of the prototype structure, with, as in the simple case above, a specific correspondence between the symmetry elements of the two phases and of the prototype structure. A well documented example of this situation is provided by two of the three transitions occurring in barium titanate (Lines & Glass, 1977).

A subclassification of *structural* transitions into *ferroic classes* is of interest (Aizu, 1969; Tolédano & Tolédano, 1987, and references therein). Indeed the distinction of ferroic classes allows one to establish a relationship between the point symmetries of the two phases surrounding a phase transition, the observed twinning, and the nature of the physical properties mainly affected by the phase transition.

The group–subgroup relationship that exists, in the standard situation, between the *space groups* of the two phases adjacent to a structural transition implies that the *point group* of one phase is either a *subgroup* of the point group of the other phase or is *identical* to it.

If the two point groups are *identical*, the corresponding transition is classified as *non-ferroic*.

In the general case, the point group of one phase (the *ferroic phase*) is a strict subgroup of the point group of the other phase (the *prototype phase*). The transition is then classified as *ferroic*. Originally, a somewhat more abstract definition was given (Aizu, 1969): a crystal was said to be ferroic if it can exist in two or more *orientation states* having equal stabilities in the absence of external forces, and when the various orientation states have crystal structures that only differ in their global spatial orientations. The latter definition, which focuses on the situation of the *ferroic phase*, derives from the former one: the *lowering of point symmetry* that accompanies the transition between the prototype phase and the ferroic phase results in the existence of various *variants* or twin orientations having the same structures within a global reorientation (see also Sections 3.2.1, 3.2.3, 3.3.7, 3.3.10 and 3.4.1).

The various orientation states can coexist in a given sample and then determine a *twinning pattern*. Geometrical and physical considerations pertaining to twinned structures are developed in Chapters 3.2 and 3.3 of this volume. In particular, it can be shown that the structure of one orientation state can be brought to coincide with the structure of another orientation state by means of a set of geometrical transformations R which all belong to the space group of the *prototype phase*.

If we adopt a common frame of reference for all the orientation states of the ferroic phase, the tensors representing certain macroscopic quantities (see Chapter 1.1) will have different values in the different states (*e.g.* distinct nonzero components). If a certain macroscopic tensor has components differing in two states, a and b, these components are thus modified by the action of the geometrical transformations R which transforms (reorients) one structure into the other. Hence they are *not invariant* by geometrical operations belonging to the group of symmetry of the *prototype phase*: their value is necessarily zero in this phase.

Ferroic transitions therefore possess three characteristics:

(i) They are associated with a lowering of crystallographic point symmetry.

(ii) Components of certain macroscopic tensors aquire nonzero values below T_c.

(iii) The same tensors allow one to distinguish, at a macroscopic level, the various orientation states arising in the ferroic phase.

The subclassification of ferroics into *ferroic classes* has a crystallographic and a physical content. The crystallographic aspect is based on the type of point-symmetry lowering occurring at the transition, while the physical aspect focuses on the *rank of the tensor* (necessarily traceless) characterizing the different orientation states of the crystal in the ferroic phase and on the nature of the physical quantity (electrical, mechanical, ...) related to the relevant tensor (see Chapter 1.1). Table 3.1.1.1 specifies this twofold classification.

Note that a given transition related to a class defined by a tensor of rank n can belong to several classes defined by tensors of higher rank: *e.g.* a ferroelectric transition can also be ferroelastic and will also display characteristics of a higher-order ferroic.

The point-symmetry changes defining each class have been enumerated in various works (see for instance Aizu, 1973, and references therein).

The interest of the above classification is that it provides a guiding framework for the experimental investigations. Hence, the recognition that a transition is ferroelectric (respectively, ferroelastic) directs the investigation of the transition towards the examination of the dielectric (respectively, mechanical) properties of the system in the expectation that these will be the quantities mainly affected by the transition. This expectation is

Table 3.1.1.1. *Ferroic classification of structural parameters*

	Class		
	Ferroelectric	Ferroelastic	Higher-order ferroic
Symmetry change	(1) Non-polar to polar crystal point group (reference situation) or (2) polar to polar group with additional polar axes	Change of crystal system (syngony) (except from hexagonal to rhombohedral)	Change of point group not complying with the two preceding classes
Examples	(1) $2/m \Rightarrow 2$ (2) $mm2 \Rightarrow m$	$mmm \Rightarrow 2/m$ (orthorhombic $\Rightarrow$ monoclinic)	$622 \Rightarrow 32$ $4/mmm \Rightarrow 4/m$
Rank of relevant tensor	1 (vector)	2	≥ 3
Physical nature of the tensorial quantity	Dielectric polarization	Strain	Component of the piezoelectric or elastic tensor
Main physical properties affected by the transition	Dielectric, optical	Mechanical, elastic	Piezoelectric
Prototype example (temperature of transition)	Trigycine sulfate (322 K)	Lanthanum pentaphosphate, LaP_5O_{14} (420 K)	Quartz, SiO_2 (846 K); niobium dioxide, NbO_2 (1080 K)

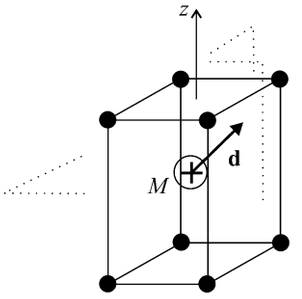

Fig. 3.1.2.1. Model of a structural transition. The filled circles at the vertices of the cell are singly charged negative ions and the empty circle at the centre is a singly charged positive ion. **d** is an arbitrary displacement of the central ion.

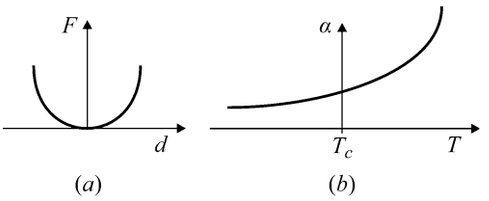

Fig. 3.1.2.2. (*a*) Variation of the free energy as function of the amplitude of the displacement of the central ion in Fig. 3.1.2.1. (*b*) Typical temperature dependence in the vicinity of T_c of the coefficient of a second-degree term in the Landau expansion (3.1.2.1) whenever this coefficient is strictly positive at T_c: one can see that this positivity is also valid slightly above and below T_c.

based on the fact that the dielectric polarization (respectively, the thermal strain tensor) acquires spontaneous components across the transition.

Conversely, if neither of these two classes of ferroics is involved in the transition considered, one knows that one must focus the study on components of higher-rank macroscopic tensors in order to reveal the characteristic anomalies associated with the transition. Also, the knowledge of the ferroic class of a transition specifies the nature of the macroscopic tensorial quantity that must be measured in order to reveal the domain structure. For instance, ferroelastic domains correspond to different values of symmetric second-rank tensors. Aside from the spontaneous strain tensor, we can consider the dielectric permittivity tensor at optical frequencies. The latter tensor determines the optical indicatrix, which will be differently oriented in space for the distinct domains. Consequently, with suitably polarized light one should always be able to 'visualize' ferroelastic domains. Conversely, such visualization will never be possible by the same method for a non-ferroelastic system.

3.1.2. Thermodynamics of structural transitions

By J.-C. Tolédano

3.1.2.1. *Introduction*

In the study of structural phase transitions, the crystallographer is often confronted by an ambiguous situation. Small changes in atomic positions determine structures having different space groups, and the data are generally compatible with several possible symmetry assignments. In order to make a choice, the crystallographer must be able to rely on some theoretical substrate, which will allow him to discard certain of the possible assignments.

The relevant theoretical framework in this field is the thermodynamical and symmetry considerations that form the *Landau theory of phase transitions*. In this chapter, we describe the ideas and results of this theory.

In the next section, we give an introduction to the main ideas of the theory by using an example consisting of a simple speculative type of structural phase transition. In Section 3.1.2.3, we discuss various situations of experimental interest relative to the thermodynamical aspect of the theory: first and second order of the transition, metastable states and thermal hysteresis. In Section 3.1.2.4, we provide a brief description, in two steps, of the general arguments constituting the foundation of the theory. In Section 3.1.2.5, we discuss the case of a structural transition actually occurring in nature and having a greater complexity than the speculative case considered in Section 3.1.2.2. In this section we also analyse the relationship between the *ferroic* character of a transition (see Section 3.1.1) and its order-parameter symmetry.

3.1.2.2. *Basic ideas of Landau's theory of phase transitions*

The Landau theory of phase transitions is a phenomenological theory. It does not aim to establish that a phase transition exists in a given system. The existence of a transition is an experimental fact considered as a starting point of the theory. The explanatory power of the theory is to establish the overall consistency of the microscopic characteristics of the transition (space symmetry and structural changes, anomalies in the phonon spectrum *etc*.) and the results of the measurement of various relevant macroscopic quantities of thermal, dielectric, optical or mechanical nature.

The continuous ('second-order') character of the transition plays an essential role in working out the general foundations of the theory. However, though its strict field of validity is that of continuous transitions, the theory also satisfactorily applies to a large fraction of discontinuous transitions.

The Landau theory defines two basic concepts: the *order parameter* (OP) and the transition free energy (LFE). It is worth pointing out that these concepts keep their usefulness in the modern statistical theory of critical phenomena, even though these phenomena do not generally comply with the results of Landau's theory. From the symmetry properties of the *order parameter* and of the *Landau free energy*, it is possible to infer, on the one hand, a certain number of observable symmetry characteristics of the system: degeneracy of the 'low-symmetry' phase (*i.e.* number of energetically equivalent domain orientations in this phase), enumeration of the possible symmetries of the 'low-symmetry' phase for a given symmetry of the 'high-symmetry' phase. On the other hand, macroscopic physical quantities can be classified as functions of their symmetries with respect to the order parameter. This classification leads to that of the various types of anomalous behaviours that can be induced by the occurrence of a phase transition.

In order to give an intuitive approach to the basic arguments of the Landau theory, and to its use, we first analyse an artificially simplified example of a crystalline phase transition.

3.1.2.2.1. *Description of a prototype example*

Fig. 3.1.2.1 represents a unit cell of a speculative crystalline structure with a simple tetragonal Bravais lattice, in which a phase transition is assumed to take place. Negative ions (filled circles) occupy the vertices of the tetragonal cell (lattice constants $a = b \neq c$). A positive ion M^+ is at the centre of the cell.

This configuration is assumed to be the equilibrium state of the system above the temperature T_c of the transition (see Fig. 3.1.2.2). *Below* T_c, equilibrium is assumed to correspond to a structure that only differs from the high-temperature structure by the fact that M^+ lies out of the centre of the cell in an unspecified direction. Hence the latter equilibrium is characterized by the magnitude and direction of the displacement $\mathbf{d}_0 = (d_x, d_y, d_z)$ of the central ion. At high temperature, the equilibrium corresponds to $\mathbf{d}_0 = 0$.

3.1.2.2.2. *Basic assumptions and strategy*

Our aim is to determine the above displacement as a function of temperature. Landau's strategy is to determine $\mathbf{d}_0$ by a *variational method*. One considers an arbitrary displacement $\mathbf{d}$ of the M^+ ion. For given temperature T and pressure p (or volume V), and specified values of the components of $\mathbf{d}$, there is, in principle, a definite value $F(T, p, d_x, d_y, d_z)$ for the free energy F of the system. This function is a *variational free energy* since it is calculated for an arbitrary displacement. The equilibrium displacement $\mathbf{d}_0(T, p)$ is defined as the displacement that minimizes the variational free energy F. The equilibrium free energy of the system is $F_{\rm eq}(T, p) = F(T, p, \mathbf{d}_0)$. Note that, strictly speaking, in the case of a given pressure, one would have to consider a variational Gibbs function $(F + pV)$ in order to determine the equilibrium of the system. We will respect the current use in the framework of Landau's theory of denoting this function F and call it a *free energy*, though this function might actually be a Gibbs potential.

The former strategy is not very useful as long as one does not know the form of the variational free energy as a function of the components of the displacement. The second step of Landau's theory is to show that, given general assumptions, one is able to determine simply the form of $F(T, p, \mathbf{d})$ in the required range of values of the functions' arguments.

The basic assumption is that of *continuity of the phase transition*. It is in fact a dual assumption. On the one hand, one assumes that the equilibrium displacement $\mathbf{d}_0(T, p)$ has components varying continuously across the transition at T_c. On the other hand, one assumes that F is a continuous and derivable function of $(T, p, \mathbf{d})$, which can be expanded in the form of a *Taylor expansion* as function of these arguments.

Invoking the continuity leads to the observation that, on either side of T_c, $|\mathbf{d}_0|$ is small, and that, accordingly, one can restrict the determination of the functional form of $F(T, p, \mathbf{d})$ to small values of (d_x, d_y, d_z) and of $|T - T_c|$. F will then be equal to the sum of the first relevant terms of a Taylor series in the preceding variables.

3.1.2.2.3. *Symmetry constraints and form of the free energy*

The central property of the variational free energy which allows one to specify its form is a symmetry property. F is a function of (d_x, d_y, d_z) which is *invariant by the symmetry transformations of the high-temperature equilibrium structure*. In other terms, an arbitrary displacement $\mathbf{d}$ and the displacement $\mathbf{d}'$ obtained by applying to $\mathbf{d}$ one of the latter symmetry transformations correspond to the same value of the free energy.

Indeed, both displacements determine an identical set of mutual distances between the positive and negative ions of the system and the free energy only depends on this 'internal' configuration of the ions.

Note that, in the case considered here (Fig. 3.1.2.1), the set of symmetry transformations comprises, aside from the lattice translations, fourfold rotations around the z axis, mirror symmetries into planes and the products of these transformations. The set of rotations and reflections forms a *group* G of order 16, which is the crystallographic point group $4/mmm$ (or D_{4h}).

Also note that this symmetry property of the free energy also holds for each degree of the Taylor expansion of F since the geometrical transformations of G act linearly on the components of $\mathbf{d}$. Hence, terms of different degrees belonging to the expansion of F will not 'mix', and must be separately invariant.

Let us implement these remarks in the case in Fig. 3.1.2.1. It is easy to check that by successive application to the components of $\mathbf{d}$ of the mirror symmetries perpendicular to the three axes, no linear combination of these components is invariant by G: each of the three former symmetry transformations reverses one component of $\mathbf{d}$ and preserves the two others. *Linear terms are therefore absent from the expansion*.

As for second-degree terms, the same symmetry transformations preclude the existence of combinations of bilinear products of the type $d_x d_y$. Actually, one finds that the fourfold symmetry imposes that the most general form of the second-degree contribution to the variational free energy is a linear combination of d_z^2 and of $(d_x^2 + d_y^2)$. Hence the Taylor expansion of F, restricted to its lowest-degree terms, is

$$F = F_o(T, p) + \frac{\alpha_1(T, p)}{2} d_z^2 + \frac{\alpha_2(T, p)}{2} \left(d_x^2 + d_y^2\right). \qquad (3.1.2.1)$$

3.1.2.2.4. *Reduction of the number of relevant degrees of freedom: order parameter*

Let us now derive the *key result of the theory*, namely, that either the component d_z or the pair of components (d_x, d_y) will take nonzero values below T_c (but not both). The meaning of this result will be clarified by symmetry considerations.

The derivation of this result relies on the fact that one, and one only, of the two coefficients α_i in equation (3.1.2.1) must vanish and change sign at T_c, and that the other coefficient must remain positive in the neighbourhood of T_c.

(a) Before establishing the latter property in (b) hereunder, let us show that its validity implies the stated key result of the theory. Indeed, if one α_i coefficient is strictly positive (*e.g.* $\alpha_1 > 0$), then the minimum of F with respect to the components of $\mathbf{d}$ (*e.g.* d_z) multiplying this coefficient in (3.1.2.1) occurs for zero equilibrium values of these components (*e.g.* $d_z^0 = 0$) in the vicinity of T_c, *above and below this temperature*. Hence, depending on the coefficient α_i which remains positive, either d_z or the pair (d_x, d_y) can be omitted, in the first place, from the free-energy expansion. *The remaining set of components is called the order parameter of the transition*. At this stage, this fundamental quantity is defined as the set of degrees of freedom, the coefficient of which in the second-degree contribution to F vanishes and changes sign at T_c. The number of independent components of the order parameter (one in the case of d_z, two in the case of the pair d_x, d_y) is called the dimension of the order parameter.

Note that the preceding result means that the displacement of the M^+ ion below T_c cannot occur in an arbitrary direction of space. It is either directed along the z axis, or in the (x, y) plane.

(b) Let us now establish the property of the α_i postulated above.

At T_c, the equilibrium values of the components of $\mathbf{d}$ are zero. Therefore, at this temperature, the variational free energy (3.1.2.1) is minimum for $d_x, d_y, d_z = 0$. Considering the form (3.1.2.1) of F, this property implies that we have (Fig. 3.1.2.2) $\alpha_i(T_c) \geq 0$ $(i = 1, 2)$.

Note that these inequalities cannot be strict for both coefficients α_i, because their positiveness would hold on either side of T_c in the vicinity of this temperature. Consequently, the minimum of F would correspond to $\mathbf{d} = 0$ on either side of the transition while the situation assumed is only compatible with this result *above* T_c. Using the converse argument that the equilibrium values of the components of $\mathbf{d}$ are not *all* equal to zero below T_c leads easily to the conclusion that one, at least, of the two coefficients α_i must vanish at T_c and become negative below this temperature.

Let us now show that the two coefficients α_i cannot vanish simultaneously at T_c. This result relies on the 'reasonable' assumption that the two coefficients α_i are *different* functions of temperature and pressure (or volume), no constraint in this respect being imposed by the symmetry of the system.

Fig. 3.1.2.3 shows, in the (T, p) plane, the two lines corresponding to the vanishing of the two functions α_i. The simultaneous vanishing of the two coefficients occurs at an isolated point

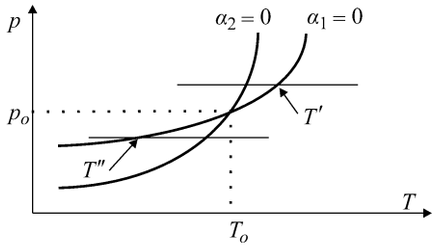

Fig. 3.1.2.3. Plots representative of the equations $\alpha_1(p, T) = 0$ and $\alpha_2(p, T) = 0$. The simultaneous vanishing of these coefficients occurs for a single couple of temperature and pressure (p_0,T_0).

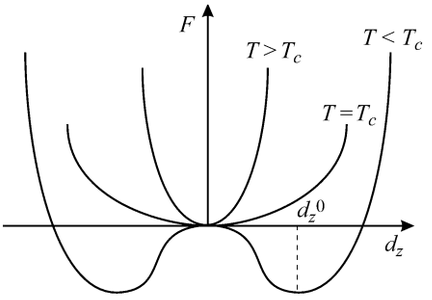

Fig. 3.1.2.4. Plots of the Landau free energy as a function of the order parameter, for values of the temperature above or below T_c or coincident with T_c. The shape of the plot changes qualitatively from a one-minimum plot to a two-minimum plot.

(T_0, p_0). Let us consider, for instance, the situation depicted in Fig. 3.1.2.3. For $p > p_0$, on lowering the temperature, α_1 vanishes at T' and α_2 remains positive in the neighbourhood of T'. Hence, the equilibrium value of the set (d_x, d_y) remains equal to zero on either side of T'. A transition at this temperature will only concern a possible change in d_z^0.

Likewise for p below p_0, a transition at T'' will only concern a possible change of the set of components (d_x^0, d_y^0), the third component d_z remaining equal to zero on either sides of T''. Hence an infinitesimal change of the pressure (for instance a small fluctuation of the atmospheric pressure) from above p_0 to below p_0 will *modify qualitatively the nature of the phase transformation* with the direction of the displacement changing abruptly from z to the (x, y) plane. As will be seen below, the crystalline symmetries of the phases stable below T' and T'' are different. This is a singular situation, of *instability*, of the type of phase transition, not encountered in real systems. Rather, the standard situation corresponds to pressures away from p_0, for which a slight change of the pressure does not modify significantly the direction of the displacement. In this case, one coefficient α_i only vanishes and changes sign at the transition temperature, as stated above.

3.1.2.2.5. *Stable state below T_c and physical anomalies induced by the transition*

We have seen that either d_z or the couple (d_x, d_y) of components of the displacement constitute the order parameter of the transition and that the free energy needs only to be expanded as a function of the components of the order parameter. Below the transition, the corresponding coefficient α_i is negative and, accordingly, the free energy, limited to its second-degree terms, has a maximum for $\mathbf{d} = 0$ and no minimum. Such a truncated expansion is not sufficient to determine the equilibrium state of the system. The stable state of the system must be determined by positive terms of higher degrees. Let us examine first the simplest case, for which the order parameter coincides with the d_z component.

The same symmetry argument used to establish the form (3.1.2.1) of the Landau free energy allows one straightforwardly to assert the absence of a third-degree term in the expansion of F as a function of the order parameter d_z, and to check the effective occurrence of a fourth-degree term. If we assume that this simplest form of expansion is sufficient to determine the equilibrium state of the system, the coefficient of the fourth-degree term must be positive in the neighbourhood of T_c. Up to the latter degree, the form of the relevant contributions to the free energy is therefore

$$F = F_o(T, p) + \frac{\alpha(T - T_c)}{2} d_z^2 + \frac{\beta}{4} d_z^4. \qquad (3.1.2.2)$$

In this expression, α_1, which is an odd function of $(T - T_c)$ since it vanishes and changes sign at T_c, has been expanded linearly. Likewise, the lowest-degree expansion of the function $\beta(T - T_c)$ is a *positive constant* in the vicinity of T_c. The function F_0, which is the zeroth-degree term in the expansion, represents the normal 'background' part of the free energy. It behaves smoothly since it does not depend on the order parameter. A plot of $[F(d_z) - F_0]$ for three characteristic temperatures is shown in Fig. 3.1.2.4.

The minima of F, determined by the set of conditions

$$\frac{\partial F}{\partial d_z} = 0; \quad \frac{\partial^2 F}{\partial^2 d_z} > 0, \qquad (3.1.2.3)$$

occur above T_c for $d_z = 0$, as expected. For $T < T_c$ they occur for

$$d_z^0 = \pm\sqrt{\alpha \frac{(T_c - T)}{\beta}}. \qquad (3.1.2.4)$$

This behaviour has a general validity: the order parameter of a transition is expected, in the framework of Landau's theory, to possess a square-root dependence as a function of the deviation of the temperature from T_c.

Note that one finds two minima corresponding to the same value of the free energy and opposite values of d_z^0. The corresponding upward and downward displacements of the M^+ ion (Fig. 3.1.2.1) are distinct states of the system possessing the same stability.

Other physical consequences of the form (3.1.2.2) of the free energy can be drawn: absence of latent heat associated with the crossing of the transition, anomalous behaviour of the specific heat, anomalous behaviour of the *dielectric susceptibility* related to the order parameter.

The *latent heat* is $L = T\Delta S$, where ΔS is the difference in entropy between the two phases at T_c. We can derive S in each phase from the equilibrium free energy $F(T, p, d_z^0(T, p))$ using the expression

$$S = -\frac{\mathrm{d}F}{\mathrm{d}T}\bigg|d_z^0 = -\left[\frac{\partial F}{\partial T}\bigg|d_z^0 + \frac{\partial F}{\partial d_z}\frac{\mathrm{d}(d_z)}{\mathrm{d}T}\bigg|d_z^0\right]. \qquad (3.1.2.5)$$

However, since F is a minimum for $d_z = d_z^0$, the second contribution vanishes. Hence

$$S = -\frac{\alpha}{2}\left(d_z^0\right)^2 - \frac{\partial F_0}{\partial T}. \qquad (3.1.2.6)$$

Since both d_z^0 and $(\partial F_0/\partial T)$ are continuous at T_c, there is no entropy jump $\Delta S = 0$, and *no latent heat at the transition*.

Several values of the specific heat can be considered for a system, depending on the quantity that is maintained constant. In the above example, the displacement $\mathbf{d}$ of a positive ion determines the occurrence of an electric dipole (or of a macroscopic polarization $\mathbf{P}$). The quantity ε, which is thermodynamically conjugated to d_z, is therefore proportional to an electric field (the conjugation between quantities η and ζ is expressed by the fact that infinitesimal work on the system has the form $\zeta\,\mathrm{d}\eta$ – *cf.*

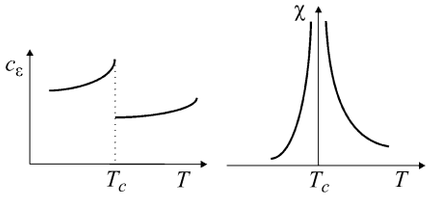

(*a*) (*b*)

Fig. 3.1.2.5. (*a*) Qualitative temperature dependence of the specific heat at a continuous transition. (*b*) Temperature dependence of the susceptibility at a continuous transition.

Sections 1.1.1.4 and 1.1.1.5). Let us show that the specific heat at *constant electric field* has a specific type of anomaly.

This specific heat is expressed by

$$c_\varepsilon = T\frac{\partial S}{\partial T}\bigg|\varepsilon. \tag{3.1.2.7}$$

Using (3.1.2.6), we find

$$T > T_c: \quad c_\varepsilon^0 = -\frac{\partial^2 F_0(T,p)}{\partial T^2}, \tag{3.1.2.8}$$

$$T < T_c: \quad c_\varepsilon = -\frac{\partial^2 F_0(T,p)}{\partial T^2} - \frac{\alpha}{2}\frac{\mathrm{d}(d_z^0)^2}{\mathrm{d}T}T = c_\varepsilon^0 + \frac{\alpha^2}{2\beta}. \tag{3.1.2.8a}$$

Hence above and below T_c the specific heat is a different, smoothly varying function of temperature, determined by the background free energy $F_0(T,p)$ and by the smooth variation of the β coefficient. Fig. 3.1.2.5(*a*) reproduces the anomaly of the specific heat, which, on cooling through T_c, has the form of an upward step.

Finally, let us consider the anomaly of the susceptibility χ, which, in the case considered, is proportional to the dielectric susceptibility of the material. It is defined as

$$\chi = \lim_{\varepsilon\to 0}\frac{\partial d_z}{\partial \varepsilon}\bigg|d_z^0. \tag{3.1.2.9}$$

In order to calculate χ, it is necessary to examine the behaviour of the system in the presence of a small field, ε, conjugated to the order parameter. In this case, the appropriate thermodynamical potential whose minimum determines the equilibrium of the system is not F but $G = F - d_z\varepsilon$. Minimizing G with respect to d_z leads to

$$d_z\{\alpha(T - T_c) + \beta d_z^2\} = \varepsilon. \tag{3.1.2.10}$$

For small values of ε, the solution of this equation must tend towards the equilibrium values $d_z = 0$. Deriving these solutions with respect to ε, we obtain

$$\chi(T > T_c) = \frac{1}{\alpha(T - T_c)}; \quad \chi(T < T_c) = \frac{1}{2\alpha(T - T_c)}. \tag{3.1.2.11}$$

The susceptibility goes to infinity when $T \to T_c$ from either side of the transition (Fig. 3.1.2.5*b*). The set of anomalies in c_ε and χ described in this paragraph represents the basic effects of temperature on quantities that are affected by a phase transition. They constitute the 'canonical signature' of a phase transition of the *continuous* type.

Certain complications arise in the cases where the transition is not strictly continuous, where the order parameter is coupled to other degrees of freedom, and where the order parameter is not one-dimensional. We consider one of these complications in Section 3.1.2.3.

3.1.2.2.6. *Symmetry considerations*

3.1.2.2.6.1. *Order-parameter symmetry*

Up to now, we have defined the order parameter as a set of degrees of freedom determining a second-degree contribution to the free energy, the coefficient of which has a specific temperature dependence proportional to $(T - T_c)$. Actually, the order parameter can also be defined on the basis of its specific symmetry characteristics.

Let us consider the manner by which the components (d_x, d_y, d_z) transform when we apply to the crystal each of the 16 symmetry operations of the group $G = 4/mmm$. Table 3.1.2.1 specifies the results of these transformations.

In the first place, we note that d_z is transformed either into itself or into $(-d_z)$. If we consider this coordinate as the basis vector of a one-dimensional vector space, we can conclude that this *vector space* (*i.e.* the space formed by the set of vectors that are linear combinations of the basis) is *invariant* by all the transformations of the group G. Such a space, containing obviously no space of smaller dimension, is, according to the definitions given in Chapter 1.2, *a one-dimensional irreducible invariant space with respect to the group G*.

Each of the components (d_x, d_y) is not transformed into a proportional component by *all* the elements of G. Certain of these elements transform d_x into $\pm d_y$, and conversely. Hence d_x and d_y are not, separately, bases for one-dimensional irreducible invariant spaces. However, their set generates a two-dimensional vector space that has the property to be invariant and irreducible by all the transformations of G.

Note that the set of the three components (d_x, d_y, d_z) carries a three-dimensional vector space which, obviously, has the property to be invariant by all the transformations of G. However, this vector space *contains* the two invariant spaces carried respectively by d_z and by (d_x, d_y). Hence it is not irreducible.

In conclusion, from a symmetry standpoint, the order parameter of a phase transition is a set of degrees of freedom that carries an irreducible vector space (an irreducible representation) with respect to the action of the group G, the latter group being the symmetry group of the high-symmetry phase.

3.1.2.2.6.2. *Degeneracy of the low-symmetry phase*

We had noted above that the structure is invariant by G in the stable state of the system above T_c. When $\mathbf{d} \neq 0$, the structure becomes invariant by a smaller set of transformations. Let us enumerate these transformations for each possible stable state of the system below T_c.

When the order parameter coincides with d_z, we determined, below T_c, two stable states, $d_z^0 = \pm[\alpha(T_c - T)/\beta]^{1/2}$. The crystalline structures determined by these displacements of the M^+ ion parallel to the z axis are both invariant by the same set of eight symmetry transformations. These comprise the cyclic group of order 4 generated by the fourfold rotation around z, and by the reflections in planes containing this axis. This set is the group

Table 3.1.2.1. *Transformation of the components of* **d** *under the symmetry operations of group* $G = 4/mmm$

G	E	C_4	C_2	C_4^3	σ_x	σ_y	σ_{xy}	$\sigma_{xy'}$
d_z	d_z	d_z	d_z	d_z	d_z	d_z	d_z	d_z
d_x	d_x	d_y	$-d_x$	$-d_y$	$-d_x$	d_x	$-d_y$	d_y
d_y	d_y	$-d_x$	$-d_y$	d_x	d_y	$-d_y$	$-d_x$	d_x
G	I	S_4^3	σ_z	S_4	U_x	U_y	U_{xy}	$U_{xy'}$
d_z	$-d_z$	$-d_z$	$-d_z$	$-d_z$	$-d_z$	$-d_z$	$-d_z$	$-d_z$
d_x	$-d_x$	$-d_y$	d_x	d_y	d_x	$-d_x$	$-d_y$	d_y
d_y	$-d_y$	d_x	d_y	$-d_x$	$-d_y$	d_y	d_x	$-d_x$

$C_{4v} = 4mm$, a *subgroup F of G*. The transition is thus accompanied by a lowering of the symmetry of the system.

Also note that the two states $\pm d_z^{\xi}$ are transformed into each other by certain of the symmetry operations such as the mirror symmetry σ_z 'lost' below T_c. These two states correspond to the same value of the free energy [the minimum value determined in equation (3.1.2.3)]: they are equally stable. This can also be checked by applying to the system the mirror symmetry σ_z. This transformation keeps unchanged the value of F since the free energy is invariant by all the transformations belonging to G (to which σ_z belongs). The state d_z is, however, not preserved, and is transformed into $(-d_z)$.

We have not determined explicitly the stable states of the system in the case of a two-dimensional order parameter (d_x, d_y). A simple discussion along the line developed for the one-dimensional order parameter d_z would show that the relevant form of the free energy is

$$F = F_0 + \frac{\alpha(T - T_c)}{2}\left(d_x^2 + d_y^2\right) + \beta_1\left(d_x^4 + d_y^4\right) + \beta_2 d_x^2 d_y^2 \tag{3.1.2.12}$$

and that the possible stable states below T_c are:

(i) $d_x^0 = \pm[\alpha(T_c - T)/\beta_1]^{1/2}$, $d_y = 0$;

(ii) $d_y^0 = \pm[\alpha(T_c - T)/\beta_2]^{1/2}$, $d_x = 0$;

(iii) and (iv) $d_x^0 = \pm d_y = \pm[\alpha(T_c - T)/(\beta_1 + \beta_2)]^{1/2}$.

Like the case of d_z, there is a lowering of the crystal symmetry below T_c. In the four cases, one finds that the respective symmetry groups of the structure are (i) $F = C_{2v} = mm2_x$; (ii) $F' = C_{2v} = mm2_y$; (iii) $F = C_{2v} = mm2_{xy}$; (iv) $F' = C_{2v} = mm2_{xy}$.

States (i) and (ii) correspond to each other through one of the 'lost' transformations of G (the rotations by $\pi/2$). They therefore possess the same free energy and stability. The second set of states (iii) and (iv) also constitute, for the same reason, a pair of states with the same value of the equilibrium free energy.

Note that the symmetry groups associated with equally stable states are conjugate relative to G, that is they satisfy the relationship $F' = gFg^{-1}$, with g belonging to G.

3.1.2.3. *Free-energy models for discontinuous transitions*

Expression (3.1.2.2) for the free energy, discussed in the preceding section, only contains terms of even degrees as a function of the order parameter. We have stressed that this property derives from symmetry considerations. Let us provisionally ignore the symmetry constraints and assume that the phase transition in a given system is described by a free energy containing a term of degree three as a function of the order parameter.

$$F = F_0 + \frac{\alpha(T - T_0)}{2}\eta^2 + \frac{\delta}{3}\eta^3 + \frac{\beta}{4}\eta^4. \tag{3.1.2.13}$$

The stable state of this system at each temperature is determined by the minimum of F. The extrema of this function are provided by

$$\frac{\partial F}{\partial \eta} = \eta\left[\alpha(T - T_0) + \delta\eta + \beta\eta^2\right] = 0, \tag{3.1.2.14}$$

the solutions of which are

$$\eta = 0 \quad \text{and} \quad \eta = \frac{1}{2\beta}\left[-\delta \pm \sqrt{\delta^2 + 4\alpha\beta(T_0 - T)}\right]. \tag{3.1.2.15}$$

A straightforward analysis based on (3.1.2.13) and (3.1.2.15) shows that, depending on the range of temperatures, the free energy has one of the forms schematically represented in Fig. 3.1.2.6(a). This form changes at three characteristic temperatures.

(i) Above $T_1 = (T_0 + \delta^2/4\alpha\beta)$, the free energy has one extremum (a minimum) for $\eta = 0$. The stable state of the system corresponds to a zero value of the order parameter.

(ii) For $T_0 < T < T_1$, the free energy has two minima, one for $\eta = 0$ and the other one for $\eta = (1/2\beta)\{-\delta \pm [\delta^2 + 4\alpha\beta(T_1 - T)]^{1/2}\}$. These minima define one stable state (the deepest minimum) and one metastable state. Note that the zero value of the order parameter constitutes the stable state in the range $T_c < T < T_1$ with $T_c = T_0 + \delta^2/9\beta\alpha$. *Hence, the observed phase transition corresponding to a change from a zero value to a nonzero value of the order parameter occurs at* T_c. Below this temperature, and down to T_0, the system has a stable state at $\eta \neq 0$ and a metastable state at $\eta = 0$.

(iii) Finally, below T_0, the free energy has two minima both corresponding to $\eta \neq 0$, the value $\eta = 0$ being a relative maximum.

The remarkable physical consequences of this sequence of shapes are the following.

In the first place, it appears that *the equilibrium value of the order parameter changes discontinuously at* T_c. The free energy (3.1.2.13) therefore provides us with a model of discontinuous phase transitions. Referring to equation (3.1.2.6), we can see that a discontinuity of the order parameter is necessarily associated with a nonzero latent heat (or entropy) for the transition. More precisely, the downward jump experienced, on heating, by the equilibrium value of the order parameter corresponds to an endothermal transition. Such a transition is also termed (following Ehrenfest's classification) a *first-order transition*, since the entropy, which is a *first derivative* of the free energy, is discontinuous.

On the other hand, the occurrence of metastable states, in certain temperature ranges, generates *thermal hysteresis*. Indeed, on cooling from above T_1, the system is likely to remain in the state $\eta = 0$ down to the temperature T_0, even though between T_1 and T_0 this state is not the stable state of the system. Conversely, on heating, the system will remain in a state $\eta \neq 0$ up to T_1, even though this state does not constitute the stable state of the system between T_c and T_1. Hence, the variations of the order parameter will schematically vary as in Fig. 3.1.2.6(b), the temperature dependence below the discontinuity being determined by equation (3.1.2.15). Likewise, the susceptibility will vary as in Fig. 3.1.2.6(c).

The form (3.1.2.13) of the free energy is not the only model form for discontinuous transitions. Another canonical form is

$$F = F_0 + \frac{\alpha(T - T_0)}{2}\eta^2 - \frac{\beta}{4}\eta^4 + \frac{\gamma}{6}\eta^6, \tag{3.1.2.16}$$

where η, β and γ are positive coefficients. The negative coefficient of the fourth-degree term has the effect of introducing more than one minimum in a certain temperature range. Fig. 3.1.2.7 shows the different shapes of the plot of $F(\eta)$ over different temperature ranges. The situation is similar to the one already discussed in the presence of a third-degree contribution to the free energy. It corresponds to a discontinuous transition associated with a latent heat as well as to the existence of a range of thermal hysteresis.

Two relevant questions arise from consideration of the above models of first-order transitions.

In the first place, one can object to the use of a polynomial expansion of the free energy in cases involving a discontinuity of the order parameter while the assumption of continuity of the phase transition has been used as an essential substrate of the argument developed. However, the approach will clearly keep its validity if a transition, though discontinuous, involves 'small' discontinuties. The criterion for estimating if a discontinuity is small relies on the comparison between the atomic displacements involved by the transition and the distances between atoms in the structure. If the displacements are a small fraction of the distances between atoms, then the method used can be consid-

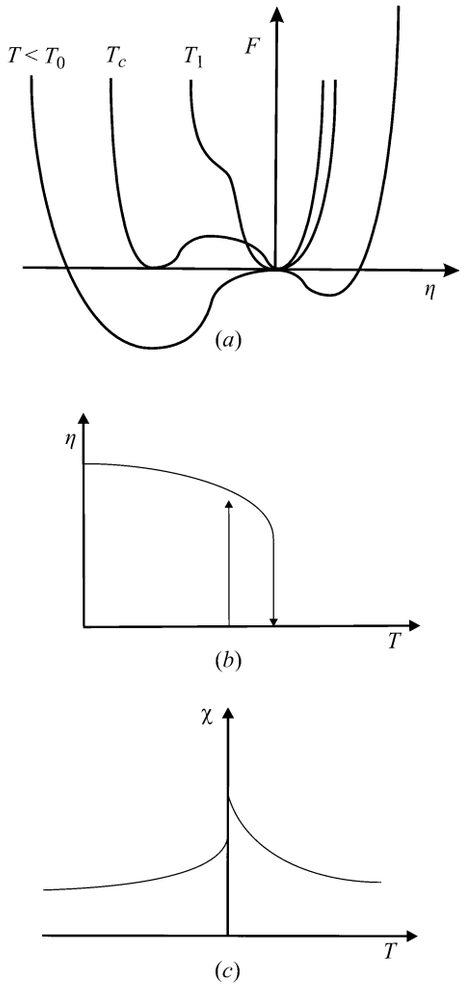

Fig. 3.1.2.6. (*a*) Plots of the free energy as a function of the order parameter for various temperature values in the framework of the model of a discontinuous transition associated with equation (3.1.2.13). (*b*) Temperature dependence of the equilibrium value of the order parameter, as determined by the model of a discontinuous transition. (*c*) Temperature dependence of the susceptibility in this model.

ered as valid. Indeed, the total free energy of the system depends on the distance between atoms, because this distance controls the strength of the interaction energy within the system. Hence, the transition only changes in a minor way the value of the system's free energy.

On the other hand, one has to check that there are systems of physical interest for which the crystallographic symmetry allows free-energy forms of the type (3.1.2.13), (3.1.2.16). Indeed, the crystallographic symmetry relative to the example in Section 3.1.2.2 was such that the presence of a third-degree term in the Landau free energy was excluded.

Such verification is not necessary for the free energy of type (3.1.2.16). This free energy is only characterized by a *specific sign* of the coefficient of the fourth-degree term, a circumstance that is not defined by symmetry considerations.

By contrast, an actual crystallographic model of a transition described by (3.1.2.13), which involves a term of degree three, is required to support the relevance of the corresponding model. Such a model is provided, for instance, by a crystal the high-temperature phase of which has a rhombohedral symmetry (*e.g.* *R*3*m*), and which undergoes a transition corresponding to an atomic displacement **d** perpendicular to the ternary axis (Fig. 3.1.2.8).

If we refer the components to a rectangular frame of coordinates, the matrices representing the mode of transformation of the components (d_x, d_y) under application of the generating

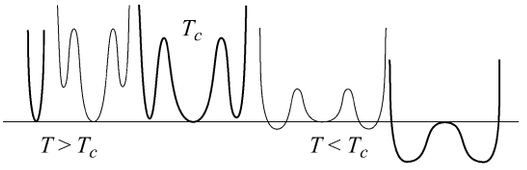

Fig. 3.1.2.7. Plots of the free energy as a function of the order parameter for various temperatures in the framework of the model of a discontinuous transition associated with equation (3.1.2.16). The temperature decreases from right to left, the transition being reached for the temperature corresponding to the third plot.

elements of the group *R*3*m* have a form reproduced in existing tables. It is easy to check that the form of the Landau free energy resulting from a search of invariant polynomials of successive degrees is

$$F = F_0 + \frac{\alpha(T - T_0)}{2}\left(d_x^2 + d_y^2\right) + \frac{\delta}{3}\left(d_x^2 - 3d_y^2\right) + \frac{\beta}{4}\left(d_x^2 + d_y^2\right)^2. \tag{3.1.2.17}$$

We note that the form of the free energy of this system, determined by its symmetry, involves a third-degree term. Let us show that the thermodynamic properties corresponding to this form are qualitatively identical to the ones derived from the canonical free energy (3.1.2.13). In this view, let us put $d_x = \eta\cos\theta$ and $d_y = \eta\sin\theta$. The free energy takes the form

$$F = F_0 + \frac{\alpha(T - T_0)}{2}\eta^2 + \frac{\delta}{3}\eta^3\cos\theta\left(\cos^2\theta - 3\sin^2\theta\right) + \frac{\beta}{4}\eta^4. \tag{3.1.2.18}$$

For such a free energy, it is remarkable that for $\eta \neq 0$ the directions θ of the extrema, which are determined by $\partial F/\partial\theta = 0$, are independent of the value of η. These directions form two sets which we denote A ($\theta = 0, 2\pi/3, 4\pi/3$) and B ($\pi/3, \pi, -\pi/3$). If we replace in equation (3.1.2.18) η by one of these values, we obtain

$$F = F_0 + \frac{\alpha(T - T_0)}{2}\eta^2 \pm \frac{\delta}{3}\eta^3 + \frac{\beta}{4}\eta^4, \tag{3.1.2.19}$$

the sign in front of the δ coefficient being $+$ for the A set of θ angles and $-$ for the B set. We are therefore brought back to a form close to the canonical one [equation (3.1.2.13)]. Note that for $\delta > 0$, the stable second minimum of the free energy [equation (3.1.2.15)] corresponded to $\eta < 0$, *i.e.* to $\delta\eta < 0$. Hence in (3.1.2.19), η being a positive modulus, the second stable minimum will correspond to a negative coefficient for η^3. Depending on the sign of δ, the direction θ of this minimum will either be the set A or the set B of θ values.

3.1.2.4. *Generalization of the approach*

Let us summarize the results obtained in the study of the specific models described in the preceding sections. We have shown that an order parameter (*e.g.* d_z or d_x, d_y) is a set of scalar degrees of freedom that allows the description of the symmetry and physical changes accompanying the phase transition in a system. The equilibrium values of the n components of the order parameter are zero for $T \geq T_c$ and *not all zero* for $T < T_c$. The n components define a vector space that is an irreducible invariant

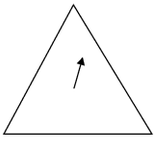

Fig. 3.1.2.8. Schematic representation of the displacement associated with the order parameter in a crystal having trigonal (rhombohedral) symmetry.

space by the group G, which is the crystallographic symmetry group of the high-temperature phase. A variational free energy F associated with the transition, and termed the Landau free energy, can be expanded as a function of the components of the order parameter. The second-degree term of this expansion has a coefficient that vanishes and changes sign at the transition temperature. The form of F is determined by the symmetry properties of the order parameter, *i.e.* by the mode of transformation of the components of the order parameter into each other when the operations of G are applied to them. The specific form of F determines the symmetries of the potentially stable phases below T_c, the degeneracy of these phases, the temperature dependencies of relevant physical quantities and, in certain cases, the thermodynamic order of the phase transition.

In this section, let us briefly outline the arguments used in order to formulate the theory in a general framework.

These arguments rely in part on the properties of the irreducible representations of a group. The reader can refer to Chapter 1.2 for a comprehensive presentation of irreducible representations. We will consider here representations of a group G carried by a set of degrees of freedom $(\eta_1, \eta_2, \eta_3, \ldots)$, and use essentially the following properties.

(a) If the set is irreducible and non-totally symmetric (trivial), there is no linear combination $f_1(\eta_i) = \alpha_1\eta_1 + \alpha_2\eta_2 + \ldots$ of the η_i that is invariant by all the elements of G.

(b) If the set is irreducible, there is a single homogeneous polynomial of degree two that is invariant by the group G. Its form is $f_2 = \sum \eta_i^2$.

(c) If $g(\mathbf{r})$ is an arbitrary function of the space coordinates $[\mathbf{r} = (x, y, z)]$, one can always write

$$g(\mathbf{r}) = \sum_{\gamma} \sum_{j} \varphi_{\gamma,j}(\mathbf{r}), \tag{3.1.2.20}$$

where each set of functions $\varphi_{\gamma,j}$ $(j = 1, 2, \cdots, p)$ defines a space generated by the p functions which is invariant and irreducible by the group G and corresponds to the irreducible representation labelled τ_γ of G.

3.1.2.4.1. *Description of the phase transition*

In order to generalize the considerations developed in the preceding sections, we have to define, independently from any specific structure, the basic ingredients of the theory: definition of a variational set of degrees of freedom; construction of a free energy; determination of the stable states on either side of a transition temperature.

In a first step, we describe an arbitrary atomic configuration of a system by the set of densities $\rho_i(\mathbf{r})$ of the particles of type (i). This set constitutes variational degrees of freedom, which can be used to construct the variational free energy of the system $F[T, \rho_i(\mathbf{r})]$. The equilibrium of the system is defined by the set of functions $\rho_i^{\rm eq}(T, \mathbf{r})$ that minimize the free energy.

The symmetry of the system at a given temperature is defined as the set of geometrical transformations that leave invariant all the $\rho_i^{\rm eq}$. This set forms a group.

We are then in a position to define a *continuous transition* at T_c by two conditions:

(i) The $\rho_i^{\rm eq}(T, \mathbf{r})$ are functions whose forms change continuously across T_c.

(ii) The symmetry group of the system just above T_c is different to the symmetry just below T_c.

Hence the phase transition, though associated with a *continuous* change of the spatial configuration of the atoms, is associated with a *sudden* change of the symmetry.

3.1.2.4.2. *Order parameter*

As compared with the set (d_x, d_y, d_z) used in the example of Section 3.1.2.2, the variational functions $\rho_i(\mathbf{r})$ have the drawback of not being *small and scalar* quantities, thus making an expansion of the free energy more complicated.

Without loss of generality, let us restrict ourselves to a single type of (i) particles. In order to remove the difficulty mentioned above we put

$$\rho(\mathbf{r}) = \rho_0(\mathbf{r}) + \sum \sum \eta_{\gamma,j}\varphi_{\gamma,j}(\mathbf{r}), \tag{3.1.2.21}$$

where $\rho_0 = \rho^{\rm eq}(T_c, \mathbf{r})$ is the equilibrium density at T_c. Let us denote by G the symmetry group of this equilibrium density. The sum in the second part of (3.1.2.21) is a small increment since the transition is continuous. This increment has been expanded, as in (3.1.2.20), as a function of irreducible functions with respect to the group G. Moreover, each function has been expressed as the product of a normalized function $\varphi_{\gamma,j}$ and of small scalar parameters $\eta_{\gamma,j}$. It is easy to convince oneself that it is possible to consider that under the action of G either the $\varphi_{\gamma,j}$ transform into each other, the $\eta_{\gamma,j}$ being fixed coefficients, or the $\eta_{\gamma,j}$ transform into each other, the functions $\varphi_{\gamma,j}$ being fixed. *We shall adopt the second convention*. The variational free energy can then be written in the form

$$F = F\big[T, \eta_{\gamma,j}, \varphi_{\gamma,j}(\mathbf{r})\big]. \tag{3.1.2.22}$$

At each temperature, the characteristics of the system are specified by the following conditions:

(i) The equilibrium corresponds to the values $\eta_{\gamma,j}$ that make the free energy a minimum. These values define through (3.1.2.21) the equilibrium density of particles in the system.

(ii) The symmetry of the system is defined as the group of invariance of the determined equilibrium density.

Note that, in $(\rho - \rho_0)$, the contribution of the degrees of freedom $\eta_{\gamma,j}$ spanning a *totally symmetric representation* can be ignored in the first place. One can show that such a contribution would have the same symmetry on either side of the transition. Therefore it is not crucially associated with the symmetry change defining the phase transition.

Following the ideas introduced in Section 3.1.2.2, the free-energy form is obtained as a Taylor expansion as a function of the small parameters $\eta_{\gamma,j}$. Besides, each polynomial term of a given degree of this expansion is invariant by G. Indeed, F, being a scalar, is unchanged by any rotation or reflection. Among the transformations, those belonging to G have the additional property of leaving invariant the density ρ_0 which is, besides T and the $\eta_{\gamma,j}$, an argument of the function F.

It is easy to check that the group-theoretical rules recalled at the beginning of this section determine the absence of an invariant linear term in the expansion. Moreover, these rules specify the form of the second-degree contribution. We have

$$F = F_0(T) + \sum \alpha_\gamma \big(\sum \eta_{\gamma,j}^2\big). \tag{3.1.2.23}$$

On the other hand, the equilibrium density is

$$\rho^{\rm eq} - \rho_0 = \sum \sum \eta_{\gamma,j}^0 \varphi_{\gamma,j}(\mathbf{r}). \tag{3.1.2.24}$$

Let us first consider the system at T_c. The equilibrium values of all the $\eta_{\gamma,j}$ are zero. Hence, on the basis of (3.1.2.23), we conclude that all the α_γ satisfy the condition $\alpha_\gamma > 0$ (since the second-degree expansion must be minimum at the origin). Note that this condition *cannot be strict for all* γ. Otherwise, these coefficients would also be positive in the vicinity of T_c, on either side of this temperature. As a consequence, the equilibrium values $\eta_{\gamma,j}^0$ would all be zero and the symmetry would be unchanged. *Hence, one at least of the* α_γ *has to vanish and to change sign at* T_c. An argument already invoked in Section 3.1.2.2 allows one to assert that one α_γ coefficient only has this property. The $\eta_{\gamma,j}$ corresponding to the other indices γ keep zero equilibrium values in the vicinity of T_c and can be ignored in the first place. We can therefore drop in (3.1.2.23) all degrees of freedom except the ones associated with

the α_γ coefficient that vanishes at T_c. The set $\eta_{\gamma,j}$ ($j = 1, 2, \ldots, m$) constitutes the *m-dimensional order parameter of the transition considered*. As this set comprises all the degrees of freedom contributing to a single second-degree term in the free energy, it necessarily constitutes a basis for an irreducible vector space with respect to G, according to the group-theoretical rules recalled above.

3.1.2.4.3. *Stable states and symmetry in the vicinity of T_c*

Above T_c, due to the positivity of α (we can drop the γ index), the equilibrium values of the η_j are zero and the symmetry is G, identical to the symmetry at T_c. Below T_c, α is negative and the minimum of F occurs away from the origin in the $\{\eta_j\}$ space. The symmetry of the system is defined by all the transformations leaving invariant the density:

$$\rho^{\rm eq} = \rho_0 + \sum \eta_j^0 \varphi_j(\mathbf{r}). \qquad (3.1.2.25)$$

Since the η_j^0 contribution to the second member is small, these transformations have to be selected among those belonging to the invariance group of ρ_0. The space $\{\eta_j\}$ defines a *non-trivial representation* of the latter group since the linear combination of the order-parameter components present in $\rho^{\rm eq}$ cannot be invariant by all the transformations of G. The symmetry group of the system below T_c is therefore a subgroup F of G.

As pointed out in Section 3.1.2.2, in order to determine the minimum of F below T_c, it is necessary to expand the free energy to degrees higher than two. The relevant expression of the free energy is then

$$F = F_0(T, \rho_0) + \tfrac{1}{2}\alpha(T - T_c)\big(\sum \eta_j^2\big) + f_3(\eta_j) + f_4(\eta_j) + \ldots, \qquad (3.1.2.26)$$

where we have developed the coefficient α, which is an odd function of $(T - T_c)$ to the lowest degree in $(T - T_c)$. It can be shown that the existence of a third-degree term $f_3(\eta_j)$ depends exclusively on the nature of the representation τ_γ associated with the order parameter. If the symmetry of the order parameter is such that a third-degree term is not symmetry forbidden, the transition will be of the type analysed in Section 3.1.2.3: it will be discontinuous.

For any symmetry of the order parameter, fourth-degree terms $f_4(\eta_j)$ will always be present in the free-energy expansion (there will be at least one such term that is the square of the second-degree term). No further general statement can be made. Depending on the form and coefficients of this term, a continuous or discontinuous transition will be possible towards one or several distinct low-symmetry phases. The form of the $f_4(\eta_j)$ term can be determined by searching the most general fourth-degree polynomial that is invariant by the set of transformations belonging to G.

In summary, in the light of the preceding considerations, the study of a phase transition according to the Landau scheme can be developed along the following lines:

(a) Search, as a starting information on the system, the symmetry group G of the more symmetric phase surrounding the transition and the nature of the irreducible representation τ_γ associated with the order parameter. Both can be obtained from a crystallographic investigation as illustrated by the example in the next section.

(b) Check the possibility of a third-degree invariant on symmetry grounds.

(c) Construct the free energy by determining the form of the invariant polynomials of the required degrees.

(d) Determine, as a function of the coefficients of the free-energy expansion, the absolute minimum of F.

(e) For each minimum, determine the invariance group of the density $\rho^{\rm eq}$, *i.e.* the 'low-symmetry' group of the system.

(f) Derive the temperature dependence of the quantities related to the order parameter component η_j.

(g) Consider (as discussed in the next section) the coupling of the order parameter to other relevant 'secondary' degrees of freedom, and derive the temperature dependence of these quantities.

3.1.2.5. *Application to the structural transformation in a real system*

Let us examine the particular ingredients needed to apply Landau's theory to an example of *structural* transitions, *i.e.* a transition between crystalline phases.

3.1.2.5.1. *Nature of the groups and of their irreducible representations*

The phases considered being crystalline, their invariance groups, G or F, coincide with *crystallographic space groups*. Let us only recall here that each of these groups of infinite order is constituted by elements of the form $\{R|\mathbf{t}\}$ where R is a point-symmetry operation and $\mathbf{t}$ a translation. The symmetry operations R generate the point group of the crystal. On the other hand, among the translations $\mathbf{t}$ there is a subset forming an infinite group of 'primitive' translations $\mathbf{T}$ generating the three-dimensional Bravais lattice of the crystal.

For a space group G, there is an infinite set of unequivalent irreducible representations. An introduction to their properties can be found in Chapter 1.2 as well as in a number of textbooks. They cannot be tabulated in a synthetic manner as the better-known representations of finite groups. They have to be constructed starting from simpler representations. Namely, each representation is labelled by a double index.

(i) The first index is a $\mathbf{k}$ vector in reciprocal space, belonging to the first Brillouin zone of this space. The former vector defines a subgroup $G(\mathbf{k})$ of G. This group is the set of elements $\{R|\mathbf{t}\}$ of G whose component R leaves $\mathbf{k}$ unmoved, or transforms it into an 'equivalent' vector (*i.e.* differing from $\mathbf{k}$ by a reciprocal-lattice vector). The group $G(\mathbf{k})$ has irreducible representations labelled $\tau_m(\mathbf{k})$ of dimension n_m which are defined in available tables.

(ii) A representation of G can be denoted $\Gamma_{\mathbf{k},m}$. It can be constructed according to systematic rules on the basis of the knowledge of $\tau_m(\mathbf{k})$. Its dimension is $n_m r$ where r is the number of vectors in the 'star' of $\mathbf{k}$. This star is the set of vectors, unequivalent to $\mathbf{k}$, having the same modulus as $\mathbf{k}$ and obtained from $\mathbf{k}$ by application of all the point-symmetry elements R of G.

3.1.2.5.2. *The example of gadolinium molybdate, $Gd_2(MoO_4)_3$*

Gadolinium molybdate (GMO) is a substance showing one complication with respect to the example in Section 3.1.2.2. Like the prototype example already studied, it possesses below its phase transition an electric dipole (and a spontaneous polarization) resulting from the displacement of ions. However, one does not observe the expected divergence of the associated susceptibility (Fig. 3.1.2.5).

3.1.2.5.2.1. *Experimental identification of the order-parameter symmetry*

The high-temperature space group G is known for GMO from X-ray diffraction experiments. It is the tetragonal space group $P\bar{4}2_1m$. The corresponding point group $\bar{4}2m$ has eight elements, represented in Fig. 3.1.2.9.

The $\mathbf{k}$ vector labelling the irreducible representation associated with the order parameter can be directly deduced from a comparison of the diffraction spectra above and below T_c. We have seen that the difference of the two stable structures surrounding the transition is specified by the equilibrium density:

$$\rho(T, \mathbf{r}) - \rho(T_c, \mathbf{r}) = \sum \eta_{k,m} \varphi_{\mathbf{k},m}(\mathbf{r}). \qquad (3.1.2.27)$$

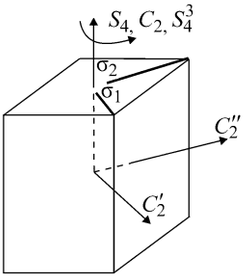

Fig. 3.1.2.9. Rotations/reflections belonging to the point group of gadolinium molybdate.

One can show, using the properties of the irreducible representations of the space groups, that the Fourier transform of the difference of densities given above is proportional to $\delta(\mathbf{K}-\mathbf{k})$, *i.e.* this Fourier transform is nonzero only for a $\mathbf{K}$ vector equal to the $\mathbf{k}$ vector indexing the order parameter. The implication of this property is that below T_c, the X-ray spectrum of the system will contain additional reflections whose locations in reciprocal space are defined by the vector of the order parameter. Experimentally, the vectors joining the Bragg spots existing in both phases to the *closest superlattice spots only appearing below* T_c are the vectors $\mathbf{k}$ defining partly the irreducible representation $\Gamma_{\mathbf{k},m}$ that specifies the symmetry properties of the order parameter.

In GMO, X-ray diffraction measurements show that superlattice spots appear below T_c at one of the four equivalent $\mathbf{k}$ vectors

$$\pm\frac{\mathbf{a}_1^* \pm \mathbf{a}_2^*}{2}. \qquad (3.1.2.28)$$

The operations of the point group $\bar{4}2m$ transform these vectors into each other. The star of $\mathbf{k}$ is therefore reduced to a single vector. On the other hand, consultation of available tables provides us with the possible representations $\tau_{\mathbf{k},m}$ necessary to construct the representation $\Gamma_{\mathbf{k},m}$ of the order parameter (the entries of the tables being the $\mathbf{k}$ vector determined and the space group G). There are three unequivalent $\tau_{\mathbf{k},m}$, which are reproduced in Table 3.1.2.2.

The ambiguity in the symmetry of the order parameter has now to be lifted. In this approach, the method is to work out for each τ_m the symmetries G of the phases that are possibly stable below T_c. One then compares the results with the observed space group below T_c, which, for GMO, is the orthorhombic space group *Pba*2.

The group F of interest is the invariance group of the density difference [equation (3.1.2.27)]. Note that this difference can be considered as a 'vector' with components η_i in the irreducible space of the order parameter. In each irreducible space, the action of the elements of G on a vector is represented by the set of matrices reproduced in Table 3.1.2.2. Let us first examine τ_1 in this table. Clearly, the matrices relative to $\{S_4|0\}$, $\{S_4^3|0\}$, $\{C_2'|\mathbf{t}\}$ and $\{C_2''|\mathbf{t}\}$ rotate by $\pi/2$ any vector of the two-dimensional space carrying the representation. These elements will not leave any direction unmoved and consequently they will not belong to F. The other elements either preserve any vector (and they then obviously belong to F) or they reverse any direction. However, in the latter case, the product of any two of these elements belongs to F.

Summarizing these remarks, we obtain a single possible group F consisting of the elements $\{E|0\}$, $\{C_2|\mathbf{a}_1\}$, $\{\sigma_1|\mathbf{t}\}$, $\{\sigma_2|\mathbf{t}+\mathbf{a}_1\}$ and by the infinite translation group generated by the vectors $(\mathbf{a}_1 \pm \mathbf{a}_2)$ and $\mathbf{a}_3$. The symbol for this space group is *Pmm*2.

A similar inspection yields for the representation τ_2 the group *Pba*2 and for τ_3 three possible groups (*P*4, *Pbm*2 and *P*2). Comparison with the experimental observation, recalled above, allows one to identify unambiguously the appropriate representation as τ_2. In conclusion, the irreducible representation associated with the order parameter of the transition in GMO can be denoted $\Gamma_{\mathbf{k},m}$. Its $\mathbf{k}$ vector is $\mathbf{k} = \pm(\mathbf{a}_1^* \pm \mathbf{a}_2^*)/2$, and its 'small representation' is $\tau_2(\mathbf{k})$. The number of components of the order parameter is two, equal to the dimension of $\Gamma_{\mathbf{k},m}$, which itself is equal to the product of the number of vectors in the star of $\mathbf{k}$ (one) and of the dimension of τ_2 (two).

3.1.2.5.2.2. *Construction of the free energy and stable states*

Denote by (η_1, η_2) the two components of the order parameter. The Landau free energy can be constructed by selecting the homogeneous polynomials of different degrees that are invariant by the *distinct* matrices of τ_2. There are four such matrices. It is easy to check that the most general form of fourth-degree polynomial invariant by the action of these four matrices is

$$F = F_0 + \frac{\alpha(T-T_c)}{2}\left(\eta_1^2+\eta_2^2\right) + \frac{\beta_1}{4}\left(\eta_1^4+\eta_2^4\right) + \frac{\beta_2}{2}\eta_1^2\eta_2^2 + \frac{\beta_3}{2}\eta_1\eta_2\left(\eta_1^2-\eta_2^2\right). \qquad (3.1.2.29)$$

A discussion of the minima of this free energy can be made according to the same method as in Section 3.1.2.3, by putting $\eta_1 = \rho\cos\theta$, $\eta_2 = \rho\sin\theta$. One then finds that, in accordance with the symmetry considerations developed in Section 3.1.2.5.2.1, there is a single possible symmetry below T_c. The equilibrium state of the system corresponds to an angle θ whose value depends on the values of the coefficients in the expansion. The modulus ρ has the standard temperature dependence $\rho \propto (T_c - T)^{1/2}$.

As in the model/example described in Section 3.1.2.2, below T_c there are several stable states having the same free energy. Indeed, one can easily check in expression (3.1.2.29) that if (η_1^0, η_2^0) is an absolute minimum of the free energy (3.1.2.29), the states $(-\eta_2^0, \eta_1^0)$, $(-\eta_1^0, \eta_2^0)$, $(-\eta_1^0, -\eta_2^0)$ are symmetry-related

Table 3.1.2.2. *Matrices defining the irreducible representations of Pba*2 *for* $\mathbf{k} = \mathbf{a}_1^* + \mathbf{a}_2^*$

	G										
	$\{E\|0\}$	$\{S_4\|0\}$	$\{C_2\|0\}$	$\{S_4^3\|0\}$	$\{\sigma_1\|\mathbf{t}\}$	$\{\sigma_2\|\mathbf{t}\}$	$\{C_2'\|\mathbf{t}\}$	$\{C_2''\|\mathbf{t}\}$	$\mathbf{a}_1$	$\mathbf{a}_2$	$\mathbf{a}_3$
τ_1	$\begin{matrix}1&0\\0&1\end{matrix}$	$\begin{matrix}0&1\\-1&0\end{matrix}$	$\begin{matrix}-1&0\\0&-1\end{matrix}$	$\begin{matrix}0&-1\\1&0\end{matrix}$	$\begin{matrix}1&0\\0&1\end{matrix}$	$\begin{matrix}-1&0\\0&-1\end{matrix}$	$\begin{matrix}0&1\\-1&0\end{matrix}$	$\begin{matrix}0&-1\\1&0\end{matrix}$	$\begin{matrix}-1&0\\0&-1\end{matrix}$	$\begin{matrix}-1&0\\0&-1\end{matrix}$	$\begin{matrix}1&0\\0&1\end{matrix}$
τ_2	$\begin{matrix}1&0\\0&1\end{matrix}$	$\begin{matrix}0&1\\-1&0\end{matrix}$	$\begin{matrix}-1&0\\0&-1\end{matrix}$	$\begin{matrix}0&-1\\1&0\end{matrix}$	$\begin{matrix}-1&0\\0&-1\end{matrix}$	$\begin{matrix}1&0\\0&1\end{matrix}$	$\begin{matrix}0&-1\\1&0\end{matrix}$	$\begin{matrix}0&1\\-1&0\end{matrix}$	$\begin{matrix}-1&0\\0&-1\end{matrix}$	$\begin{matrix}-1&0\\0&-1\end{matrix}$	$\begin{matrix}1&0\\0&1\end{matrix}$
τ_3	$\begin{matrix}1&0\\0&1\end{matrix}$	$\begin{matrix}1&0\\0&-1\end{matrix}$	$\begin{matrix}1&0\\0&1\end{matrix}$	$\begin{matrix}1&0\\0&-1\end{matrix}$	$\begin{matrix}0&1\\1&0\end{matrix}$	$\begin{matrix}0&1\\1&0\end{matrix}$	$\begin{matrix}0&-1\\1&0\end{matrix}$	$\begin{matrix}0&-1\\1&0\end{matrix}$	$\begin{matrix}-1&0\\0&-1\end{matrix}$	$\begin{matrix}-1&0\\0&-1\end{matrix}$	$\begin{matrix}1&0\\0&1\end{matrix}$

minima corresponding to the same value of the equilibrium free energy.

The intensities of the diffraction 'superlattice' spots, being proportional to the square of the atomic displacement ρ, vary linearly as a function of temperature. On the other hand, the diverging susceptibility associated with the order parameter is related to a rapid increase of the diffuse scattering of X-rays or neutrons at the location of the superlattice spots in reciprocal space. Hence, consistent with the macroscopic measurements, it is not related to a divergence of the dielectric susceptibility.

3.1.2.5.2.3. *Macroscopic behaviour of GMO*

In GMO, macroscopic quantities are degrees of freedom that are distinct from the order parameter. Indeed, their symmetry properties are different, since any lattice translation will leave them invariant, while this is not the case for the order parameter (see Section 3.1.2.5.2.1). Nevertheless, certain of the macroscopic quantities behave singularly at the transition. These degrees of freedom can be decomposed, as shown in Section 3.1.2.4, as the sum of irreducible degrees of freedom. Having a symmetry different from that of the order parameter, they were neglected in the first step of the description of the phase transition. In a more detailed description, they have to be taken into account.

Let us, for instance, consider the P_z component of the dielectric polarization of GMO, as well as the ε component of the strain tensor which represents a shear in the xy plane of the crystal. The matrices in Table 3.1.2.3 recall the mode of transformation of the order-parameter components as well as those of these two quantities under the action of the G group.

We can complete the expression of the free energy of the system by adding to F in (3.1.2.29) the contributions of the preceding degrees of freedom up to the second degree (which, as will be seen, is comparable to the fourth degree used for the order parameter). The resulting expression is provided by (3.1.2.30) below, in which we have neglected a bilinear term in P_z and ε as this term does not change the qualitative result we want to establish.

$$F_1 = F + \frac{b}{2}P_z^2 + \frac{c}{2}\varepsilon^2 + \delta_1 P_z\left(\eta_1^2 - \eta_2^2\right) + \delta_2\varepsilon\left(\eta_1^2 - \eta_2^2\right), \tag{3.1.2.30}$$

where F is provided by equation (3.1.2.29). At equilibrium, the derivatives of F_1 with respect to P_z and ε vanish. These conditions yield

$$P_z = -\frac{\delta_1}{b}\left(\eta_1^2 - \eta_2^2\right); \quad \varepsilon = -\frac{\delta_2}{c}\left(\eta_1^2 - \eta_2^2\right). \tag{3.1.2.31}$$

As stressed in Section 3.1.2.5.2.2, the equilibrium direction in the order-parameter space corresponds to the trivial $\theta = 0$ angle. Hence $\left(\eta_1^2 - \eta_2^2\right) \neq 0$ below T_c, resulting in the fact that nonzero values of P_z and ε will onset below the transition temperature. Besides, the form (3.1.2.31) indicates that the two macroscopic quantities considered, which are proportional to the square of the order parameter, are expected to vary linearly as a function of temperature below T_c. Note that terms such as P_z^2 are of the same order of magnitude as fourth-degree terms of the order parameter.

We can also determine the behaviour of the dielectric susceptibility χ, by calculating the variations of the equilibrium value of P_z as a function of an applied electric field **E** parallel to the polarization. We proceed as in Section 3.1.2.2, and minimize the potential $G_1 = (F_1 - P_z E)$ with respect to the order parameter and to the polarization. In order to obtain the qualitative behaviour of χ, we simplify the free energy by considering a single component of the order parameter. We also neglect the shear strain component ε. The set of simplified equations

$$\chi = \frac{\partial P_z}{\partial E}|E = 0; \quad bP_z + \delta\eta^2 = E \tag{3.1.2.32}$$
$$\frac{\partial F_1}{\partial E} = \eta\left\{\alpha(T - T_c) + \left(\beta - \frac{2\delta_1^2}{b}\right)\eta^2 + \frac{2\delta_1}{b}E\right\}$$

yields the following expression of the susceptibility:

$$\chi = \frac{1}{b} \quad \text{for} \quad T > T_c \quad \text{and} \quad \chi = \frac{1}{b} + \frac{2\delta_1^2}{b\left(\beta - 2\delta_1^2/b\right)} \quad \text{for} \quad T < T_c. \tag{3.1.2.33}$$

We find an upward step of the dielectric susceptibility on cooling. Likewise, consideration of the 'elastic' susceptibility relative to the shear strain component ε would determine an upward step of the elastic compliance (Fig. 3.1.2.10). The more usually measured elastic constant, which is the inverse of the compliance, undergoes a downward step on cooling.

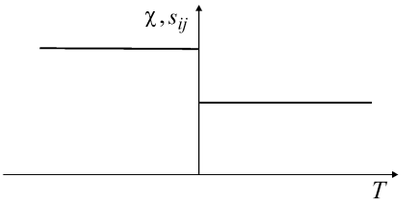

Fig. 3.1.2.10. Temperature dependence of the macroscopic susceptibility (or elastic compliance, s_{ij}) in gadolinium molybdate. Compare with the 'normal' behaviour in Fig. 3.1.2.5(b).

We have seen in the preceding paragraph that the low-symmetry phase of gadolinium molybdate possesses four equally stable states differing by the values of the order-parameter components. Equation (3.1.2.31) shows that two of the states are associated with the same sign of the polarization P_z or of the shear strain ε, while the two other states possess opposite values of P_z and ε. According to the definitions given in Section 3.1.1, gadolinium molybdate belongs to the category of ferroelectrics as well as to that of ferroelastics.

The example of GMO clearly shows that the ferroic classification is less informative than the one based on the order-parameter symmetry. The latter determines the full symmetry change (orientational and translational), while the former only specifies the orientational symmetry change. On the other hand, the ferroic classification is not informative about the physical behaviour as a function of temperature. Thus, the model ferroelectric in Section 3.1.2.2 has a diverging dielectric susceptibility at T_c, while a GMO-type ferroelectric keeps a finite susceptibility. The ferroic classification has nevertheless the advantage of specifying the nature of the macroscopic quantities that are expected to behave anomalously at the transition, and are therefore worth measuring.

Table 3.1.2.3. *Action of the generators of Pba2 on the order parameter and on the polarization and strain components*

	E	S_4	σ_1	$\mathbf{a}_1$	$\mathbf{a}_2$	$\mathbf{a}_3$
η_1 η_2	1 0 0 1	0 1 −1 0	−1 0 0 −1	−1 0 0 −1	−1 0 0 −1	1 0 0 1
P_z ε	1 1	−1 −1	1 1	1 1	1 1	1 1

3.1.3. Equitranslational phase transitions. Property tensors at ferroic phase transitions

By V. Janovec and V. Kopský

In the Landau theory, presented in the preceding Section 3.1.2, symmetry considerations and thermodynamics are closely interwoven. These two aspects can be, at least to some extent, disentangled and some basic symmetry conditions formulated and utilized without explicitly invoking thermodynamics. Statements which follow directly from symmetry are exact but usually do not yield numerical results. These can be obtained by a subsequent thermodynamic or statistical treatment.

The central point of this section is Table 3.1.3.1, which contains results of symmetry analysis for a large class of equitranslational phase transitions and presents data on changes of property tensors at most ferroic phase transitions. Notions and statements relevant to these two applications are explained in Sections 3.1.3.1 and 3.1.3.2, respectively. Table 3.1.3.1 with a detailed explanation is displayed in Section 3.1.3.3. Examples illustrating possible uses of the table are given in Section 3.1.3.4.

3.1.3.1. *Equitranslational phase transitions and their order parameters*

A basic role is played in symmetry considerations by the relation between the space group $\mathcal{G}$ of the high symmetry *parent* or *prototype* phase, the space group $\mathcal{F}$ of the low-symmetry *ferroic* phase and the order parameter η: The low-symmetry group $\mathcal{F}$ consists of all operations of the high-symmetry group $\mathcal{G}$ that leave the order parameter η invariant. By the term *order parameter* we mean the primary order parameter, *i.e.* that set of degrees of freedom whose coefficient of the quadratic invariant changes sign at the phase-transition temperature (see Sections 3.1.2.2.4 and 3.1.2.4.2).

What matters in these considerations is not the physical nature of η but the transformation properties of η, which are expressed by the representation Γ_η of $\mathcal{G}$. The order parameter η with d_η components can be treated as a vector in a d_η-dimensional carrier space V_η of the representation Γ_η, and the low-symmetry group $\mathcal{F}$ comprises all operations of $\mathcal{G}$ that do not change this vector. If Γ_η is a real one-dimensional representation, then the low-symmetry group $\mathcal{F}$ consists of those operations $g \in \mathcal{G}$ for which the matrices $D^{(\eta)}(g)$ [or characters $\chi_\eta(g)$] of the representation Γ_η equal one, $D^{(\eta)}(g) = \chi_\eta(g) = 1$. This condition is satisfied by one half of all operations of $\mathcal{G}$ (index of $\mathcal{F}$ in $\mathcal{G}$ is two) and thus the real one-dimensional representation Γ_η determines the ferroic group $\mathcal{F}$ unambiguously.

A real multidimensional representation Γ_η can induce several low-symmetry groups. A *general vector* of the carrier space V_η of Γ_η is invariant under all operations of a group Ker Γ_η, called the *kernel of representation* Γ_η, which is a normal subgroup of $\mathcal{G}$ comprising all operations $g \in \mathcal{G}$ for which the matrix $D^{(\eta)}(g)$ is the unit matrix. Besides that, *special vectors* of V_η – specified by relations restricting values of order-parameter components (*e.g.* some components of η equal zero, some components are equal *etc.*) – may be invariant under larger groups than the kernel Ker Γ_η. These groups are called *epikernels* of Γ_η (Ascher & Kobayashi, 1977). The kernel and epikernels of Γ_η represent potential symmetries of the ferroic phases associated with the representation Γ_η. Thermodynamic considerations can decide which of these phases is stable at a given temperature and external fields.

Another fundamental result of the Landau theory is that components of the order parameter of all continuous (second-order) and some discontinuous (first-order) phase transitions transform according to an irreducible representation of the space group $\mathcal{G}$ of the high-symmetry phase (see Sections 3.1.2.4.2 and 3.1.2.3). Since the components of the order parameter are real numbers, this condition requires irreducibility over the field of real numbers (so-called *physical irreducibility* or *R-irreducibility*). This means that the matrices $D^{(\eta)}(g)$ of R-irreducible representations (abbreviated *R-ireps*) can contain only real numbers. (Physically irreducible matrix representations are denoted by $D^{(\alpha)}$ instead of the symbol Γ_α used in general considerations.)

As explained in Section 1.2.3 and illustrated by the example of gadolinium molybdate in Section 3.1.2.5, an irreducible representation $\Gamma_{\mathbf{k},m}$ of a space group is specified by a vector $\mathbf{k}$ of the first Brillouin zone, and by an irreducible representation $\tau_m(\mathbf{k})$ of the little group of $\mathbf{k}$, denoted $G(\mathbf{k})$. It turns out that the vector $\mathbf{k}$ determines the change of the translational symmetry at the phase transition (see *e.g* Tolédano & Tolédano, 1987; Izyumov & Syromiatnikov, 1990; Tolédano & Dmitriev, 1996). Thus, unless one restricts the choice of the vector $\mathbf{k}$, one would have an infinite number of phase transitions with different changes of the translational symmetry.

In this section, we restrict ourselves to representations with zero $\mathbf{k}$ vector (this situation is conveniently denoted as the Γ point). Then there is no change of translational symmetry at the transition. In this case, the group $\mathcal{F}$ is called an *equitranslational* or *translationengleiche* (t) *subgroup of* $\mathcal{G}$, and this change of symmetry will be called an *equitranslational symmetry descent* $\mathcal{G} \Downarrow^t \mathcal{F}$. An *equitranslational phase transition* is a transition with an equitranslational symmetry descent $\mathcal{G} \Downarrow^t \mathcal{F}$.

Any ferroic space-group-symmetry descent $\mathcal{G} \Downarrow \mathcal{F}$ uniquely defines the corresponding symmetry descent $G \Downarrow F$, where G and F are the point groups of the space groups $\mathcal{G}$ and $\mathcal{F}$, respectively. Conversely, the equitranslational subgroup $\mathcal{F}$ of a given space group $\mathcal{G}$ is uniquely determined by the point-group symmetry descent $G \Downarrow F$, where G and F are point groups of space groups $\mathcal{G}$ and $\mathcal{F}$, respectively. In other words, a point-group symmetry descent $G \Downarrow F$ defines the set of all equitranslational space-group symmetry descents $\mathcal{G} \Downarrow^t \mathcal{F}$, where $\mathcal{G}$ runs through all space groups with the point group G. All equitranslational space-group symmetry descents $\mathcal{G} \Downarrow^t \mathcal{F}$ are available in the software *GI★KoBo*-1, where more details about the equitranslational subgroups can also be found.

Irreducible and reducible representations of the parent point group G are related in a similar way to irreducible representations with vector $\mathbf{k} = \mathbf{0}$ for all space groups $\mathcal{G}$ with the point group G by a simple process called *engendering* (Jansen & Boon, 1967). The translation subgroup $\mathbf{T}_G$ of $\mathcal{G}$ is a normal subgroup and the point group G is isomorphic to a factor group $\mathcal{G}/\mathbf{T}_G$. This means that to every element $g \in G$ there correspond all elements $\{g|\mathbf{t} + \mathbf{u}_G(g)\}$ of the space group $\mathcal{G}$ with the same linear constituent g, the same non-primitive translation $\mathbf{u}_G(g)$ and any vector $\mathbf{t}$ of the translation group $\mathbf{T}_G$ (see Section 1.2.3.1). If a representation of the point group G is given by matrices $D(g)$, then the corresponding engendered representation of a space group $\mathcal{G}$ with vector $\mathbf{k} = \mathbf{0}$ assigns the same matrix $D(g)$ to all elements $\{g|\mathbf{t} + \mathbf{u}_G(g)\}$ of $\mathcal{G}$.

From this it further follows that a representation Γ_η of a point group G describes transformation properties of the primary order parameter for all equitranslational phase transitions with point-symmetry descent $G \Downarrow F$. This result is utilized in the presentation of Table 3.1.3.1.

3.1.3.2. *Property tensors at ferroic phase transitions. Tensor parameters*

The primary order parameter expresses the 'difference' between the low-symmetry and high-symmetry structures and can be, in a microscopic description, identified with spontaneous displacements of atoms (frozen in soft mode) or with an increase of order of molecular arrangement. To find a microscopic interpretation of order parameters, it is necessary to perform mode analysis (see *e.g.* Rousseau *et al.*, 1981; Aroyo & Perez-Mato, 1998), which takes into account the microscopic structure of the parent phase.

Physical properties of crystals in a continuum description are described by *physical property tensors* (see Section 1.1.1.2), for short *property tensors* [equivalent expressions are *matter tensors* (Nowick, 1995; Wadhawan, 2000) or *material tensors* (Shuvalov, 1988)]. Property tensors are usually expressed in a Cartesian (rectangular) coordinate system [in Russian textbooks called a *crystallophysical system of coordinates* (Sirotin & Shaskolskaya, 1982; Shuvalov, 1988)] which is related to the *crystallographic coordinate system* (*IT* A, 2002) by convention (see *IEEE Standard on Piezoelectricity*, 1987; Sirotin & Shaskolskaya, 1982; Shuvalov, 1988). In what follows, *Cartesian coordinates* will mean coordinates in the crystallophysical system and tensor components will mean components in this coordinate system.

As explained in Section 1.1.4, the number of independent components of property tensors depends on the point-group symmetry of the crystal: the higher this symmetry is, the smaller this number is. Lowering of point-group symmetry at ferroic phase transitions is, therefore, always accompanied by an increased number of independent components of some property tensors. This effect manifests itself by the appearance of *morphic* (Strukov & Levanyuk, 1998) or *spontaneous tensor components*, which are zero in the parent phase and nonzero in the ferroic phase, and/or by symmetry-breaking increments of nonzero components in the ferroic phase that break relations between these tensor components which hold in the parent phase. Thus, for example, the strain tensor has two independent components $u_{11} = u_{22}, u_{33}$ in a tetragonal phase and four independent components $u_{11} \neq u_{22}, u_{33}, u_{12}$ in a monoclinic phase. In a tetragonal-to-monoclinic phase transition there is one morphic component u_{12} and one relation $u_{11} = u_{22}$ is broken by the *symmetry-breaking increment* $\delta u_{11} = -\delta u_{22}$.

Changes of property tensors at a ferroic phase transition can be described in an alternative manner in which no symmetry-breaking increments but only morphic terms appear. As we have seen, the transformation properties of the primary order parameter η are described by a d_η-dimensional R-irreducible matrix representation $D^{(\eta)}$ of the group G. One can form d_η linear combinations of Cartesian tensor components that transform according to the same representation $D^{(\eta)}$. These linear combinations will be called *components of a principal tensor parameter* of the ferroic phase transition with a symmetry descent $G \Downarrow F$. Equivalent designations are *covariant tensor components* (Kopský, 1979*a*) or *symmetry coordinates* (Nowick, 1995) of representation Γ_η of group G. Unlike the primary order parameter of a ferroic phase transition, a principal tensor parameter is not uniquely defined since one can always form further principal tensor parameters from Cartesian components of higher-rank tensors. However, only the principal tensor parameters formed from components of one, or even several, property tensors up to rank four are physically significant.

A principal tensor parameter introduced in this way has the same basic properties as the primary order parameter: it is zero in the parent phase and nonzero in the ferroic phase, and transforms according to the same R-irep $D^{(\eta)}$. However, these two quantities have different physical nature: the primary order parameter of an equitranslational phase transition is a homogeneous microscopic distortion of the parent phase, whereas the principal tensor parameter describes the macroscopic manifestation of this microscopic distortion. Equitranslational phase transitions thus possess the unique property that their primary order parameter can be represented by principal tensor parameters which can be identified and measured by macroscopic techniques.

If the primary order parameter transforms as a vector, the corresponding principal tensor parameter is a dielectric polarization (*spontaneous polarization*) and the equitranslational phase transition is called a *proper ferroelectric phase transition*. Similarly, if the primary order parameter transforms as components of a symmetric second-rank tensor, the corresponding principal tensor parameter is a *spontaneous strain* (or *spontaneous deformation*) and the equitranslational phase transition is called a *proper ferroelastic phase transition.*

A conspicuous feature of equitranslational phase transitions is a steep anomaly (theoretically an infinite singularity for continuous transitions) of the generalized susceptibility associated with the primary order parameter, especially the dielectric susceptibility near a proper ferroelectric transition (see Section 3.1.2.2.5) and the elastic compliance near a proper ferroelastic transition (see *e.g.* Tolédano & Tolédano, 1987; Tolédano & Dmitriev, 1996; Strukov & Levanyuk, 1998).

Any symmetry property of a ferroic phase transition has its pendant in domain structure. Thus it appears that any two ferroic single domain states differ in the values of the principal tensor parameters, *i.e.* principal tensor parameters ensure tensor distinction of any two ferroic domain states. If, in particular, the principal order parameter is polarization, then any two ferroic domain states differ in the direction of spontaneous polarization. Such a ferroic phase is called a *full ferroelectric phase* (Aizu, 1970). In this case, the number of ferroic domain states equals the number of ferroelectric domain states. Similarly, if any two ferroic domain states exhibit different spontaneous strain, then the ferroic phase is a *full ferroelastic phase*. An equivalent condition is an equal number of ferroic and ferroelastic domain states (see Sections 3.4.2.1 and 3.4.2.2).

The principal tensor parameters do not cover all changes of property tensors at the phase transition. Let $D^{(\lambda)}$ be a d_λ-dimensional matrix R-irep of G with an epikernel (or kernel) L which is an intermediate group between F and G, in other words, L is a supergroup of F and a subgroup of G,

$$F \subset L \subset G. \tag{3.1.3.1}$$

This means that a vector λ of the d_λ-dimensional carrier space V_λ of $D^{(\lambda)}$ is invariant under operations of L. The vector λ specifies a *secondary order parameter* of the transition, *i.e.* λ is a morphic quantity, the appearance of which lowers the symmetry from G to L (for more details on secondary order parameters see Tolédano & Tolédano, 1987; Tolédano & Dmitriev, 1996). Intermediate groups (3.1.3.1) can be conveniently traced in lattices of subgroups displayed in Figs. 3.1.3.1 and 3.1.3.2.

One can form linear combinations of Cartesian tensor components that transform according to $D^{(\lambda)}$. These combinations are components of a *secondary tensor parameter* which represents a macroscopic appearance of the secondary order parameter λ.

If a secondary tensor parameter is a spontaneous polarization and no primary order parameter with this property exists, the phase transition is called an *improper ferroelectric phase transition* (Dvořák, 1974; Levanyuk & Sannikov, 1974). Similarly, an *improper ferroelastic phase transition* is specified by existence of a secondary tensor parameter that transforms as components of the symmetric second-rank tensor (spontaneous strain) and by absence of a primary order parameter with this property. Unlike proper ferroelectric and proper ferroelastic phase transitions, which are confined to equitranslational phase transitions, the improper ferroelectric and improper ferroelastic phase transitions appear most often in non-equitranslational phase transitions. Classic examples are an improper ferroelectric phase transition in gadolinium molybdate (see Section 3.1.2.5.2) and an improper ferroelastic phase transition in strontium titanate (see Section 3.1.5.2.3). Examples of equitranslational improper ferroelectric and ferroelastic symmetry descents can be found in Table 3.1.3.2.

Secondary tensor parameters and corresponding susceptibilities exhibit less pronounced changes near the transition than those associated with the primary order parameter (see *e.g.* Tolédano & Tolédano, 1987; Tolédano & Dmitriev, 1996; Strukov & Levanyuk, 1998).

Table 3.1.3.1. *Point-group symmetry descents associated with irreducible representations*

Property tensors that appear in this table: ε enantiomorphism, chirality; P_i dielectric polarization; u_μ strain; g_μ optical activity; $d_{i\mu}$ piezoelectric tensor; $A_{i\mu}$ electrogyration tensor; $\pi_{\mu\nu}$ piezo-optic tensor ($i = 1, 2, 3$; $\mu, \nu = 1, 2, \ldots, 6$). Applications of this table to symmetry analysis of equitranslational phase transitions and to changes of property tensors at ferroic transitions are explained in Section 3.1.3.3.

(*a*) Triclinic parent groups

R-irep Γ_η	Standard variables	Ferroic symmetry F_1		n_F	Principal tensor parameters	Domain states n_f	n_a	n_e
Parent symmetry *G*: 1 C_1								
No ferroic symmetry descent								
Parent symmetry *G*: $\bar{1}$ C_i								
A_u	x_1^-	1	C_1	1	All components of odd parity tensors	2	1	2

(*b*) Monoclinic parent groups

R-irep Γ_η	Standard variables	Ferroic symmetry F_1		n_F	Principal tensor parameters	Domain states n_f	n_a	n_e
Parent symmetry *G*: 2_z C_{2z}								
B	x_3	1	C_1	1	$P_1, P_2; u_4, u_5$	2	2	2
Parent symmetry *G*: m_z C_{sz}								
A''	x_3	1	C_1	1	$\varepsilon; P_3; u_4, u_5$	2	2	2
Parent symmetry *G*: $2_z/m_z$ C_{2hz}								
B_g	x_3^+	$\bar{1}$	C_i	1	u_4, u_5	2	2	0
A_u	x_1^-	2_z	C_{2z}	1	$\varepsilon; P_3$	2	1	2
B_u	x_3^-	m_z	C_{sz}	1	P_1, P_2	2	1	2

(*c*) Orthorhombic parent groups

R-irep Γ_η	Standard variables	Ferroic symmetry F_1		n_F	Principal tensor parameters	Domain states n_f	n_a	n_e
Parent symmetry *G*: $2_x2_y2_z$ D_2								
B_{1g}	x_2	2_z	C_{2z}	1	$P_3; u_6$	2	2	2
B_{3g}	x_3	2_x	C_{2x}	1	$P_1; u_4$	2	2	2
B_{2g}	x_4	2_y	C_{2y}	1	$P_2; u_5$	2	2	2
Parent symmetry *G*: $m_xm_y2_z$ C_{2vz}								
A_2	x_2	2_z	C_{2z}	1	u_6	2	2	1
B_2	x_3	m_x	C_{sx}	1	$P_2; u_4$	2	2	2
B_1	x_4	m_y	C_{sy}	1	$P_1; u_5$	2	2	2
Parent symmetry *G*: $m_xm_ym_z$ D_{2h}								
B_{1g}	x_2^+	$2_z/m_z$	C_{2hz}	1	u_6	2	2	0
B_{3g}	x_3^+	$2_x/m_x$	C_{2hx}	1	u_4	2	2	0
B_{2g}	x_4^+	$2_y/m_y$	C_{2hy}	1	u_5	2	2	0
A_{1u}	x_1^-	$2_x2_y2_z$	D_2	1	$\varepsilon; g_1, g_2, g_3; d_{14}, d_{25}, d_{36}$	2	1	0
B_{1u}	x_2^-	$m_xm_y2_z$	C_{2vz}	1	P_3	2	1	2
B_{3u}	x_3^-	$2_xm_ym_z$	C_{2vx}	1	P_1	2	1	2
B_{2u}	x_4^-	$m_x2_ym_z$	C_{2vy}	1	P_2	2	1	2

(*d*) Tetragonal parent groups

R-irep Γ_η	Standard variables	Ferroic symmetry F_1		n_F	Principal tensor parameters	Domain states n_f	n_a	n_e
Parent symmetry *G*: 4_z C_{4z}								
B	x_3	2_z	C_{2z}	1	$\delta u_1 = -\delta u_2, u_6$	2	2	1
${}^1E \oplus {}^2E$ (Li)	(x_1, y_1)	1	C_1	1	$(P_1, P_2); (u_4, -u_5)$	4	4	4
Parent symmetry *G*: $\bar{4}_z$ S_{4z}								
B	x_3	2_z	C_{2z}	1	$\varepsilon; P_3; \delta u_1 = -\delta u_2, u_6$	2	2	2
${}^1E \oplus {}^2E$	(x_1, y_1)	1	C_1	1	$(P_1, -P_2); (u_4, -u_5)$	4	4	4
Parent symmetry *G*: $4_z/m_z$ C_{4hz}								
B_g	x_3^+	$2_z/m_z$	C_{2hz}	1	$\delta u_1 = -\delta u_2, u_6$	2	2	0
A_u	x_1^-	4_z	C_{4z}	1	$\varepsilon; P_3$	2	1	2
B_u	x_3^-	$\bar{4}_z$	S_{4z}	1	$g_1 = -g_2, g_6; d_{31} = -d_{32}, d_{36}, d_{14} = d_{25}, d_{15} = -d_{24}$	2	1	0
${}^1E_g \oplus {}^2E_g$	(x_1^+, y_1^+)	$\bar{1}$	C_i	1	$(u_4, -u_5)$	4	4	0
${}^1E_u \oplus {}^2E_u$	(x_1^-, y_1^-)	m_z	C_{sz}	1	(P_1, P_2)	4	2	4

Table 3.1.3.1 (*cont.*)

R-irep Γ_η	Standard variables	Ferroic symmetry F_1		n_F	Principal tensor parameters	Domain states n_f	n_a	n_e
Parent symmetry *G*: $\mathbf{4_z 2_x 2_{xy}}$ $\boldsymbol{D_{4z}}$								
A_2	x_2	4_z	C_{4z}	1	P_3	2	1	2
B_1	x_3	$2_x 2_y 2_z$	D_2	1	$\delta u_1 = -\delta u_2$	2	2	0
B_2	x_4	$2_{x\bar{y}} 2_{xy} 2_z$	$\hat{\boldsymbol{D}}_{2z}$	1	u_6	2	2	0
E	$(x_1, 0)$	2_x	C_{2x}	2	P_1; u_4	4	4	4
	(x_1, x_1)	2_{xy}	C_{2xy}	2	$P_1 = P_2$; $u_4 = -u_5$	4	4	4
(Li)	(x_1, y_1)	1	C_1	1	(P_1, P_2); $(u_4, -u_5)$	8	8	8
Parent symmetry *G*: $\mathbf{4_z m_x m_{xy}}$ $\boldsymbol{C_{4vz}}$								
A_2	x_2	4_z	C_{4z}	1	ε; $g_1 = g_2$, g_3; $d_{14} = -d_{25}$	2	1	1
B_1	x_3	$m_x m_y 2_z$	C_{2vz}	1	$\delta u_1 = -\delta u_2$	2	2	1
B_2	x_4	$m_{x\bar{y}} m_{xy} 2_z$	$\hat{\boldsymbol{C}}_{2vz}$	1	u_6	2	2	1
E	$(x_1, 0)$	m_x	C_{sx}	2	P_2; u_4	4	4	4
	(x_1, x_1)	m_{xy}	C_{sxy}	2	$P_2 = -P_1$; $u_4 = -u_5$	4	4	4
	(x_1, y_1)	1	C_1	1	$(P_2, -P_1)$; $(u_4, -u_5)$	8	8	8
Parent symmetry *G*: $\mathbf{\bar{4}_z 2_x m_{xy}}$ $\boldsymbol{D_{2dz}}$								
A_2	x_2	$\bar{4}_z$	S_{4z}	1	g_6; $d_{31} = -d_{32}$, $d_{15} = -d_{24}$	2	1	0
B_1	x_3	$2_x 2_y 2_z$	D_2	1	ε; $\delta u_1 = -\delta u_2$	2	2	0
B_2	x_4	$m_{x\bar{y}} m_{xy} 2_z$	$\hat{\boldsymbol{C}}_{2vz}$	1	P_3; u_6	2	2	2
E	$(x_1, 0)$	2_x	C_{2x}	2	P_1; u_4	4	4	4
	(x_1, x_1)	m_{xy}	C_{sxy}	2	$P_1 = -P_2$; $u_4 = -u_5$	4	4	4
	(x_1, y_1)	1	C_1	1	$(P_1, -P_2)$; $(u_4, -u_5)$	8	8	8
Parent symmetry *G*: $\mathbf{\bar{4}_z m_x 2_{xy}}$ $\boldsymbol{\hat{D}_{2dz}}$								
A_2	x_2	$\bar{4}_z$	S_{4z}	1	$g_1 = -g_2$; d_{36}, $d_{14} = d_{25}$	2	1	0
B_2	x_3	$m_x m_y 2_z$	C_{2vz}	1	P_3; $\delta u_1 = -\delta u_2$	2	2	2
B_1	x_4	$2_{x\bar{y}} 2_{xy} 2_z$	$\hat{D}_{2z}$	1	ε; u_6	2	2	0
E	$(x_1, 0)$	m_x	C_{sx}	2	P_2; u_4	4	4	4
	(x_1, x_1)	2_{xy}	C_{2xy}	2	$P_2 = P_1$; $u_4 = -u_5$	4	4	4
	(x_1, y_1)	1	C_1	1	(P_2, P_1); $(u_4, -u_5)$	8	8	8
Parent symmetry *G*: $\mathbf{4_z/m_z m_x m_{xy}}$ $\boldsymbol{D_{4hz}}$								
A_{2g}	x_2^+	$4_z/m_z$	C_{4hz}	1	$A_{31} = A_{32}$, A_{33}, $A_{15} = A_{24}$	2	1	0
B_{1g}	x_3^+	$m_x m_y m_z$	D_{2h}	1	$\delta u_1 = -\delta u_2$	2	2	0
B_{2g}	x_4^+	$m_{x\bar{y}} m_{xy} m_z$	$\hat{D}_{2hz}$	1	u_6	2	2	0
A_{1u}	x_1^-	$4_z 2_x 2_{xy}$	D_{4z}	1	ε; $g_1 = g_2$, g_3; $d_{14} = -d_{25}$	2	1	0
A_{2u}	x_2^-	$4_z m_x m_{xy}$	C_{4vz}	1	P_3	2	1	2
B_{1u}	x_3^-	$\bar{4}_z 2_x m_{xy}$	D_{2dz}	1	$g_1 = -g_2$; $d_{14} = d_{25}$, d_{36}	2	1	0
B_{2u}	x_4^-	$\bar{4}_z m_x 2_{xy}$	$\hat{D}_{2dz}$	1	g_6; $d_{31} = -d_{32}$, $d_{15} = -d_{24}$	2	1	0
E_g	$(x_1^+, 0)$	$2_x/m_x$	C_{2hx}	2	u_4	4	4	0
	(x_1^+, x_1^+)	$2_{xy}/m_{xy}$	C_{2hxy}	2	$u_4 = -u_5$	4	4	0
	(x_1^+, y_1^+)	$\bar{1}$	C_i	1	$(u_4, -u_5)$	8	8	0
E_u	$(x_1^-, 0)$	$2_x m_y m_z$	C_{2vx}	2	P_1	4	2	4
	(x_1^-, x_1^-)	$m_{x\bar{y}} 2_{xy} m_z$	C_{2vxy}	2	$P_1 = P_2$	4	2	4
	(x_1^-, y_1^-)	m_z	C_{sz}	1	(P_1, P_2)	8	8	8

(*e*) Trigonal parent groups

R-irep Γ_η	Standard variables	Ferroic symmetry F_1		n_F	Principal tensor parameters	Domain states n_f	n_a	n_e
Parent symmetry *G*: $\mathbf{3_z}$ $\boldsymbol{C_3}$								
E	(x_1, y_1)	1	C_1	1	(P_1, P_2) $(u_1 - u_2, -2u_6)$, $(u_4, -u_5)$	3	3	3
(La, Li)					$\delta u_1 = -\delta u_2$			
Parent symmetry *G*: $\mathbf{\bar{3}_z}$ $\boldsymbol{C_{3i}}$								
A_u	x_1^-	3_z	C_3	1	ε; P_3	2	1	2
E_g (La)	(x_1^+, y_1^+)	$\bar{1}$	C_i	1	$(u_1 - u_2, -2u_6)$, $(u_4, -u_5)$ $\delta u_1 = -\delta u_2$	3	3	0
E_u	(x_1^-, y_1^-)	1	C_1	1	(P_1, P_2)	6	3	6
Parent symmetry *G*: $\mathbf{3_z 2_x}$ $\boldsymbol{D_{3x}}$								
A_2	x_2	3_z	C_3	1	P_3	2	1	2
E	$(x_1, 0)$	2_x	C_{2x}	3	P_1; $\delta u_1 = -\delta u_2$, u_4	3	3	3
(La, Li)	(x_1, y_1)	1	C_1	1	(P_1, P_2); $(u_1 - u_2, -2u_6)$, $(u_4, -u_5)$	6	6	6
Parent symmetry *G*: $\mathbf{3_z m_x}$ $\boldsymbol{C_{3vx}}$								
A_2	x_2	3_z	C_3	1	ε; $g_1 = g_2$, g_3; $d_{11} = -d_{12} = -d_{26}$, $d_{14} = -d_{25}$	2	1	1
E	$(x_1, 0)$	m_x	C_{sx}	3	P_2; $\delta u_1 = -\delta u_2$, u_4	3	3	3
(La)	(x_1, y_1)	1	C_1	1	$(P_2, -P_1)$; $(u_1 - u_2, -2u_6)$, $(u_4, -u_5)$	6	6	6

Table 3.1.3.1 (*cont.*)

R-irep Γ_η	Standard variables	Ferroic symmetry F_1		n_F	Principal tensor parameters	Domain states n_f	n_a	n_e
Parent symmetry *G*: $\bar{3}_z m_x$ D_{3dx}								
A_{2g}	x_2^+	$\bar{3}_z$	C_{3i}	1	$A_{22} = -A_{21} = -A_{16}, A_{31} = A_{32}, A_{33}, A_{15} = A_{24}$	2	1	0
A_{1u}	x_1^-	$3_z 2_x$	D_{3x}	1	ε; $g_1 = g_2, g_3$; $d_{11} = -d_{12} = -d_{26}, d_{14} = -d_{25}$	2	1	0
A_{2u}	x_2^-	$3_z m_x$	C_{3vx}	1	P_3	2	1	2
E_g	$(x_1^+, 0)$	$2_x/m_x$	C_{2hx}	3	$\delta u_1 = -\delta u_2, u_4$	3	3	0
(La)	(x_1^+, y_1^+)	$\bar{1}$	C_i	1	$(u_1 - u_2, -2u_6), (u_4, -u_5)$	6	6	0
E_u	$(0, y_1^-)$	m_x	C_{sx}	3	P_2	6	3	6
	$(x_1^-, 0)$	2_x	C_{2x}	3	P_1	6	3	6
	(x_1^-, y_1^-)	1	C_1	1	(P_1, P_2)	12	6	12
Parent symmetry *G*: $3_z 2_y$ D_{3y}								
A_2	x_2	3_z	C_3	1	P_3	2	1	2
E	$(0, y_1)$	2_y	C_{2y}	3	P_2; $\delta u_1 = -\delta u_2, u_5$	3	3	3
(La, Li)	(x_1, y_1)	1	C_1	1	(P_1, P_2); $(2u_6, u_1 - u_2), (u_4, -u_5)$	6	6	6
Parent symmetry *G*: $3_z m_y$ C_{3vy}								
A_2	x_2	3_z	C_3	1	ε; $g_1 = g_2, g_3$; $d_{22} = -d_{21} = -d_{16}, d_{14} = -d_{25}$	2	1	1
E	$(0, y_1)$	m_y	C_{sy}	3	P_1; $\delta u_1 = -\delta u_2, u_5$	3	3	3
(La)	(x_1, y_1)	1	C_1	1	$(P_2, -P_1)$; $(2u_6, u_1 - u_2), (u_4, -u_5)$	6	6	6
Parent symmetry *G*: $\bar{3}_z m_y$ D_{3dy}								
A_{2g}	x_2^+	$\bar{3}_z$	C_{3i}	1	$A_{11} = -A_{12} = -A_{26}, A_{31} = A_{32}, A_{33}, A_{15} = A_{24}$	2	1	0
A_{1u}	x_1^-	$3_z 2_y$	D_{3y}	1	ε; $g_1 = g_2, g_3$; $d_{22} = -d_{21} = -d_{16}, d_{14} = -d_{25}$	2	1	0
A_{2u}	x_2^-	$3_z m_y$	C_{3vy}	1	P_3	2	1	2
E_g	$(0, y_1^+)$	$2_y/m_y$	C_{2hy}	3	$\delta u_1 = -\delta u_2, u_5$	3	3	0
(La)	(x_1^+, y_1^+)	$\bar{1}$	C_i	1	$(2u_6, u_1 - u_2), (u_4, -u_5)$	6	6	0
E_u	$(0, y_1^-)$	2_y	C_{2y}	3	P_2	6	3	6
	$(x_1^-, 0)$	m_y	C_{sy}	3	P_1	6	3	6
	(x_1^-, y_1^-)	1	C_1	1	(P_1, P_2)	12	6	12

(*f*) Hexagonal parent groups

Covariants with standardized labels and conversion equations:

$$g_1^- = g_1 + g_2; \quad g_{2x}^- = g_1 - g_2, \quad g_{2y}^- = 2g_6$$
$$g_1 = \tfrac{1}{2}(g_1^- + g_{2x}^-), \quad g_2 = \tfrac{1}{2}(g_1^- - g_{2x}^-); \quad \delta g_1 = -\delta g_2 = \tfrac{1}{2} g_{2x}^-$$
$$d_1^- = d_{14} - d_{25}; \quad d_{2x,2}^- = d_{14} + d_{25}, \quad d_{2y,2}^- = d_{24} - d_{15}$$
$$d_{2,1}^- = d_{31} + d_{32}; \quad d_{2x,1}^- = 2d_{36}, \quad d_{2y,1}^- = d_{32} - d_{31}$$
$$d_{14} = \tfrac{1}{2}(d_1^- + d_{2x,2}^-), \quad d_{25} = \tfrac{1}{2}(-d_1^- + d_{2x,2}^-); \quad \delta d_{14} = \delta d_{25} = \tfrac{1}{2} d_{2x}^-$$
$$d_{36} = \tfrac{1}{2} d_{2x,1}^-, \quad d_{31} = \tfrac{1}{2}(d_{2,1}^- - d_{2y,1}^-); \quad d_{32} = \tfrac{1}{2}(d_{2,1}^- + d_{2y,1}^-).$$

R-irep Γ_η	Standard variables	Ferroic symmetry F_1		n_F	Principal tensor parameters	Domain states n_f	n_a	n_e
Parent symmetry *G*: 6_z C_6								
B	x_3	3_z	C_3	1	$d_{11} = -d_{12} = -d_{26}, d_{22} = -d_{21} = -d_{16}$	2	1	1
E_2	(x_2, y_2)	2_z	C_{2z}	1	$(u_1 - u_2, 2u_6)$ $\delta u_1 = -\delta u_2$	3	3	1
(La, Li)								
E_1	(x_1, y_1)	1	C_1	1	(P_1, P_2)	6	6	6
(Li)					$(u_4, -u_5)$			
Parent symmetry *G*: $\bar{6}_z$ C_{3h}								
A''	x_3	3_z	C_3	1	ε; P_3	2	1	2
E'	(x_2, y_2)	m_z	C_{sz}	1	(P_2, P_1)	3	3	3
(La)					$(u_1 - u_2, 2u_6)$ $\delta u_1 = -\delta u_2$			
E''	(x_1, y_1)	1	C_1	1	$(u_4, -u_5)$	6	6	6
Parent symmetry *G*: $6_z/m_z$ C_{6h}								
B_g	x_3^+	$\bar{3}_z$	C_{3i}	1	$A_{11} = -A_{12} = -A_{26}, A_{22} = -A_{21} = -A_{16}$	2	1	0
A_u	x_1^-	6_z	C_6	1	ε; P_3	2	1	2
B_u	x_3^-	$\bar{6}_z$	C_{3h}	1	$d_{11} = -d_{12} = -d_{26}, d_{22} = -d_{21} = -d_{16}$	2	1	0
E_{2g}	(x_2^+, y_2^+)	$2_z/m_z$	C_{2hz}	1	$(u_1 - u_2, 2u_6)$ $\delta u_1 = -\delta u_2$	3	3	0
(La)								
E_{1g}	(x_1^+, y_1^+)	$\bar{1}$	C_i	1	$(u_4, -u_5)$	6	6	0
E_{2u}	(x_2^-, y_2^-)	2_z	C_{2z}	1	$(g_1 - g_2, 2g_6)$ $g_1 = -g_2, g_6$	6	3	2
					$(2d_{36}, d_{32} - d_{31})$ $d_{32} = -d_{31}, d_{36}$			
					$(d_{14} + d_{25}, d_{24} - d_{15})$ $d_{14} = d_{25}, d_{24} = -d_{15}$			
E_{1u}	(x_1^-, y_1^-)	m_z	C_{sz}	1	(P_1, P_2)	6	3	6

Table 3.1.3.1 (*cont.*)

R-irep Γ_η	Standard variables	Ferroic symmetry F_1		n_F	Principal tensor parameters	Domain states n_f	n_a	n_e
Parent symmetry G:		$\mathbf{6_z 2_x 2_y}$	$\boldsymbol{D_6}$					
A_2	x_2	6_z	C_6	1	P_3	2	1	2
B_1	x_3	$3_z 2_x$	D_{3x}	1	$d_{11} = -d_{12} = -d_{26}$	2	1	0
B_2	x_4	$3_z 2_y$	D_{3y}	1	$d_{22} = -d_{21} = -d_{16}$	2	1	0
E_2	$(x_2, 0)$	$2_x 2_y 2_z$	D_2	3	$\delta u_1 = -\delta u_2$	3	3	0
(La, Li)	(x_2, y_2)	2_z	C_{2z}	1	$(u_1 - u_2, 2u_6)$	6	6	2
E_1	$(x_1, 0)$	2_x	C_{2x}	3	P_1; u_4	6	6	6
	$(0, y_1)$	2_y	C_{2y}	3	P_2; u_5	6	6	6
(Li)	(x_1, y_1)	1	C_1	1	(P_1, P_2); $(u_4, -u_5)$	12	12	12
Parent symmetry G:		$\mathbf{6_z m_x m_y}$	$\boldsymbol{C_{6v}}$					
A_2	x_2	6_z	C_6	1	ε; $g_1 = g_2, g_3$; $d_{14} = -d_{25}$	2	1	1
B_2	x_3	$3_z m_x$	C_{3vx}	1	$d_{22} = -d_{21} = -d_{16}$	2	1	1
B_1	x_4	$3_z m_y$	C_{3vy}	1	$d_{11} = -d_{12} = -d_{26}$	2	1	1
E_2	$(x_2, 0)$	$m_x m_y 2_z$	C_{2vz}	3	$\delta u_1 = -\delta u_2$	3	3	1
(La)	(x_2, y_2)	2_z	C_{2z}	1	$(u_1 - u_2, 2u_6)$	6	6	1
E_1	$(x_1, 0)$	m_x	C_{sx}	3	P_2; u_4	6	6	6
	$(0, y_1)$	m_y	C_{sy}	3	P_1; u_5	6	6	6
	(x_1, y_1)	1	C_1	1	$(P_2, -P_1)$; $(u_4, -u_5)$	12	12	12
Parent symmetry G:		$\mathbf{\bar{6}_z 2_x m_y}$	$\boldsymbol{D_{3h}}$					
A_2'	x_2	$\bar{6}_z$	C_{3h}	1	$d_{22} = -d_{21} = -d_{16}$	2	1	0
A_1''	x_3	$3_z 2_x$	D_{3x}	1	ε; $g_1 = g_2, g_3$; $d_{14} = -d_{25}$	2	1	0
A_2''	x_4	$3_z m_y$	C_{3vy}	1	P_3	2	1	2
E'	$(x_2, 0)$	$2_x m_y m_z$	C_{2vx}	3	P_1; $\delta u_1 = -\delta u_2$	3	3	3
(La)	(x_2, y_2)	m_z	C_{sz}	1	$(P_1, -P_2)$; $(u_1 - u_2, 2u_6)$	6	6	6
E''	$(x_1, 0)$	2_x	C_{2x}	3	u_4	6	6	3
	$(0, y_1)$	m_y	C_{sy}	3	u_5	6	6	6
	(x_1, y_1)	1	C_1	1	$(u_4, -u_5)$	12	12	12
Parent symmetry G:		$\mathbf{\bar{6}_z m_x 2_y}$	$\boldsymbol{\hat{D}_{3h}}$					
A_2'	x_2	$\bar{6}_z$	C_{3h}	1	$d_{11} = -d_{12} = -d_{26}$	2	1	0
A_2''	x_3	$3_z m_x$	C_{3vx}	1	P_3	2	1	2
A_1'	x_4	$3_z 2_y$	D_{3y}	1	ε; $g_1 = g_2, g_3$; $d_{14} = -d_{25}$	2	1	0
E'	$(x_2, 0)$	$m_x 2_y m_z$	C_{2vy}	3	P_2; $\delta u_1 = -\delta u_2$	3	3	3
(La)	(x_2, y_2)	m_z	C_{sz}	1	(P_2, P_1); $(u_1 - u_2, 2u_6)$	6	6	6
E''	$(x_1, 0)$	m_x	C_{sx}	3	u_4	6	6	6
	$(0, y_1)$	2_y	C_{2y}	3	u_5	6	6	3
	(x_1, y_1)	1	C_1	1	$(u_4, -u_5)$	12	12	12
Parent symmetry G:		$\mathbf{6_z/m_z m_x m_y}$	$\boldsymbol{D_{6h}}$					
A_{2g}	x_2^+	$6_z/m_z$	C_{6h}	1	$A_{31} = A_{32}, A_{33}, A_{15} = A_{24}$	2	1	0
B_{1g}	x_3^+	$\bar{3}_z m_x$	D_{3dx}	1	$A_{11} = -A_{12} = -A_{26}$	2	1	0
B_{2g}	x_4^+	$\bar{3}_z m_y$	D_{3dy}	1	$A_{22} = -A_{21} = -A_{16}$	2	1	0
A_{1u}	x_1^-	$6_z 2_x 2_y$	D_6	1	ε; $g_1 = g_2, g_3$; $d_{14} = -d_{25}$	2	1	0
A_{2u}	x_2^-	$6_z m_x m_y$	C_{6v}	1	P_3	2	1	2
B_{1u}	x_3^-	$\bar{6}_z 2_x m_y$	D_{3h}	1	$d_{11} = -d_{12} = -d_{26}$	2	1	0
B_{2u}	x_4^-	$\bar{6}_z m_x 2_y$	$\hat{D}_{3h}$	1	$d_{22} = -d_{21} = -d_{16}$	2	1	0
E_{2g}	$(x_2^+, 0)$	$m_x m_y m_z$	D_{2h}	3	$\delta u_1 = -\delta u_2$	3	3	0
(La)	(x_2^+, y_2^+)	$2_z/m_z$	C_{2hz}	1	$(u_1 - u_2, 2u_6)$	6	6	0
E_{1g}	$(x_1^+, 0)$	$2_x/m_x$	C_{2hx}	3	u_4	6	6	0
	$(0, y_1^+)$	$2_y/m_y$	C_{2hy}	3	u_5	6	6	0
	(x_1^+, y_1^+)	$\bar{1}$	C_i	1	$(u_4, -u_5)$	12	12	0
E_{1u}	$(x_1^-, 0)$	$2_x m_y m_z$	C_{2vx}	3	P_1	6	3	6
	$(0, y_1^-)$	$m_x 2_y m_z$	C_{2vy}	3	P_2	6	3	6
	(x_1^-, y_1^-)	m_z	C_{sz}	1	(P_1, P_2)	12	6	12
E_{2u}	$(x_2^-, 0)$	$2_x 2_y 2_z$	D_2	3	$\delta g_1 = -\delta g_2$; d_{36}, $\delta d_{14} = \delta d_{25}$	6	3	0
	$(0, y_2^-)$	$m_x m_y 2_z$	C_{2vz}	3	g_6: $d_{32} = -d_{31}$, $d_{24} = -d_{15}$	6	3	2
	(x_2^-, y_2^-)	2_z	C_{2z}	1	$(g_1 - g_2, 2g_6)$; $(2d_{36}, d_{32} - d_{31})$, $(d_{14} + d_{25}, d_{24} - d_{15})$	12	6	2

In tensor distinction of domains, the secondary tensor parameters play a secondary role in a sense that some but not all ferroic domain states exhibit different values of the secondary tensor parameters. This property forms a basis for the concept of partial ferroic phases (Aizu, 1970): A ferroic phase is a *partial ferroelectric (ferroelastic)* one if some but not all domain states differ in spontaneous polarization (spontaneous strain). A non-ferroelectric phase denotes a ferroic phase which is either non-polar or which possesses a unique polar direction available already in the parent phase. A non-ferroelastic phase exhibits no spontaneous strain.

3.1.3.3. *Tables of equitranslational phase transitions associated with irreducible representations*

The first systematic symmetry analysis of Landau-type phase transitions was performed by Indenbom (1960), who found all equitranslational phase transitions that can be accomplished

Table 3.1.3.1 (*cont.*)

(*g*) Cubic parent groups

Covariants with standardized labels and conversion equations:

$$u_{3x} = u_{3x}^{+} = u_3 - a(u_1 + u_2); \quad u_{3y} = u_{3y}^{+} = b(u_1 - u_2)$$
$$\delta u_1 = -\tfrac{1}{3}u_{3x}^{+} + \tfrac{1}{\sqrt{3}}u_{3y}^{+}; \quad \delta u_2 = -\tfrac{1}{3}u_{3x}^{+} - \tfrac{1}{\sqrt{3}}u_{3y}^{+}; \quad \delta u_3 = \tfrac{2}{3}u_{3x}^{+}$$
$$g_1^{-} = g_1 + g_2 + g_3; \quad g_{3x}^{-} = g_3 - a(g_1 + g_2); \quad g_{3y}^{-} = b(g_1 - g_2)$$
$$g_1 = \tfrac{1}{3}g_1^{-} - \tfrac{1}{3}g_{3x}^{-} + \tfrac{1}{\sqrt{3}}g_{3y}^{-}; \quad g_2 = \tfrac{1}{3}g_1^{-} - \tfrac{1}{3}g_{3x}^{-} - \tfrac{1}{\sqrt{3}}g_{3y}^{-}; \quad g_3 = \tfrac{1}{3}g_1^{-} + \tfrac{2}{3}g_{3x}^{-}$$
$$d_1^{-} = d_{14} + d_{25} + d_{36}; \quad d_{3x}^{-} = b(d_{14} - d_{25}), \quad d_{3y}^{-} = a(d_{14} + d_{25}) - d_{36}$$
$$d_{14} = \tfrac{1}{3}d_1^{-} + \tfrac{1}{\sqrt{3}}d_{3x}^{-} + \tfrac{1}{3}d_{3y}^{-}; \quad d_{25} = \tfrac{1}{3}d_1^{-} - \tfrac{1}{\sqrt{3}}d_{3x}^{-} + \tfrac{1}{3}d_{3y}^{-}; \quad d_{36} = \tfrac{1}{3}d_1^{-} - \tfrac{2}{3}d_{3y}^{-}$$
$$d_{1x} = d_{13} - d_{12}; \quad d_{1y} = d_{21} - d_{23}; \quad d_{1z} = d_{32} - d_{31}$$
$$d_{2x} = d_{13} + d_{12}; \quad d_{2y} = d_{21} + d_{23}; \quad d_{2z} = d_{32} + d_{31}$$
$$d_{13} = \tfrac{1}{2}(d_{1x} + d_{2x}); \quad d_{21} = \tfrac{1}{2}(d_{1y} + d_{2y}); \quad d_{32} = \tfrac{1}{2}(d_{1z} + d_{2z})$$
$$d_{12} = \tfrac{1}{2}(d_{2x} - d_{1x}); \quad d_{23} = \tfrac{1}{2}(d_{2y} - d_{1y}); \quad d_{31} = \tfrac{1}{2}(d_{2z} - d_{1z})$$

$a = \frac{1}{2}$, $b = \frac{\sqrt{3}}{2}$, $\pi^{a}_{\mu\nu} = (\pi_{\mu\nu} - \pi_{\nu\mu})$, $\mu = 1, 2, \ldots, 6$, $\nu = 1, 2, \ldots, 6$.

R-irep Γ_η	Standard variables	Ferroic symmetry F_1		n_F	Principal tensor parameters	Domain states n_f	n_a	n_e
Parent symmetry *G*: 23 *T*								
E (La)	(x_3, y_3)	$2_x2_y2_z$	D_2	1	$[u_3 - a(u_1+u_2), b(u_1-u_2)]$ $\delta u_1 + \delta u_2 + \delta u_3 = 0$	3	3	0
T	$(0, 0, z_1)$	2_z	C_{2z}	3	P_3; u_6	6	6	6
	(x_1, x_1, x_1)	3_p	C_{3p}	4	$P_1 = P_2 = P_3$; $u_4 = u_5 = u_6$	4	4	4
(La, Li)	(x_1, y_1, z_1)	1	C_1	1	(P_1, P_2, P_3); (u_4, u_5, u_6)	12	12	12
Parent symmetry *G*: $m\bar{3}$ T_h								
A_u	x_1^{-}	23	T	1	ε; $g_1 = g_2 = g_3$; $d_{14} = d_{25} = d_{36}$	2	1	0
E_g (La)	(x_3^{+}, y_3^{+})	$m_xm_ym_z$	D_{2h}	1	$[u_3 - a(u_1+u_2), b(u_1-u_2)]$ $\delta u_1 + \delta u_2 + \delta u_3 = 0$	3	3	0
E_u	(x_3^{-}, y_3^{-})	$2_x2_y2_z$	D_2	1	$[g_3 - a(g_1+g_2), b(g_1-g_2)]$ $\delta g_1 + \delta g_2 + \delta g_3 = 0$ $[b(d_{14}-d_{25}), a(d_{14}+d_{25}) - d_{36}]$ $\delta d_{14} + \delta d_{25} + \delta d_{36} = 0$	6	3	0
T_g	$(0, 0, z_1^{+})$	$2_z/m_z$	C_{2hz}	3	u_6	6	6	0
	$(x_1^{+}, x_1^{+}, x_1^{+})$	$\bar{3}_p$	C_{3ip}	4	$u_4 = u_5 = u_6$	4	4	0
(La)	$(x_1^{+}, y_1^{+}, z_1^{+})$	$\bar{1}$	C_i	1	(u_4, u_5, u_6)	12	12	0
T_u	$(0, 0, z_1^{-})$	$m_xm_y2_z$	C_{2vz}	3	P_3	6	3	6
	$(x_1^{-}, x_1^{-}, x_1^{-})$	3_p	C_{3p}	4	$P_1 = P_2 = P_3$	8	4	8
	$(x_1^{-}, y_1^{-}, z_1^{-})$	1	C_1	1	(P_1, P_2, P_3)	24	12	24
Parent symmetry *G*: 432 *O*								
A_2	x_2	23	T	1	$d_{14} = d_{25} = d_{36}$	2	1	0
E	$(x_3, 0)$	$4_z2_x2_{xy}$	D_{4z}	3	$\delta u_1 = \delta u_2 = -\frac{1}{2}\delta u_3$	3	3	0
(La)	(x_3, y_3)	$2_x2_y2_z$	D_2	1	$[u_3 - a(u_1+u_2), b(u_1-u_2)]$ $\delta u_1 + \delta u_2 + \delta u_3 = 0$	6	6	0
T_1	$(0, 0, z_1)$	4_z	C_{4z}	3	P_3	6	3	6
	$(x_1, x_1, 0)$	2_{xy}	C_{2xy}	6	$P_1 = P_2$	12	12	12
	(x_1, x_1, x_1)	3_p	C_{3p}	4	$P_1 = P_2 = P_3$	8	4	8
(Li)	(x_1, y_1, z_1)	1	C_1	1	(P_1, P_2, P_3)	24	24	24
T_2	$(0, 0, z_2)$	$2_{x\bar{y}}2_{xy}2_z$	$\hat{D}_{2z}$	3	u_6	6	6	0
	$(x_2, -x_2, z_2)$	2_{xy}	C_{2xy}	6	$u_4 = -u_5$, u_6	12	12	12
	(x_2, x_2, x_2)	$3_p2_{x\bar{y}}$	D_{3p}	4	$u_4 = u_5 = u_6$	4	4	0
(La, Li)	(x_2, y_2, z_2)	1	C_1	1	(u_4, u_5, u_6)	24	24	24

continuously. A table of all crystallographic point groups G along with all their physically irreducible representations, corresponding ferroic point groups F and related data has been compiled by Janovec *et al.* (1975). These data are presented in an improved form in Table 3.1.3.1 together with corresponding principal tensor parameters and numbers of ferroic, ferroelectric and ferroelastic domain states. This table facilitates solving of the following typical problems:

(1) *Inverse Landau problem* (Ascher & Kobayashi, 1977) of equitranslational phase transitions: For a given equitranslational symmetry descent $\mathcal{G} \Downarrow^{t} \mathcal{F}$ (determined for example from diffraction experiments), find the representation Γ_η of $\mathcal{G}$ that specifies the transformation properties of the primary order parameter. Solution: In Table 3.1.3.1, one finds a physically irreducible representation Γ_η of the point group G of $\mathcal{G}$ with epikernel F (point group of $\mathcal{F}$). For some symmetry descents from cubic point groups $G = 432$, $\bar{4}3m$ and $m\bar{3}m$, the inverse Landau problem has two solutions, which are given in Table 3.1.3.2.

If for a given symmetry descent $\mathcal{G} \Downarrow^{t} \mathcal{F}$ no appropriate *R*-irep exists in Table 3.1.3.1, then the primary order parameter η transforms according to a reducible representation of G. These transitions are always discontinuous and can be accomplished with several reducible representations. Some symmetry descents can be associated with an irreducible representation and with several reducible representations. All these transitions are treated in the software *GI★KoBo*-1 and in Kopský (2001). All point-group symmetry descents are listed in Table 3.4.2.7 and can be traced in lattices of subgroups (see Figs. 3.1.3.1 and 3.1.3.2).

Table 3.1.3.1 (*cont.*)

R-irep Γ_η	Standard variables	Ferroic symmetry F_1		n_F	Principal tensor parameters	Domain states n_f	n_a	n_e
Parent symmetry *G*: $\bar{4}3m$ T_d								
A_2	x_2	23	T	1	ε; $g_1 = g_2 = g_3$ $A_{14} = A_{25} = A_{36}$; $\pi^a_{23} = \pi^a_{31} = \pi^a_{12}$	2	1	0
E	$(x_3, 0)$	$\bar{4}_z 2_x m_{xy}$	D_{2dz}	3	$\delta u_1 = \delta u_2 = -\frac{1}{2}\delta u_3$	3	3	0
(La)	(x_3, y_3)	$2_x 2_y 2_z$	D_2	1	$[u_3 - a(u_1 + u_2), b(u_1 - u_2)]$ $\delta u_1 + \delta u_2 + \delta u_3 = 0$	6	6	0
T_1	$(0, 0, z_1)$	$\bar{4}_z$	S_{4z}	3	g_6; $d_{32} = -d_{31}$, $d_{24} = -d_{15}$	6	3	0
	$(x_1, x_1, 0)$	m_{xy}	C_{sxy}	6	$g_4 = g_5$ $d_{13} = -d_{23}$, $d_{12} = -d_{21}$ $d_{35} = -d_{34}$, $d_{26} = -d_{16}$	12	12	12
	(x_1, x_1, x_1)	3_p	C_{3p}	4	$g_4 = g_5 = g_6$ $d_{13} = d_{21} = d_{32}$, $d_{12} = d_{23} = d_{31}$ $d_{35} = d_{16} = d_{24}$, $d_{26} = d_{34} = d_{15}$	8	4	4
	(x_1, y_1, z_1)	1	C_1	1	(g_4, g_5, g_6) $(d_{13} - d_{12}, d_{21} - d_{23}, d_{32} - d_{31})$ $(d_{35} - d_{26}, d_{16} - d_{34}, d_{24} - d_{15})$	24	24	24
T_2	$(0, 0, z_2)$	$m_{x\bar{y}} m_{xy} 2_z$	$\hat{C}_{2vz}$	3	P_3; u_6	6	6	6
	$(x_2, -x_2, z_2)$	m_{xy}	C_{sxy}	6	$P_1 = -P_2$, P_3; $u_4 = -u_5$, u_6	12	12	12
	(x_2, x_2, x_2)	$3_p m_{x\bar{y}}$	C_{3vp}	4	$P_1 = P_2 = P_3$; $u_4 = u_5 = u_6$	4	4	4
(La)	(x_2, y_2, z_2)	1	C_1	1	(P_1, P_2, P_3); (u_4, u_5, u_6)	24	24	24
Parent symmetry *G*: $m\bar{3}m$ O_h								
A_{2g}	x_2^+	$m\bar{3}$	T_h	1	$A_{14} = A_{25} = A_{36}$; $\pi^a_{23} = \pi^a_{31} = \pi^a_{12}$	2	1	0
A_{1u}	x_1^-	432	O	1	ε; $g_1 = g_2 = g_3$;	2	1	0
A_{2u}	x_2^-	$\bar{4}3m$	T_d	1	$d_{14} = d_{25} = d_{36}$	2	1	0
E_g	$(x_3^+, 0)$	$4_z / m_z m_x m_{xy}$	D_{4hz}	3	δu_3	3	3	0
(La)	(x_3^+, y_3^+)	$m_x m_y m_z$	D_{2h}	1	$[\delta u_3 - a(\delta u_1 + \delta u_2), b(\delta u_1 - \delta u_2)]$	6	6	0
E_u	$(x_3^-, 0)$	$4_z 2_x 2_{xy}$	D_{4z}	3	$g_1 = g_2, g_3$; $d_{14} = -d_{25}$	12	3	0
	$(0, y_3^-)$	$\bar{4}_z 2_x m_{xy}$	D_{2dz}	3	$g_1 = -g_2$; $d_{14} = d_{25} = d_{36}$	6	3	0
	(x_3^-, y_3^-)	$2_x 2_y 2_z$	D_2	1	$[g_3 - a(g_1 + g_2), b(g_1 - g_2)]$ $[b(d_{14} - d_{25}), a(d_{14} + d_{25}) - d_{36}]$	12	6	0
T_{1g}	$(0, 0, z_1^+)$	$4_z / m_z$	C_{4hz}	3	$A_{33}, A_{32} = A_{31}, A_{24} = A_{15}, A_{14} = -A_{25}$	6	3	0
	$(x_1^+, x_1^+, 0)$	$2_{xy} / m_{xy}$	C_{2hxy}	6	$A_{11} = A_{22}$, $A_{13} = A_{23}$, $A_{12} = A_{21}$ $A_{35} = A_{34}$, $A_{26} = A_{16}$	12	12	0
	(x_1^+, x_1^+, x_1^+)	$\bar{3}_p$	C_{3ip}	4	$A_{11} = A_{22} = A_{33}$ $A_{13} = A_{21} = A_{32}$, $A_{12} = A_{32} = A_{31}$ $A_{35} = A_{16} = A_{24}$, $A_{26} = A_{34} = A_{15}$	8	4	0
	(x_1^+, y_1^+, z_1^+)	$\bar{1}$	C_i	1	(A_{11}, A_{22}, A_{33}) $(A_{13} + A_{12}, A_{21} + A_{23}, A_{32} + A_{31})$ $(A_{35} + A_{26}, A_{16} + A_{34}, A_{24} + A_{15})$	24	24	0
T_{2g}	$(0, 0, z_2^+)$	$m_{x\bar{y}} m_{xy} m_z$	$\hat{D}_{2hz}$	3	u_6	6	6	0
	$(x_2^+, -x_2^+, z_2^+)$	$2_{xy} / m_{xy}$	C_{2hxy}	6	$u_4 = -u_5$, u_6	24	12	12
	(x_2^+, x_2^+, x_2^+)	$\bar{3}_p m_{x\bar{y}}$	D_{3dp}	4	$u_4 = u_5 = u_6$	4	4	0
(La)	(x_2^+, y_2^+, z_2^+)	$\bar{1}$	C_i	1	(u_4, u_5, u_6)	24	24	0
T_{1u}	$(0, 0, z_1^-)$	$4_z m_x m_{xy}$	C_{4vz}	3	P_3	6	3	6
	$(x_1^-, y_1^-, 0)$	m_z	C_{sz}	3	P_1,P_2	24	12	24
	$(x_1^-, x_1^-, 0)$	$m_{x\bar{y}} 2_{xy} m_z$	$\hat{C}_{2vxy}$	6	$P_1 = P_2$	12	6	12
	$(x_1^-, -x_1^-, z_1^-)$	m_{xy}	C_{sxy}	6	$P_1 = -P_2$, P_3	24	12	24
	(x_1^-, x_1^-, x_1^-)	$3_p m_{x\bar{y}}$	C_{3vp}	4	$P_1 = P_2 = P_3$	8	4	8
	(x_1^-, y_1^-, z_1^-)	1	C_1	1	(P_1, P_2, P_3)	48	24	48
T_{2u}	$(0, 0, z_2^-)$	$\bar{4}_z m_x 2_{xy}$	$\hat{D}_{2dz}$	3	g_6; $d_{32} = -d_{31}$, $d_{24} = -d_{15}$	6	3	0
	$(x_2^-, y_2^-, 0)$	m_z	C_{sz}	3	g_4, g_5; $d_{13}, d_{12}, d_{21}, d_{23}$ $d_{35}, d_{26}, d_{16}, d_{34}$	24	12	24
	$(x_2^-, -x_2^-, 0)$	$m_{x\bar{y}} 2_{xy} m_z$	$\hat{C}_{2vxy}$	6	$g_4 = -g_5$; $d_{13} = d_{23}$, $d_{21} = d_{21}$ $d_{35} = d_{34}$, $d_{16} = d_{26}$	12	6	12
	$(x_2^-, -x_2^-, z_2^-)$	2_{xy}	C_{2xy}	6	$g_4 = -g_5$, g_6; $d_{13} = d_{23}$, $d_{21} = d_{21}$ $d_{35} = d_{34}$, $d_{16} = d_{26}$ $d_{32} = -d_{31}$, $d_{24} = -d_{15}$	24	12	12
	(x_2^-, x_2^-, x_2^-)	$3_p 2_{x\bar{y}}$	D_{3p}	4	$g_4 = g_5 = g_6$; $d_{13} = -d_{12} = d_{21} = -d_{23} = d_{32} - d_{31}$ $d_{35} = -d_{26} = d_{16} = -d_{34} = d_{24} = -d_{15}$	8	4	0
	(x_2^-, y_2^-, z_2^-)	1	C_1	1	(g_4, g_5, g_6) $(d_{13} - d_{12}, d_{21} - d_{23}, d_{32} - d_{31})$ $(d_{35} - d_{26}, d_{16} - d_{34}, d_{24} - d_{15})$	48	24	48

The solution of the inverse Landau problem – *i.e.* the identification of the representation Γ_η relevant to symmetry descent $G \Downarrow F$ – enables one to determine the corresponding nomal mode (so-called soft mode) of the transition (see *e.g.* Rousseau *et al.*, 1981). We note that this step requires additional knowledge of the crystal structure, whereas other conclusions of the analysis hold for *any* crystal structure with a given symmetry descent $G \Downarrow F$. Normal-mode determination reveals the dynamic microscopic nature of the instability of the crystal lattice which leads to the phase transition (for more details and examples, see Section 3.1.5).

The representation Γ_η further determines the principal tensor parameters associated with the primary order parameter η. If one of them is a vector (polarization) the soft mode is infrared-active in the parent phase; if it is a symmetric second-rank tensor (spontaneous strain), the soft mode is Raman active in this phase. Furthermore, the *R*-irep Γ_η determines the polynomial in components of η in the Landau free energy (basic invariant polynomials, called *integrity bases*, are available in the software *GI⋆KoBo*-1 and in Kopský, 2001) and allows one to decide whether the necessary conditions of continuity of the transition (so-called Landau and Lifshitz conditions) are fulfilled.

(2) *Direct Landau problem of equitranslational phase transitions*: For a given space group $\mathcal{G}$ of the parent phase and the *R*-irep Γ_η (specifying the transformation properties of the primary order parameter η), find the corresponding equitranslational space group $\mathcal{F}$ of the ferroic phase. To solve this task, one first finds in Table 3.1.3.1 the point group F that corresponds to point group G of space group $\mathcal{G}$ and to the given *R*-irep Γ_η. The point-group symmetry descent $G \Downarrow F$ thus obtained specifies uniquely the equitranslational subgroup $\mathcal{F}$ of $\mathcal{G}$ that can be found in the lattices of equitranslational subgroups of space groups available in the software *GI⋆KoBo*-1 (see Section 3.1.6).

(3) *Secondary tensor parameters of an equitranslational phase transition* $\mathcal{G} \Downarrow^t \mathcal{F}$. These parameters are specified by the representation Γ_λ of G associated with a symmetry descent $\Gamma \Downarrow L$, where L is an intermediate group [see equation (3.1.3.1)]. In other words, the secondary tensor parameters of the transition $G \Downarrow F$ are identical with principal tensor parameters of the transition $G \Downarrow L$. To each intermediate group L there corresponds a set of secondary tensor parameters. All intermediate subgroups of a symmetry descent $G \Downarrow F$ can be deduced from lattices of subgroups in Figs. 3.1.3.1 and 3.1.3.2.

The representation Γ_λ specifies transformation properties of the secondary tensor parameter λ and thus determines *e.g* its infrared and Raman activity in the parent phase and enables one to make a mode analysis. Representation Γ_λ together with Γ_η determine the coupling between secondary and primary tensor parameters. The explicit form of these faint interactions (Aizu, 1973; Kopský, 1979*d*) can be found in the software *GI⋆KoBo*-1 and in Kopský (2001).

(4) *Changes of property tensors at a ferroic phase transition.* These changes are described by tensor parameters that depend only on the point-group-symmetry descent $G \Downarrow F$. This means that *the same principal tensor parameters and secondary tensor parameters appear in all equitranslational and in all non-equitranslational transitions with the same* $G \Downarrow F$. The only difference is that in non-equitranslational ferroic phase transitions a principal tensor parameter corresponds to a secondary ferroic order parameter. It still plays a leading role in tensor distinction of domains, since it exhibits different values in any two ferroic domain states (see Section 3.4.2.3). Changes of property tensors at ferroic phase transitions are treated in detail in the software *GI⋆KoBo*-1 and in Kopský (2001).

We note that Table 3.1.3.1 covers only those point-group symmetry descents $G \Downarrow F$ that are 'driven' by *R*-ireps of *G*. All possible point-group symmetry descents $G \Downarrow F$ are listed in Table 3.4.2.7. Principal and secondary tensor parameters of symmetry descents associated with reducible representations are combinations of tensor parameters appearing in Table 3.1.3.1 (for a detailed explanation, see the manual of the software *GI⋆KoBo*-1 and Kopský, 2000). Necessary data for treating these cases are available in the software *GI⋆KoBo*-1 and Kopský (2001).

3.1.3.3.1. *Explanation of Table 3.1.3.1*

Parent symmetry G: the short international (Hermann–Mauguin) and the Schoenflies symbol of the point group G of the parent phase are given. Subscripts specify the orientation of symmetry elements (generators) in the Cartesian crystallophysical coordinate system of the group G (see Figs. 3.4.2.3 and 3.4.2.4, and Tables 3.4.2.5 and 3.4.2.6).

R-irep Γ_η: physically irreducible representation Γ_η of the group G in the spectroscopic notation. This representation defines transformation properties of the primary order parameter η and of the principal tensor parameters. Each complex irreducible representation is combined with its complex conjugate and thus a real physically irreducible representation *R*-irep is formed. Matrices $D^{(\alpha)}$ of *R*-ireps are given explicitly in the the software *GI⋆KoBo*-1.

Table 3.1.3.2. *Symmetry descents* $G \Downarrow F_1$ *associated with two irreducible representations*

			Proper or improper		Domain states			Full or partial	
G	Γ_η	F_1	Ferroelectric	Ferroelastic	n_f	n_e	n_a	Ferroelectric	Ferroelastic
432	T_1 T_2	2_{xy}	proper improper	improper proper	12	12	12	full	full
	T_1 T_2	1	improper proper	improper proper	24	24	24	full	full
$\bar{4}3m$	T_1 T_2	m_{xy}	improper proper	improper proper	12	12	12	full	full
	T_1 T_2	1	improper proper	improper proper	24	24	24	full	full
$m\bar{3}m$	T_{1g} T_{2g}	$2_{xy}/m_{xy}$	non non	improper proper	12	0	12	non	full
	T_{1g} T_{2g}	$\bar{1}$	non non	improper proper	24	0	24	non	full
	T_{1u} T_{2u}	$m_{x\bar{y}}2_{xy}m_z$	proper improper	improper improper	12	12	6	full	partial
	T_{1u} T_{2u}	m_z	proper improper	improper improper	24	24	12	full	partial
	T_{1u} T_{2u}	1	proper improper	improper improper	48	48	24	full	partial

(La) below the symbol of the irreducible representation Γ_η indicates that the *Landau condition* is violated, hence the transition cannot be continuous (second order). The Landau condition requires the absence of the third-degree invariant polynomial of the order-parameter components (the symmetrized triple product $[\Gamma_\eta]^3$ must not contain the identity representation of G). For more details see Lyubarskii (1960), Kociński (1983, 1990), Tolédano & Tolédano (1987), Izyumov & Syromiatnikov (1990) and Tolédano & Dmitriev (1996).

(Li) below the symbol of the irreducible representation Γ_η means that the *Lifshitz condition* is violated, hence the transition to a homogeneous ferroic phase is not continuous. The Lifshitz condition demands the absence of invariant terms that couple bilinearly the order-parameter components with their spatial derivatives that are not exact differentials (the antisymmetric square $\{\Gamma_\eta\}^2$ has no representation in common with the vector representation of G). For more details see Lyubarskii (1960), Kociński (1983, 1990), Tolédano & Tolédano (1987), Izyumov & Syromiatnikov (1990) and Tolédano & Dmitriev (1996).

If there is no symbol (La) and/or (Li) below the symbol of the R-irep Γ_η (*i.e.* if both Landau and Lifshitz conditions are fulfilled), then the R-irep is called an *active representation*. In the opposite case, the R-irep is a *passive representation* (Lyubarskii, 1960; Kociński, 1983, 1990).

Standard variables: components of the order parameter in the carrier space of the irreducible representation Γ_η expressed in so-called *standard variables* (see the manual of the software *GI⋆KoBo*-1). Upper and lower indices and the typeface of standard variables allow one to identify to which irreducible representation Γ_η they belong. Standard variables of one-dimensional representations are denoted by x (Sans Serif typeface), two- or three-dimensional R-ireps by x, y or x, y, z, respectively. Upper indices $^+$ and $^-$ correspond to the lower indices g (*gerade*) and u (*ungerade*) of spectroscopic notation, respectively. The lower index specifies to which irreducible representation the variable belongs.

For multidimensional representations, a general vector of the carrier space V_η is given in the last row; this vector is invariant under the kernel of Γ_η that appears as a low-symmetry group in column F_1. The other rows contain special vectors defined by equal or zero values of some standard variables; these vectors are invariant under epikernels of Γ_η given in column F_1.

F_1: short international (Hermann–Mauguin) and Schoenflies symbol of the point group F_1 which describes the symmetry of the first single domain state of the ferroic (low-symmetry) phase. The subscripts define the orientation of symmetry elements (generators) of F_1 in the Cartesian crystallophysical coordinate system of the group G (see Figs. 3.4.2.3 and 3.4.2.4, and Tables 3.4.2.5 and 3.4.2.6). This specifies the orientation of the group F_1, which is a prerequisite for domain structure analysis (see Chapter 3.4).

n_F: number of subgroups conjugate to F_1 under G. If $n_F = 1$, the group F_1 is a normal subgroup of G (see Section 3.2.3).

Principal tensor parameters: covariant tensor components, *i.e.* linear combinations of Cartesian tensor components that transform according to the same matrix R-irep $D^{(\eta)}$ as the primary order parameter η. Principal tensor parameters are given in this form in the software *GI⋆KoBo*-1 and in Kopský (2001).

This presentation is in certain situations not practical, since property tensors are usually described by numerical values of their Cartesian components. Then it is important to know morphic Cartesian tensor components and symmetry-breaking increments of nonzero Cartesian components that appear spontaneously in the ferroic phase. The bridge between these two presentations is

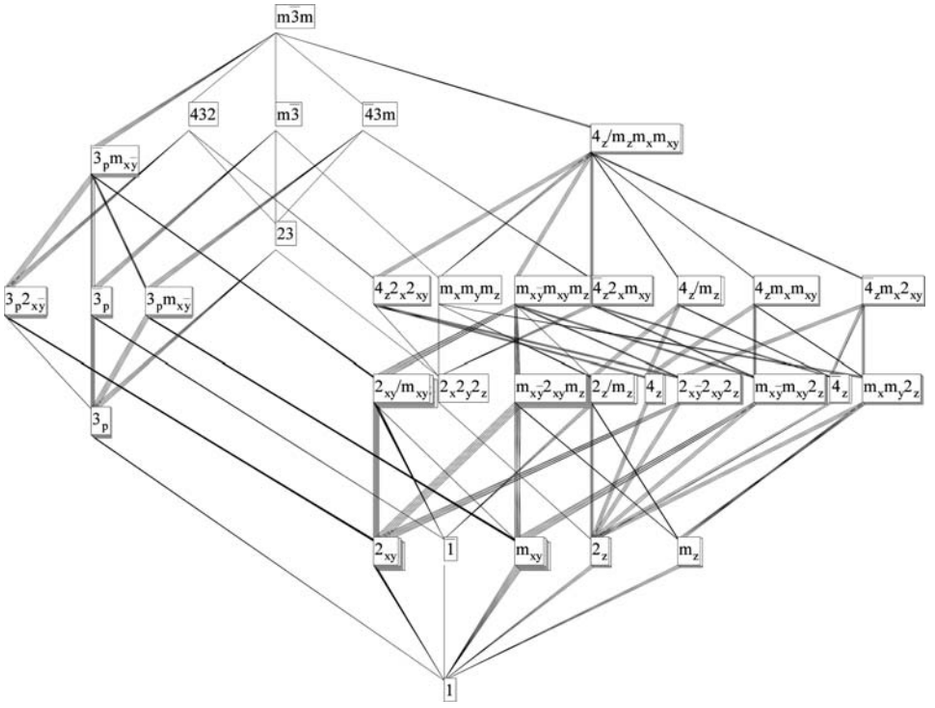

Fig. 3.1.3.1. Lattice of subgroups of the group $m\bar{3}m$. Conjugate subgroups are depicted as a pile of cards. In the software *GI⋆KoBo*-1, one can pull out individual conjugate subgroups by clicking on the pile. All conjugate subgroups are given explicitly in Table 3.4.2.7.

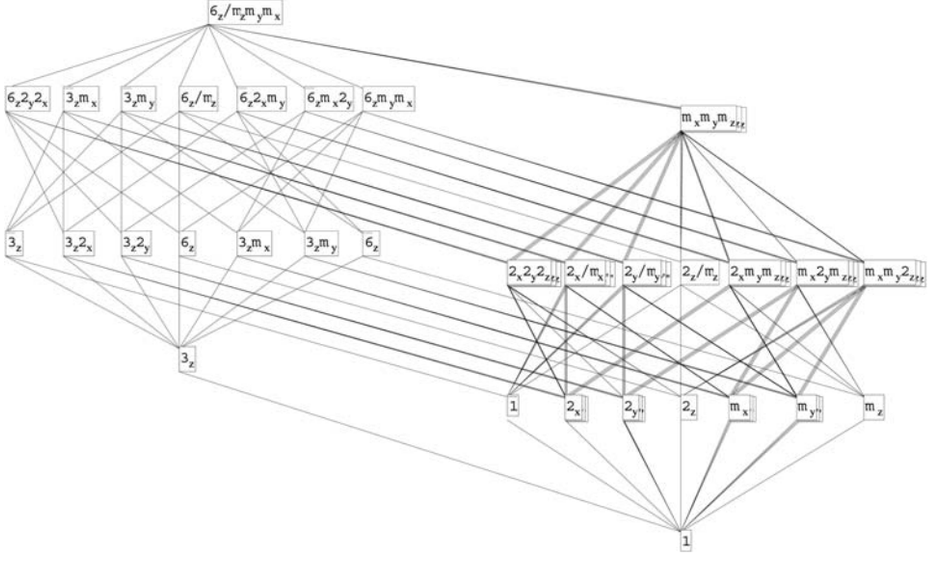

Fig. 3.1.3.2. Lattice of subgroups of the group $6/mmm$. Conjugate subgroups are depicted as a pile of cards. In the software *GI⋆KoBo*-1, one can pull out individual conjugate subgroups by clicking on the pile. All conjugate subgroups are given explicitly in Table 3.4.2.7.

provided by the *conversion equations* that express Cartesian tensor components as linear combinations of principal and secondary covariant components (for more details on tensorial covariants and conversion equations see Appendix E of the manual for *GI★KoBo*-1 and Kopský, 2001).

We illustrate the situation on a transition with symmetry descent $4_z2_x2_{xy} \Downarrow 2_x2_y2_z$. In Table 3.1.3.1, we find that the principal tensor parameter transforms according to irreducible representation B_1 with standard variable x_3. The corresponding covariant $\mathsf{u}_3 = u_1 - u_2$ can be found in Appendix E of the manual of *GI★KoBo*-1 (or in Kopský, 2001), where one also finds an invariant containing u_1 and u_2: $\mathsf{u}_{1,1} = u_1 + u_2$. The corresponding conversion equations are: $u_1 = \frac{1}{2}(\mathsf{u}_{1,1} + \mathsf{u}_3)$, $u_2 = \frac{1}{2}(\mathsf{u}_{1,1} - \mathsf{u}_3)$. In the parent phase $\mathsf{u}_3 = u_1^{(p)} - u_2^{(p)} = 0$, hence $u_1^{(p)} = u_2^{(p)} = \frac{1}{2}\mathsf{u}_{1,1}$, whereas in the ferroic phase $u_1^{(f)} = \frac{1}{2}(\mathsf{u}_{1,1} + \mathsf{u}_3) = u_1^{(p)} + \frac{1}{2}\mathsf{u}_{1,1} = u_1^{(p)} + \delta u_1$, $u_2^{(f)} = u_2^{(p)} - \frac{1}{2}\mathsf{u}_{1,1} = u_2^{(p)} + \delta u_2 = u_1^{(p)} - \delta u_1$. The symmetry-breaking increments $\delta u_1 = -\delta u_2$ describe thus the changes of the Cartesian components that correspond to the nonzero principal tensor component $u_1 - u_2$.

An analogous situation occurs frequently in trigonal and hexagonal parent groups, where $u_1 - u_2$ (or $g_1 - g_2$) transforms like the first or second component of the principal tensor parameter. In these cases, the corresponding symmetry-breaking increments of Cartesian components are again related: $\delta u_1 = -\delta u_2$ (or $\delta g_1 = -\delta g_2$).

We note that relations like $A_{11} = -A_{12} = -A_{26}$ do not imply that these components transform as the standard variable. Though these components are proportional to the principal tensor parameter in the first domain state, they cannot be transformed to corresponding components in other domain states as easily as covariant tensor components of the principal tensor parameter.

In general, it is useful to consider a tensor parameter as a vector in the carrier space of the respective representation. Then the Cartesian components are projections of this vector on the Cartesian basis of the tensor space.

The presentation of the principal tensor parameters in the column *Principal tensor parameters* of this table is a compromise: whenever conversion equations lead to simple relations between morphic Cartesian components and/or symmetry-breaking increments, we present these relations, in some cases together with corresponding covariants. In the more complicated cases, only the covariants are given. The corresponding conversion equations and labelling of covariants are given at the beginning of that part of the table which covers hexagonal and cubic parent groups G. In the main tables of the software *GI★KoBo*-1, the principal tensor parameters and the secondary tensor parameters up to rank 4 are given consistently in covariant form. Labelling of covariant components and conversion equations are given in Appendix E of the manual.

The principal tensor parameters presented in Table 3.1.3.1 represent a particular choice of property tensors for standard variables given in the second column. To save space, property tensors are selected in the following way: polarization **P** and strain u are always listed; if none of their components transform according to $D^{(\eta)}$, then components of one axial and one polar tensor (if available) appearing in Table 3.1.3.3 are given. Principal parameters of two different property tensors are separated by a semicolon. If two different components of the same property tensor transform in the same way, they are separated by a comma.

As tensor indices we use integers 1, 2, 3 instead of vector components x, y, z and contracted indices 1, 2, 3, 4, 5, 6 in matrix notation for pairs $xx, yy, zz, yz \approx zy, zx \approx xz, xy \approx yx$, respectively

Important note: To make Table 3.1.3.1 compatible with the software *GI★KoBo*-1 and with Kopský (2001), coefficients of property tensors in matrix notation with contracted indices 4, 5, 6 *do not* contain the numerical factors 2 and 4 which are usually introduced to preserve a compact form (without these factors) of linear constitutive relations [see Chapter 1.1, Nye (1985) and especially Appendices E and F of Sirotin & Shaskolskaya (1982)]. This explains the differences in matrix coefficients appearing in Table 3.1.3.1 and those presented in Chapter 1.1 or in Nye (1985) and in Sirotin & Shaskolskaya (1982). Thus *e.g.* for the symmetry descent $6_z2_x2_y \Downarrow 3_z2_x$, we find in Table 3.1.3.1 the principal tensor parameters $d_{11} = -d_{12} = -d_{26}$, whereas according to Chapter 1.1 or *e.g.* to Nye (1985) or Sirotin & Shaskolskaya (1982) these coefficients for $F_1 = 3_z2_x$ are related by equations $d_{11} = -d_{12} = -2d_{26}$.

Table 3.1.3.3. *Important property tensors*

$i = 1, 2, 3$; $\mu, \nu = 1, 2, \ldots, 6$.

Tensor components	Property	Tensor components	Property
ε	enantiomorphism		chirality
P_i	polarization	p_i	pyroelectricity
u_μ	strain	ε_{ij}	dielectric permittivity
g_μ	optical activity		
$d_{i\mu}$	piezoelectricity	$r_{i\mu}$	electro-optics
$A_{i\mu}$	electrogyration		
$\pi_{\mu\nu}$	piezo-optics	$Q_{\mu\nu}$	electrostriction

Property tensors and symbols of their components that can be found in Table 3.1.3.1 are given in the left-hand half of Table 3.1.3.3. The right-hand half presents other tensors that transform in the same way as those on the left and form, therefore, covariant tensor components of the same form as those given in the column *Principal tensor parameters*. Principal and secondary tensor parameters for all property tensors that appear in Table 3.1.3.3 are available in the software *GI★KoBo*-1.

n_f: number of ferroic single domain states that differ in the primary order parameter η and in the principal tensor parameters.

n_a: number of ferroelastic single domain states. If $n_a = n_f$, $n_a < n_f$ or $n_a = 1$, the ferroic phase is, respectively, a full, partial or non-ferroelastic one.

n_e: number of ferroelectric single domain states. If $n_e = n_f$, $n_e < n_f$ or $n_e = 0, 1$, the ferroic phase is, repectively, a full, partial or non-ferroelectric one ($n = 0$ or $n = 1$ correspond to a non-polar or to a polar parent phase, respectively) (see Section 3.4.2).

3.1.3.4. *Examples*

Example 3.1.3.4.1. Phase transition in triglycine sulfate (TGS). Assume that the space groups of both parent (high-symmetry) and ferroic (low-symmetry) phases are known: $\mathcal{G} = P2_1/c$ (C_{2h}^5), $\mathcal{F}_1 = P2_1$ (C_2^2). The same number of formula units in the primitive unit cell in both phases suggests that the transition is an equitranslational one. This conclusion can be checked in the lattice of equitranslational subgroups of the software *GI★KoBo*-1. There we find for the low-symmetry space group the symbol $P112_1(\mathbf{b}/4)$, where the vector in parentheses expresses the shift of the origin with respect to the conventional origin given in *IT* A (2002).

In Table 3.1.3.1, one finds that the corresponding point-group-symmetry descent $2_z/m_z \Downarrow 2_z$ is associated with irreducible representation $\Gamma_\eta = A_u$. The corresponding principal tensor parameters of lowest rank are the pseudoscalar ε (enantiomorphism or chirality) and the vector of spontaneous polarization with one nonzero morphic component P_3 – the transition is a proper ferroelectric one. The non-ferroelastic ($n_a = 1$) full ferroelectric phase has two ferroelectric domain states ($n_f = n_e = 2$). Other principal tensor parameters (morphic tensor components that transform according to Γ_η) are available in the software *GI★KoBo*-1: g_1, g_2, g_3, g_6; $d_{31}, d_{32}, d_{33}, d_{36}, d_{14}, d_{15}, d_{24}, d_{25}$. Property tensors with these components are listed in Table 3.1.3.3. As shown in Section 3.4.2, all these components

change sign when one passes from one domain state to the other. Since there is no intermediate group between G and F, there are no secondary tensor parameters.

Example 3.1.3.4.2. Phase transitions in barium titanate ($BaTiO_3$). We shall illustrate the solution of the inverse Landau problem and the need to correlate the crystallographic system with the Cartesian crystallophysical coordinate system. The space-group type of the parent phase is $\mathcal{G} = Pm\bar{3}m$, and those of the three ferroic phases are $\mathcal{F}_1^{(1)} = P4mm$, $\mathcal{F}_1^{(2)} = Cm2m$, $\mathcal{F}_1^{(3)} = R3m$, all with one formula unit in the primitive unit cell.

This information is not complete. To perform mode analysis, we must specify these space groups by saying that the lattice symbol P in the first case and the lattice symbol R in the third case are given with reference to the cubic crystallographic basis (**a**, **b**, **c**), while lattice symbol C in the second case is given with reference to crystallographic basis [(**a** − **b**), (**a** + **b**), **c**]. If we now identify vectors of the cubic crystallographic basis with vectors of the Cartesian basis by $\mathbf{a} = a\mathbf{e}_x$, $\mathbf{b} = a\mathbf{e}_y$, $\mathbf{c} = a\mathbf{e}_z$, where $\mathbf{e}_x$, $\mathbf{e}_y$, $\mathbf{e}_z$ are three orthonormal vectors, we can see that the corresponding point groups are $F_1^{(1)} = 4_z m_x m_{xy}$, $F_1^{(2)} = m_{x\bar{y}} 2_{xy} m_z$, $F_1^{(3)} = 3_p m_{x\bar{y}}$.

Notice that without specification of crystallographic bases one could interpret the point group of the space group $Cm2m$ as $m_x 2_y m_z$. Bases are therefore always specified in lattices of equitranslational subgroups of the space groups that are available in the software *GI★KoBo*-1, where we can check that all three symmetry descents are equitranslational.

In Table 3.1.3.1, we find that these three ferroic subgroups are epikernels of the R-irep $\Gamma_\eta = T_{1u}$ with the following principal tensor components: P_3, $P_1 = P_2$, $P_1 = P_2 = P_3$, respectively. Other principal tensor parameters can be found in the main tables of the software *GI★KoBo*-1. The knowledge of the representation Γ_η allows one to perform soft-mode analysis (see *e.g.* Rousseau *et al.*, 1981).

For the tetragonal ferroelectric phase with $F_1 = 4_z m_x m_y$, we find in Fig. 3.1.3.1 an intermediate group $L_1 = 4_z/m_z m_x m_{xy}$. In Table 3.1.3.1, we check that this is an epikernel of the R-irep E_g with secondary tensor parameter δu_3. This phase is a full (proper) ferroelectric and partial ferroelastic one.

More details about symmetry aspects of structural phase transitions can be found in monographs by Izyumov & Syromiatnikov (1990), Kociński (1983, 1990), Landau & Lifshitz (1969), Lyubarskii (1960), Tolédano & Dmitriev (1996) and Tolédano & Tolédano (1987). Group–subgroup relations of space groups are treated extensively in *IT* A1 (2003).

3.1.4. Example of a table for non-equitranslational phase transitions

By J.-C. Tolédano

In the preceding Section 3.1.3, a systematic tabulation of possible symmetry changes was provided for the class of equitranslational phase transitions. This tabulation derives from the principles described in Section 3.1.2, and relates the enumeration of the symmetry changes at structural transitions to the characteristics of the irreducible representations of the space group $\mathcal{G}$ of the 'parent' (highest-symmetry) phase adjacent to the transition. Systematic extension of this type of tabulation to the general case of transitions involving both a decrease of translational and of point-group symmetry has been achieved by several groups (Tolédano & Tolédano, 1976, 1977, 1980, 1982; Stokes & Hatch, 1988). The reader can refer, in particular, to the latter reference for an exhaustive enumeration of the characteristics of possible transitions. An illustration of the results obtained for a restricted class of parent phases (those associated with the point symmetry $4/m$ and to a simple Bravais lattice P) is presented here.

In order to clarify the content Table 3.1.4.1, let us recall (*cf.* Section 3.1.2) that Landau's theory of continuous phase transitions shows that the order parameter of a transition transforms according to a physically irreducible representation of the space group $\mathcal{G}$ of the high-symmetry phase of the crystal. A physically irreducible representation is either a real irreducible representation of $\mathcal{G}$ or the direct sum of two complex-conjugate irreducible representations of $\mathcal{G}$. To classify the order-parameter symmetries of all possible transitions taking place between a given parent (high-symmetry) phase and another (low-symmetry) phase, it is therefore necessary, for each parent space group, to list the various relevant irreducible representations.

Each irreducible representation of a given space group can be denoted $\Gamma_n(k^*)$ and identified by two quantifies. The star k^*, represented by a vector linking the origin of reciprocal space to a point of the first Brillouin zone, specifies the translational symmetry properties of the basis functions of $\Gamma_n(k^*)$. The dimension of $\Gamma_n(k^*)$ is equal to the number of components of the order parameter of the phase transition considered. A given space group has an infinite number of irreducible representations. However, physical considerations restrict a systematic enumeration to only a few irreducible representations. The restrictions arise from the fact that one focuses on continuous (or almost continuous) transitions between strictly periodic crystal structures (*i.e.* in particular, incommensurate phases are not considered), and have been thoroughly described previously (Tolédano & Tolédano, 1987, and references therein).

3.1.5. Microscopic aspects of structural phase transitions and soft modes

By J. F. Scott

3.1.5.1. *Introduction*

Phase transitions in crystals are most sensitively detected *via* dynamic techniques. Two good examples are ultrasonic attenuation and internal friction. Unfortunately, while often exquisitely sensitive to subtle second-order phase transitions [*e.g.* the work of Spencer *et al.* (1970) on $BaMnF_4$], they provide no real structural information on the lattice distortions that occur at such phase transitions, or even convincing evidence that a real phase transition has occurred (*e.g.* transition from one long-range thermodynamically stable ordered state to another). It is not unusual for ultrasonic attenuation to reveal a dozen reproducible anomalies over a small temperature range, none of which might be a phase transition in the usual sense of the phrase. At the other extreme are detailed structural analyses *via* X-ray or neutron scattering, which give unambiguous lattice details but often totally miss small, nearly continuous rigid rotations of light ions, such as hydrogen bonds or oxygen or fluorine octahedra or tetrahedra. Intermediate between these techniques are phonon spectroscopies, notably infrared (absorption or reflection) and Raman techniques. The latter has developed remarkably over the past thirty years since the introduction of lasers and is now a standard analytical tool for helping to elucidate crystal structures and phase transitions investigated by chemists, solid-state physicists and materials scientists.

3.1.5.2. *Displacive phase transitions*

3.1.5.2.1. *Landau–Devonshire theory*

Landau (1937) developed a simple mean-field theory of phase transitions which implicitly assumes that each atom or ion in a system exerts a force on the other particles that is independent of the distance between them (see Section 3.1.2.2). Although this is a somewhat unphysical crude approximation to the actual forces, which are strongly dependent upon interparticle spacings, it allows the forces of all the other particles in the system to be replaced mathematically by an effective 'field', and for the

resulting equations to be solved exactly. This mathematical simplicity preserves the qualitative features of the real physical system and its phase transition without adding unnecessary cumbersome mathematics and had earlier been used to great advantage for fluids by Van der Waals (1873) and for magnetism by Weiss (1907). Landau's theory is a kind of generalization of those earlier theories. In it he defines an 'order parameter' x, in terms of which most physical quantities of interest may be expressed *via* free energies. In a ferromagnet, the order parameter corresponds to the net magnetization; it is zero above the Curie temperature T_c and increases monotonically with decreasing temperature below that temperature. In a liquid–gas phase transition the order parameter is the difference in density in the gas and liquid phases for the fluid.

Devonshire independently developed an equivalent theory for ferroelectric crystals around 1953 (Devonshire, 1954). For ferroelectrics, the order parameter is the spontaneous dielectric polarization P. In both his formalism and that of Landau, the ideas are most conveniently expressed through the free energy of the thermodynamic system:

$$F(P, T) = A(T - T_c)P^2 + BP^4 + CP^6, \qquad (3.1.5.1a)$$

where A and C are positive quantities and B may have either sign. Scott (1999) shows that C changes sign at ferroelectric-to-superionic conducting transition temperatures. As shown in Fig. 3.1.5.1, minimization of the free energy causes the expectation value of P to go from zero above the Curie temperature to a nonzero value below. If B is positive the transition is continuous ('second-order'), whereas if B is negative, the transition is discontinuous ('first-order'), as shown in Fig. 3.1.5.2. The coefficient B may also be a function of pressure p or applied electric field **E** and may pass through zero at a critical threshold value of p or **E**. Such a point is referred to as a 'tricritical point' and is marked by a change in the order of the transition from first-order to second-order. The term '*tri*-critical' originates from the fact that in a three-dimensional graph with coordinates temperature T, pressure p and applied field **E**, there are *three* lines marking the ferroelectric–paraelectric phase boundary that meet at a single point. Crossing any of these three lines produces a continuous phase transition (Fig. 3.1.5.3).

3.1.5.2.2. *Soft modes*

Minimization of the free energy above leads to the dependence of spontaneous polarization P upon temperature given by $P(T) = P(0)[(T_c - T)/T_c]$ for continuous transitions. In the more general case discussed by Landau, the polarization P is replaced by a generic 'order parameter' $\varphi(T)$ with the same dependence. Cochran's contribution (1960, 1961) was to show that for

Table 3.1.4.1. *Possible symmetry changes across transitions from a parent phase with space group $P4/m$, $P4_2/m$, $P4/n$, $P4_2/n$, $I4/m$ or $I4_1/a$*

Equitranslational symmetry changes are not included (*cf.* Section 3.1.3). The coordinates of the points in the second column are referred to the primitive unit cell of the reciprocal lattice. The terms used in the fifth column are introduced in Section 3.1.1. The last column is characteristic of non-equitranslational transitions.

Parent space group	Irreducible representation: Brillouin zone point	Irreducible representation: Dimension of the order parameter	Possible low-symmetry space groups	Macroscopic characteristics of the transition	Change in the number of atoms per primitive unit cell
$P4/m$	$\frac{1}{2},\frac{1}{2},0$	2	$P2/m$; $P2/b$	Ferroelastic	2
		1	$P4/m$; $P4/n$	Non-ferroic	2
	$0,0,\frac{1}{2}$	2	$P2_1/m$	Ferroelastic	2
		1	$P4/m$; $P4_2/m$	Non-ferroic	2
	$\frac{1}{2},\frac{1}{2},\frac{1}{2}$	2	$B2/m$	Ferroelastic	2
		1	$I4/m$	Non-ferroic	2
	$0,\frac{1}{2},\frac{1}{2}$	2	$B2/m$	Ferroelastic	2
		1	$I4/m$	Non-ferroic	4
	$0,\frac{1}{2},0$	2	$P2/m$; $P2/b$	Ferroelastic	2
		1	$P4/m$; $P4/n$	Non-ferroic	4
$P4_2/m$	$\frac{1}{2},\frac{1}{2},0$	2	$P2/m$; $P2/b$	Ferroelastic	2
		1	$P4_2/n$; $P4_2/m$	Non-ferroic	2
	$0,0,\frac{1}{2}$	2	$P2_1/m$	Ferroelastic	2
		2	$P4_1$; $P4_3$	Ferroelectric	2
	$\frac{1}{2},\frac{1}{2},\frac{1}{2}$	2	$B2/m$	Ferroelastic	2
		1	$I4/m$	Non-ferroic	2
	$0,\frac{1}{2},\frac{1}{2}$	2	$B2/m$	Ferroelastic	2
		2	$P4_1/a$	Non-ferroic	2
	$0,\frac{1}{2},0$	2	$P2/m$; $P2/b$	Ferroelastic	2
		2	$P4_2/m$; $P4_2/n$	Non-ferroic	2
$P4/n$	$\frac{1}{2},\frac{1}{2},0$	2	$P2/b$	Ferroelastic	2
		2	$P4$	Ferroelectric	2
	$0,0,\frac{1}{2}$	2	$P2_1/b$	Ferroelastic	2
		1	$P4/n$; $P4_2/n$	Non-ferroic	2
	$\frac{1}{2},\frac{1}{2},\frac{1}{2}$	2	$B2/b$	Ferroelastic	2
		2	$I4$	Ferroelectric	2
$P4_2/n$	$\frac{1}{2},\frac{1}{2},0$	2	$P2/b$	Ferroelastic	2
	$0,0,\frac{1}{2}$	2	$P2_1/b$	Ferroelastic	2
		2	$P4_1$; $P4_3$	Ferroelectric	2
$I4/m$	$\frac{1}{2},-\frac{1}{2},-\frac{1}{2}$	2	$P2_1/m$; $P2_1/b$	Ferroelastic	2
		1	$P4/m$; $P4_2/m$; $P4/n$; $P4_2/n$	Non-ferroic	2
	$\frac{1}{2},\frac{1}{2},0$	2	$B2/m$; $B2/b$	Ferroelastic	2
		2	$P4/m$; $P4_2/m$; $P4/n$; $P4_2/n$	Non-ferroic	4
	$\frac{1}{2},0,0$	4	$B2/m$	Ferroelastic	2
		4	$P\bar{1}$	Ferroelastic	8
		4	$I4/m$; $I4_1/a$	Non-ferroic	8
	$\frac{3}{4},\frac{1}{4},-\frac{1}{4}$	2	$I4/m$; $I4_1/a$	Non-ferroic	4
$I4_1/a$	$\frac{1}{2},-\frac{1}{2},-\frac{1}{2}$	2	$P2_1/b$	Ferroelastic	2
	$\frac{1}{2},0,0$	4	$I\bar{4}$	Higher-order ferroic	8
		4	$P\bar{1}$	Ferroelastic	2
		4	$P\bar{1}$; $B2/b$	Ferroelastic	4

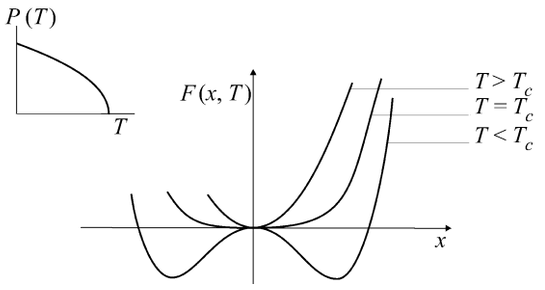

Fig. 3.1.5.1. Free energy $F(P, T)$ and order parameter $P(T)$ from the Landau–Devonshire theory [equation (3.1.5.1*a*)] for a continuous second-order ferroelectric phase transition [coefficient B positive in equation (3.1.5.1*a*)]. The insert shows the temperature dependence of the order parameter, *i.e.* the expectation value of the displacement $x(T)$.

continuous 'displacive' (as opposed to 'order–disorder') transitions, this order parameter is (or is proportional to) a normal mode of the lattice. One normal mode of the crystal must, in Cochran's theory, literally soften: the generalized force constant for this mode weakens as a function of temperature, and its frequency consequently decreases. This soft-mode theory provided an important step from the macroscopic description of Landau and Devonshire to a microscopic theory, and in particular, to vibrational (phonon) spectroscopy.

Cochran illustrated this theory using a 'shell' model in which the electrons surrounding an ion were approximated by a rigid sphere; shell–shell force constants were treated as well as shell–core and core–core terms, in the general case. The initial application was to PbTe and other rock-salt cubic structures that undergo ferroelectric structural distortions.

For this simple case, the key equations relate the optical phonon frequencies of long wavelength to two terms: a short-range force constant R'_0 and a long-range Coulombic term. It is important that in general neither of these terms has a pathological temperature dependence; in particular, neither vanishes at the Curie temperature. Rather it is the subtle cancellation of the two terms at T_c that produces a 'soft' transverse optical phonon.

The longitudinal optical phonon frequency $\omega_{\rm LO}(T)$ is positive definite and remains finite at all temperatures:

$$\mu\omega_{\rm LO}^2 = R'_0 + \frac{8\pi Z^2 e^2}{9\varepsilon V(T)}, \qquad (3.1.5.1b)$$

where μ is a reduced mass for the normal mode; Ze is an effective charge for the mode, related to the valence state of the ions involved; ε is the high-frequency dielectric constant and $V(T)$ is the unit-cell volume, which is a function of temperature due to thermal expansion.

By comparison, the transverse optical phonon frequency

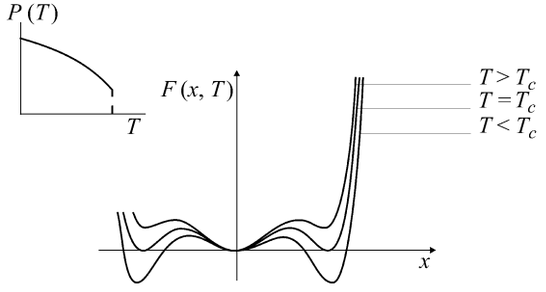

Fig. 3.1.5.2. Free energy $F(P, T)$ and order parameter $P(T)$ from the Landau–Devonshire theory [equation (3.1.5.1*a*)] for a discontinuous first-order ferroelectric phase transition [coefficient B negative in equation (3.1.5.1*a*)]. T_1 is the temperature (see Fig. 3.1.2.6) below which a secondary minimum appears in the free energy.

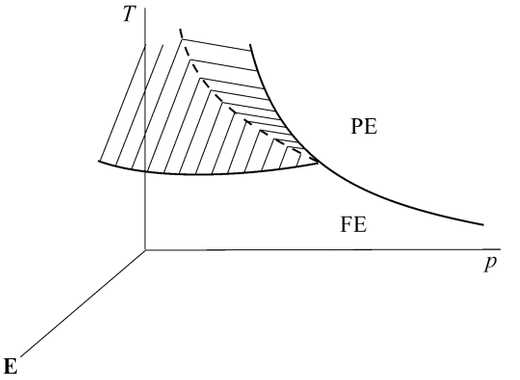

Fig. 3.1.5.3. Three-dimensional graph of phase boundaries as functions of temperature T, pressure p and applied electric field $\mathbf{E}$, showing a tricritical point where three continuous phase boundaries intersect.

$$\mu\omega_{\rm TO}^2 = R'_0 - \frac{4\pi Z^2 e^2}{3\varepsilon V(T)} \qquad (3.1.5.1c)$$

can vanish accidentally when $V(T)$ reaches a value that permits cancellation of the two terms. Note that this does not require any unusual temperature dependence of the short-range interaction term R'_0. This description appears to satisfy all well studied ferroelectrics except for the 'ultra-weak' ones epitomized by TSCC (tris-sarcosine calcium chloride), in which the Coulombic term in (3.1.5.1*b*) and (3.1.5.1*c*) is very small and the pathological dependence occurs in R'_0. This leads to a situation in which the longitudinal optical phonon is nearly as soft as is the transverse branch.

Subsequent to Cochran's shell-model developments, Cowley (1962, 1964, 1970) replaced this phenomenological modelling with a comprehensive many-body theory of phonon anharmonicity, in which the soft-mode temperature is dominated by Feynman diagrams emphasizing renormalization of phonon self-energies due to four-phonon interactions (two in and two out). This contrasts with the three-phonon interactions that dominate phonon linewidths under most conditions.

It is worth noting that the soft optical phonon branch is necessarily always observable in the low-symmetry phase *via* Raman spectroscopy in all 32 point-group symmetries. This was first proved by Worlock (1971), later developed in more detail by Pick (1969) and follows group-theoretically from the fact that the vibration may be regarded as a dynamic distortion of symmetry Γ_i which condenses at T_c to produce a static distortion of the same symmetry. Hence the vibration in the distorted phase has symmetry given by the product $\Gamma_i \times \Gamma_i$, which always contains the totally symmetric representation Γ_1 for any choice of Γ_i. If Γ_i is non-degenerate, its outer product with itself will contain only Γ_1 and there will be a single, totally symmetric soft mode; if Γ_i is degenerate, there will be two or three soft modes of different symmetries, at least one of which is totally symmetric.

Since the totally symmetric representation is Raman-active for all 32 point-group symmetries, this implies that the soft mode is always accessible to Raman spectroscopy at least in the distorted, low-symmetry phase of the crystal.

3.1.5.2.3. *Strontium titanate, $SrTiO_3$*

Among the perovskite oxides that are ferroelectric insulators, barium titanate has received by far the most attention from the scientific community since its independent characterization in several countries during World War II. The discovery of a ferroelectric that was robust, relatively inert (not water-soluble) and without hydrogen bonding was a scientific breakthrough, and its large values of dielectric constant and especially spontaneous polarization are highly attractive for devices. Although not ferroelectric in pure bulk form, strontium titanate has received

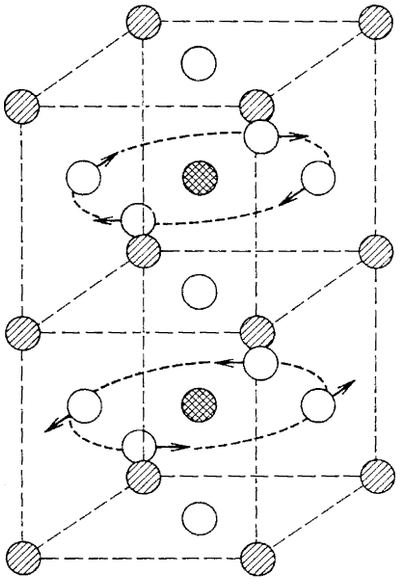

Fig. 3.1.5.4. Structure of strontium titanate above (undisplaced ions) and below (arrows) its anti-ferrodistortive phase transition at *ca.* 105 K. Below this temperature, the cubic primitive cell undergoes a tetragonal distortion and also doubles along the [001] cubic axis (domains will form along [100], [010] and [001] of the original cubic lattice). The ionic displacements approximate a rigid rotation of oxygen octahedra, out-of-phase in adjacent unit cells, except that the oxygens actually remain on the cube faces, so that a very small Ti—O bond elongation occurs.

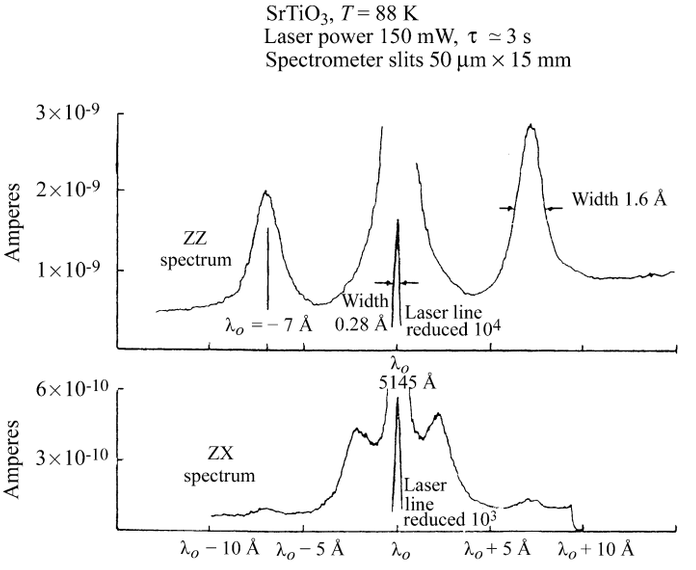

Fig. 3.1.5.6. Raman spectra of strontium titanate below its cubic–tetragonal phase transition temperature. These features disappear totally above the phase transition temperature, thereby providing a vivid indication of a rather subtle phase transition.

the second greatest amount of attention of this family over the past thirty years. It also provides a textbook example of how optical spectroscopy can complement traditional X-ray crystallographic techniques for structural determination.

Fig. 3.1.5.4 shows the structure of strontium titanate above and below the temperature ($T_0 = 105$ K) of a non-ferroelectric phase transition. Note that there is an out-of-phase distortion of oxygen ions in adjacent primitive unit cells (referred to the single formula group ABO_3 in the high-temperature phase). This out-of-phase displacement approximates a rigid rotation of oxygen octahedra about a [100], [010] or [001] cube axis, except that the oxygens actually remain in the plane of the cube faces. We note three qualitative aspects of this distortion: Firstly, it doubles the primitive unit cell from one formula group to two; this will approximately double the number of optical phonons of very long wavelength ($q = 0$) permitted in infrared and/or Raman spectroscopy. Secondly, it makes the gross crystal class tetragonal, rather than cubic (although in specimens cooled through the transition temperature in the absence of external stress, we might expect a random collection of domains with tetragonal axes along the original [100], [010], [001] cube axes, which will give macroscopic cubic properties to the multidomain aggregate). Thirdly, the transition is perfectly continuous, as shown in Fig. 3.1.5.5, where the rotation angle of the oxygen octahedra about the cube axis is plotted *versus* temperature.

Fig. 3.1.5.4 does not correspond at all to the structure inferred earlier from X-ray crystallographic techniques (Lytle, 1964). The very small, nearly rigid rotation of light ions (oxygens) in multidomain specimens caused the X-ray study to overlook the primary characteristic of the phase transition and to register instead only the unmistakable change in the c/a ratio from unity. Thus, the X-ray study correctly inferred the cubic–tetragonal characteristic of the phase transition but it got both the space

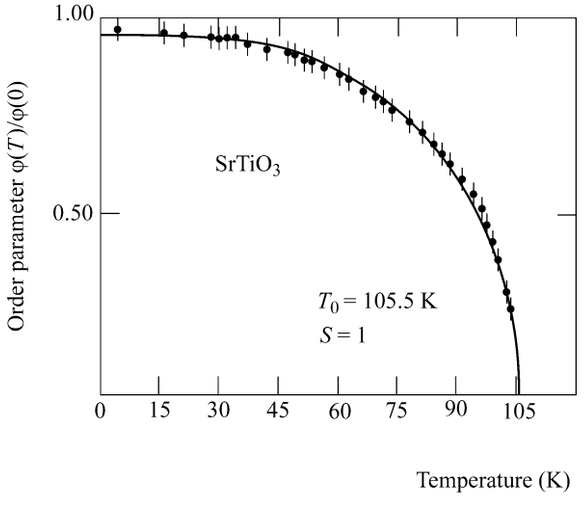

Fig. 3.1.5.5. Rotation angle *versus* temperature for the oxygen octahedron distortion below 105 K in strontium titanate described in Fig. 3.1.5.4. The solid curve is a mean-field least-squares fit to an $S = 1$ Brillouin function.

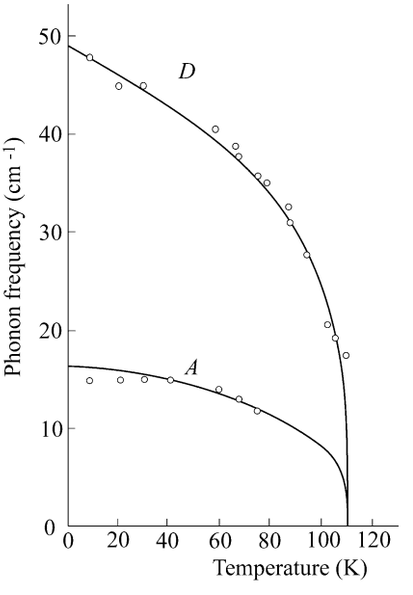

Fig. 3.1.5.7. Temperature dependence of phonon branches observed in the Raman spectra of tetragonal strontium titanate.

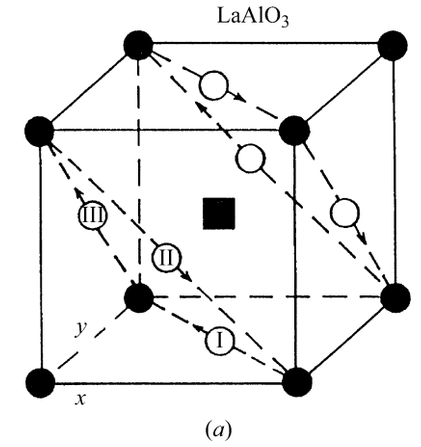

(*a*)

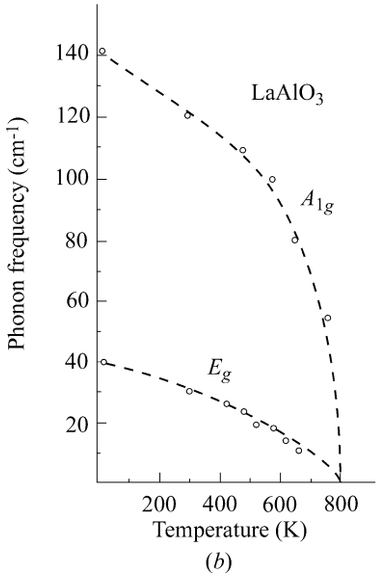

(*b*)

Fig. 3.1.5.8. (*a*) Structure of lanthanum aluminate above (undistorted) and below (arrows) its cubic–rhombohedral phase transition near 840 K. As in strontium titanate (Figs. 3.1.5.4–3.1.5.7), there is a nearly rigid rotation of oxygen octahedra (the oxygen ions actually remain on the cube faces); however, in the lanthanide aluminates (Ln = La, Pr, Nd) the rotation is about a cube [111] body diagonal, so that the resulting structure is rhombohedral, rather than tetragonal. The primitive unit cell doubles along the cubic [111] axis; domains will form with the unique axis along all originally equivalent body diagonals of the cubic lattice. (*b*) Optical phonon frequences *versus* temperature in lanthanum aluminate.

group and the size of the primitive cell wrong. The latter error has many serious implications for solid-state physicists: For example, certain electronic transitions from valence to conduction bands are actually 'direct' (involving no change in wavevector) but would have erroneously been described as 'indirect' with the structure proposed by Lytle. More serious errors of interpretation arose with the microscopic mechanisms of ultrasonic loss proposed by Cowley based upon Lytle's erroneous structure.

The determination of the correct structure of strontium titanate (Fig. 3.1.5.4) was actually made *via* EPR studies (Unoki & Sakudo, 1967) and confirmed *via* Raman spectroscopy (Fleury *et al.*, 1968). The presence of 'extra' $q = 0$ optical phonon peaks in the Raman spectra below T_0 (Fig. 3.1.5.6) is simple and unmistakable evidence of unit-cell multiplication. The fact that two optical phonon branches have frequencies that decrease continuously to zero (Fig. 3.1.5.7) as the transition temperature is approached from below shows further that the transition is 'displacive', that is, that the structures are perfectly ordered both above and below the transition temperature. This is a classic example of Cochran's soft-mode theory discussed above.

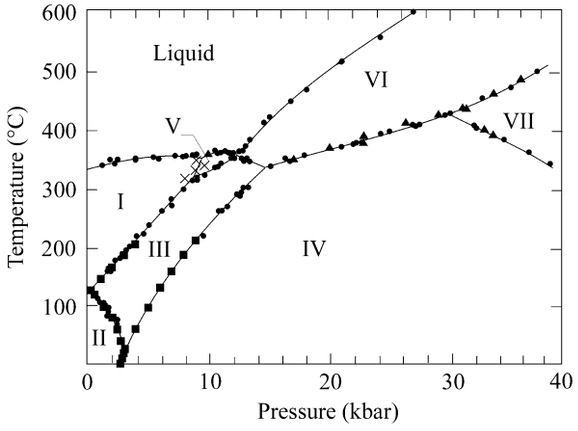

Fig. 3.1.5.9. Phase diagram of potassium nitrate, KNO_3.

3.1.5.2.4. *Lanthanum aluminate, $LaAlO_3$*

A structural distortion related to that in strontium titanate is exhibited in lanthanum aluminate at approximately 840 K. As in strontium titanate, the distortion consists primarily of a nearly rigid rotation of oxygen octahedra. However, in the lanthanide aluminates (including $NdAlO_3$ and $PrAlO_3$) the rotation is about the [111] body diagonal(s) of the prototype cubic structure. The rotation, shown in Fig. 3.1.5.8, is out-of-phase in adjacent cubic unit cells, analogous to that in strontium titanate.

Historically, this phase transition and indeed the structure of lanthanum aluminate were incorrectly characterized by X-ray crystallography (Geller & Bala, 1956) and correctly assigned by Scott (1969) and Scott & Remeika (1970) *via* Raman spectroscopy. The causes were as in the case of strontium titanate, namely that it is difficult to assess small, nearly rigid rotations of light ions in twinned specimens. In the case of lanthanum aluminate, Geller and Bala incorrectly determined the space group to be $R\bar{3}m$ (D^5_{3d}), rather than the correct $R\bar{3}2/c$ (D^6_{3d}) shown in Fig. 3.1.5.8, and they had the size of the primitive unit cell as one formula group rather than two.

3.1.5.2.5. *Potassium nitrate, KNO_3*

Potassium nitrate has a rather simple phase diagram, reproduced in Fig. 3.1.5.9. Two different structures and space groups were proposed for the ambient temperature phase I: Shinnaka (1962) proposed D^6_{3d} ($R\bar{3}2/c$) with two formula groups per primitive cell ($Z = 2$), whereas Tahvonen (1947) proposed D^5_{3d} ($R\bar{3}m$) with one formula group per primitive cell. In fact, both are wrong. The correct space group is that of Nimmo & Lucas (1973): D^6_{3d} ($R\bar{3}2/c$) with one formula group per primitive cell. Again, Raman spectroscopy of phonons shows that the Tahvonen structure predicts approximately twice as many spectral lines as can be observed. Balkanski *et al.* (1969) tried creatively but unsuccessfully to account for their spectra in terms of Tahvonen's space-group symmetry assignment for this crystal; later Scott & Pouligny (1988) showed that all spectra were compatible with the symmetry assigned by Nimmo and Lucas. In this case, in contrast to the perovskites strontium titanate and lanthanum aluminate, the confusion regarding space-group symmetry arose from the large degree of structural disorder found in phase I of KNO_3. The structures of phases II and III are unambiguous and are, respectively, aragonite D^{16}_{2h} (*Pnma*) with $Z = 4$ and C^5_{3v} ($R3m$) with $Z = 1$.

3.1.5.2.6. *Lanthanum pentaphosphate*

The lanthanide pentaphosphates (La, Pr, Nd and TbP_5O_{14}) consist of linked ribbons of PO_4 tetrahedra. In each material a structural phase transition occurs from a high-temperature D^7_{2h} (*Pncm*) point-group symmetry orthorhombic phase to a C_{2h}

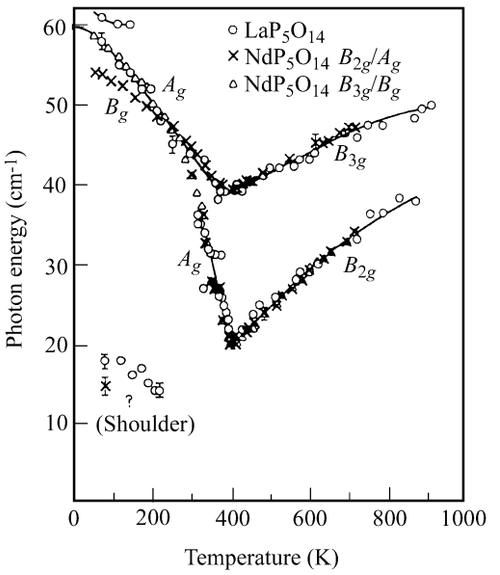

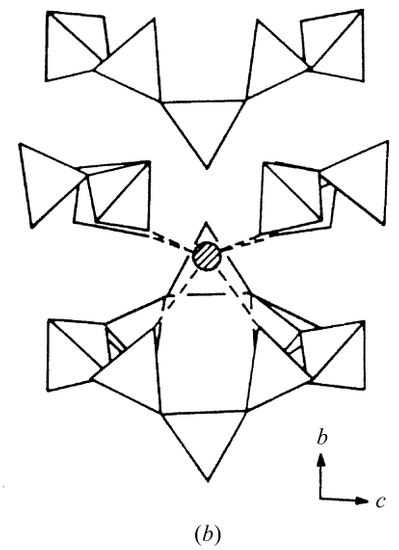

Fig. 3.1.5.10. (*a*) 'Soft' optical phonon frequency *versus* temperature in LaP_5O_{14}, showing displacive character of the phase transition. Large acousto-optic interaction prevents the optical phonon frequency from reaching zero at the transition temperature, despite the second-order character of the transition. (*b*) Lanthanum pentaphosphate structure, showing linked 'ribbons' of phosphate tetrahedra.

($P2_1/c$) monoclinic phase. The macroscopic order parameter for this transition is simply the monoclinic angle φ, or more precisely ($\varphi - 90^\circ$). In this family of materials, the X-ray crystallography was unambiguous in its determination of space-group symmetries and required no complementary optical information. However, the Raman studies (Fox *et al.*, 1976) provided two useful pieces of structural information. First, as shown in Fig. 3.1.5.10, they showed that the phase transition is entirely displacive, with no disorder in the high-symmetry phase; second, they showed that there is a microscopic order parameter that in mean field is proportional to the frequency of a 'soft' optical phonon of long wavelength ($q = 0$). This microscopic order parameter is in fact the eigenvector of that soft mode (normal coordinate), which approximates a rigid rotation of phosphate tetrahedra.

3.1.5.2.7. *Barium manganese tetrafluoride*

$BaMnF_4$ is an unusual material whose room-temperature structure is illustrated in Fig. 3.1.5.11(*a*). It consists of MnF_6 octahedra, linked by two shared corners along the polar *a* axis,

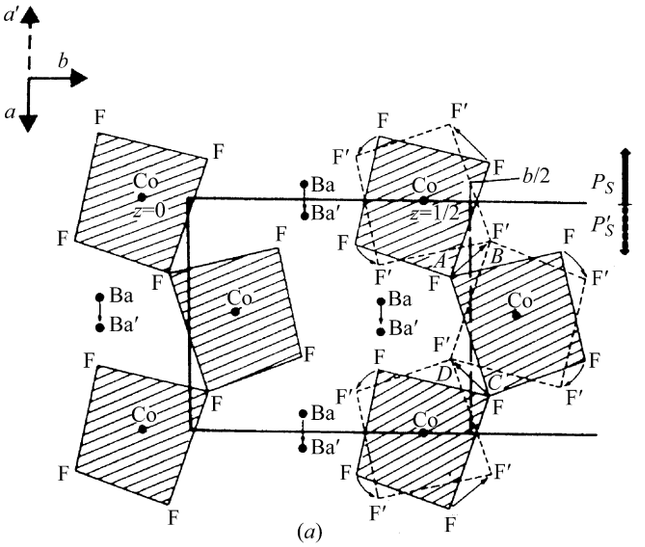

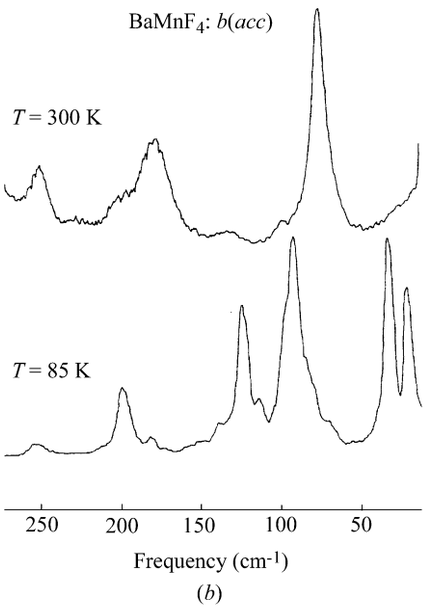

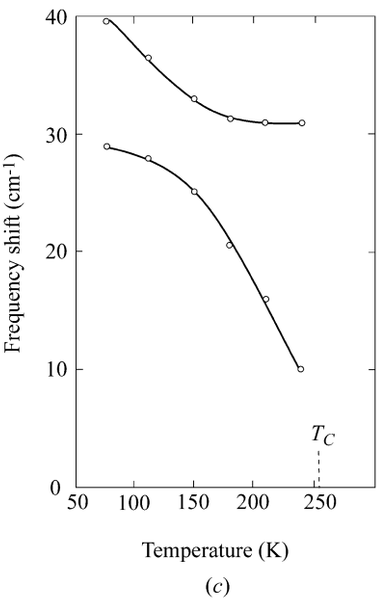

Fig. 3.1.5.11. (*a*) Structure of barium metal fluoride BaMF$_4$ (M = Co, Mn, Mg, Zn, Ni) at ambient temperature (300 K). (*b*) Raman spectroscopy of barium manganese fluoride above and below its structural phase transition temperature, *ca.* 251 K. (*c*) Temperature dependence of lower energy phonons in (*b*).

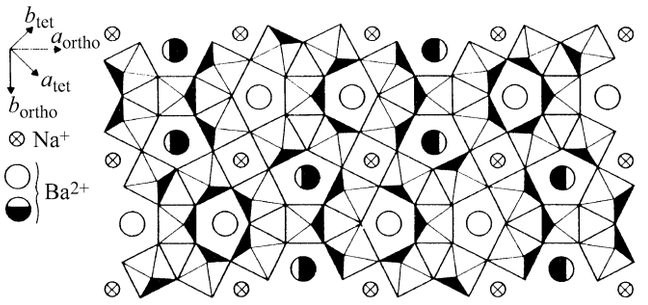

Fig. 3.1.5.12. Structure of the tungsten bronze barium sodium niobate $Ba_2NaNb_5O_{15}$ in its highest-temperature $P4/mbm$ phase above 853 K.

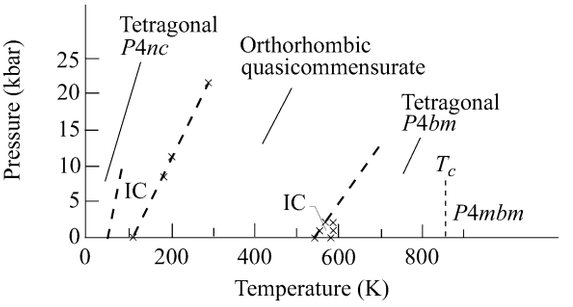

Fig. 3.1.5.13. Sequence of phases encountered with raising or lowering the temperature in barium sodium niobate.

with ribbons of such octahedra rather widely separated by the large ionic radius barium ions in the *b* direction. The resulting structure is, both magnetically and mechanically, rather two-dimensional, with easy cleavage perpendicular to the *b* axis and highly anisotropic electrical (ionic) conduction.

Most members of the BaMF$_4$ family (M = Mg, Zn, Mn, Co, Ni, Fe) have the same structure, which is that of orthorhombic C_{2v} (2*mm*) point-group symmetry. These materials are all ferroelectric (or at least pyroelectric; high conductivity of some makes switching difficult to demonstrate) at all temperatures, with an 'incipient' ferroelectric Curie temperature extrapolated from various physical parameters (dielectric constant, spontaneous polarization *etc.*) to lie 100 K or more above the melting point (*ca.* 1050 K). The Mn compound is unique in having a low-temperature phase transition. The reason is that Mn^{+2} represents (Shannon & Prewitt, 1969) an end point in ionic size (largest) for the divalent transition metal ions Mn, Zn, Mg, Fe, Ni, Co; hence, the Mn ion and the space for it in the lattice are not a good match. This size mismatch can be accommodated by the r.m.s. thermal motion above room temperature, but at lower temperatures a structural distortion must occur.

This phase transition was first detected (Spencer *et al.*, 1970) *via* ultrasonic attenuation as an anomaly near 255 K. This experimental technique is without question one of the most sensitive in discovering phase transitions, but unfortunately it gives no direct information about structure and often it signals something that is not in fact a true phase transition (in $BaMnF_4$ Spencer *et al.* emphasized that they could find no other evidence that a phase transition occurred).

Raman spectroscopy was clearer (Fig. 3.1.5.11*b*), showing unambiguously additional vibrational spectra that arise from a doubling of the primitive unit cell. This was afterwards confirmed directly by X-ray crystallography at the Clarendon Laboratory, Oxford, by Wondre (1977), who observed superlattice lines indicative of cell doubling in the *bc* plane.

The real structural distortion near 250 K in this material is even more complicated, however. Inelastic neutron scattering at Brookhaven by Shapiro *et al.* (1976) demonstrated convincingly that the 'soft' optical phonon lies not at $(0, 1/2, 1/2)$ in the Brillouin zone, as would have been expected for the *bc*-plane cell doubling suggested on the basis of Raman studies, but at $(0.39, 1/2, 1/2)$. This implies that the actual structural distortion from the high-temperature C_{2v}^{12} ($Cmc2_1$) symmetry does indeed double the primitive cell along the *bc* diagonal but in addition modulates the lattice along the *a* axis with a resulting repeat length that is incommensurate with the original (high-temperature) lattice constant *a*. The structural distortion microscopically approximates a rigid fluorine octahedra rotation, as might be expected. Hence, the chronological history of developments for this material is that X-ray crystallography gave the correct lattice structure at room temperature; ultrasonic attenuation revealed a possible phase transition near 250 K; Raman spectroscopy confirmed the transition and implied that it involved primitive cell doubling; X-ray crystallography confirmed directly the cell doubling; and finally neutron scattering revealed an unexpected incommensurate modulation as well. This interplay of experimental techniques provides a rather good model as exemplary for the field. For most materials, EPR would also play an important role in the likely scenarios; however, the short relaxation times for Mn ions made magnetic resonance of relatively little utility in this example.

3.1.5.2.8. *Barium sodium niobate*

The tungsten bronzes represented by $Ba_2NaNb_5O_{15}$ have complicated sequences of structural phase transitions. The structure is shown in Fig. 3.1.5.12 and, viewed along the polar axis, consists of triangular, square and pentagonal spaces that may or may not be filled with ions. In barium sodium niobate, the pentagonal channels are filled with Ba ions, the square channels are filled with sodium ions, and the triangular areas are empty.

The sequence of phases is shown in Fig. 3.1.5.13. At high temperatures (above $T_c = 853$ K) the crystal is tetragonal and paraelectric ($P4/mbm = D_{4h}^5$). When cooled below 853 K it becomes ferroelectric and of space group $P4bm = C_{4v}^2$ (still tetragonal). Between *ca.* 543 and 582 K it undergoes an incommensurate distortion. From 543 to *ca.* 560 K it is orthorhombic and has a '1q' modulation along a single orthorhombic axis. From 560 to 582 K it has a 'tweed' structure reminiscent of metallic lattices; it is still microscopically orthorhombic but has a short-range modulated order along a second orthorhombic direction and simultaneous short-range modulated order along an orthogonal axis, giving it an incompletely developed '2q' structure.

As the temperature is lowered still further, the lattice becomes orthorhombic but not incommensurate from 105–546 K; below 105 K it is incommensurate again, but with a microstructure quite different from that at 543–582 K. Finally, below *ca.* 40 K it becomes macroscopically tetragonal again, with probable space-group symmetry $P4nc$ (C_{4v}^6) and a primitive unit cell that is four times that of the high-temperature tetragonal phases above 582 K.

This sequence of phase transitions involves rather subtle distortions that are in most cases continuous or nearly continuous. Their elucidation has required a combination of experimental techniques, emphasizing optical birefringence (Schneck, 1982), Brillouin spectroscopy (Oliver, 1990; Schneck *et al.*, 1977; Tolédano *et al.*, 1986; Errandonea *et al.*, 1984), X-ray scattering, electron microscopy and Raman spectroscopy (Shawabkeh & Scott, 1991), among others. As with the other examples described in this chapter, it would have been difficult and perhaps impossible to establish the sequence of structures *via* X-ray techniques alone. In most cases, the distortions are very small and involve essentially only the oxygen ions.

3.1.5.2.9. *Tris-sarcosine calcium chloride (TSCC)*

Tris-sarcosine calcium chloride has the structure shown in Fig. 3.1.5.14. It consists of sarcosine molecules of formula

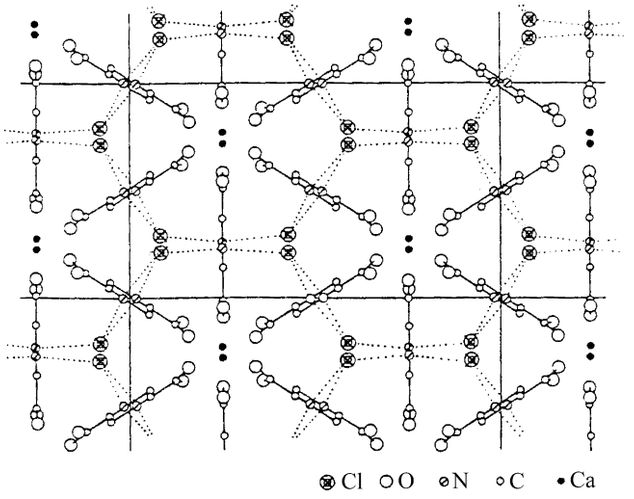

Fig. 3.1.5.14. Structure of tris-sarcosine calcium chloride, $(CH_3NHCH_2COOH)_3CaCl_2$. The hydrogen ion (proton) on the COOH group is relocated in the crystal onto the N atom to form a zwitter ion, forming an H—N—H group that hydrogen bonds to adjacent chlorine ions. Each nitrogen forms two such hydrogen bonds, whereas each chlorine has three, forming a very complex network of hydrogen bonding. The phase transition is actually displacive, involving a rather rigid rolling of whole sarcosine molecules, which stretches the N—H bonds; it is not order–disorder of hydrogen ions in a Cl···H—N double well. (The Cl···H—N wells are apparently too asymmetric for that.)

CH_3NHCH_2COOH in which the hydrogen ion comes off the COOH group and is used to hydrogen bond the nitrogen ion to a nearby chlorine, forming a zwitter ion. As is illustrated in this figure, this results in a relatively complex network of N—H···Cl bonds. The COO^- ion that results at the end group of each sarcosine is ionically bonded to adjacent calcium ions. The resulting structure is highly ionic in character and not at all that of a 'molecular crystal'. The structure at ambient temperatures is *Pnma* (D_{2h}^{16}) with $Z = 4$; below 127 K it distorts to *Pna*2$_1$ (C_{2v}^{9}) with Z still 4.

It had been supposed for some years on the basis of NMR studies of the Cl ions, as well as the conventional wisdom that 'hydrogen-bonded crystals exhibit order–disorder phase transitions', that the kinetics of ferroelectricity at the Curie temperature of 127 K in TSCC involved disorder in the proton positions along the N—H···Cl hydrogen bonds. In fact that is not correct; even the NMR data of Windsch & Volkel (1980), originally interpreted as order–disorder, actually show (Blinc *et al.*, 1970) a continuous, displacive evolution of the H-atom position along the H···Cl bond with temperature, rather than a statistical averaging

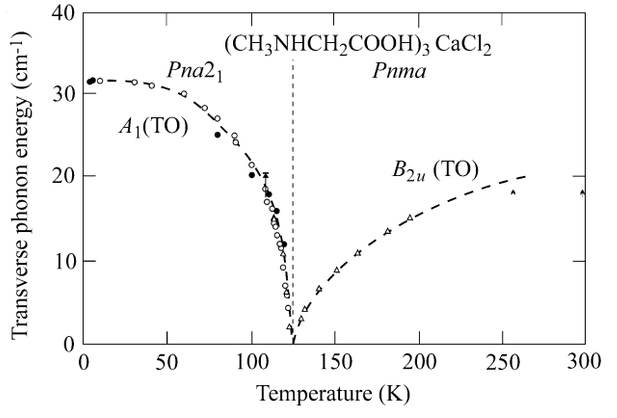

Fig. 3.1.5.15. 'Soft' optical phonon frequencies *versus* temperature in both ferroelectric and paraelectric phases of tris-sarcosine calcium chloride.

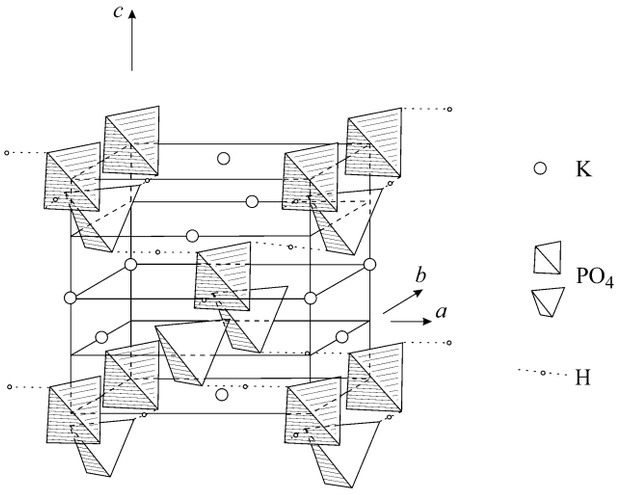

Fig. 3.1.5.16. The structure of potassium dihydrogen phosphate, KH_2PO_4, showing the O···H···O hydrogen bonds.

of two positions, which would characterize order–disorder dynamics. In addition, as shown in Fig. 3.1.5.15, there is (Kozlov *et al.*, 1983) a lightly damped 'soft' phonon branch in both the paraelectric and ferroelectric phases. TSCC is in fact a textbook example of a displacive ferroelectric phase transition. The hydrogen bonds do not exhibit disorder in the paraelectric phase. Rather, the transition approximates a rigid rotation of the sarcosine molecules, which stretches the N—H···Cl bond somewhat (Prokhorova *et al.*, 1980).

3.1.5.2.10. *Potassium dihydrogen phosphate, KH_2PO_4*

Potassium dihydrogen phosphate, colloquially termed 'KDP', has probably been the second most studied ferroelectric after barium titanate. It has been of some practical importance, and the relationship between its hydrogen bonds, shown in Fig. 3.1.5.16, the perpendicular displacement of heavier ions (K and P) and the Curie temperature has fascinated theoretical physicists, who generally employ a 'pseudo-spin model' in which the right and left displacements of the hydrogen ions along symmetric hydrogen bonds (O···H···O) can be described by a fictitious spin with up (+1/2) and down (−1/2) states.

Unlike TSCC, discussed above, KDP has perfectly symmetric hydrogen bonds. Therefore, one might expect that above a sufficiently high temperature the protons can quantum-mechanically tunnel between equivalent potential wells separated by a shallow (and temperature-dependent) barrier. Below T_C the protons order (all to the right or all to the left) in spatial regions that represent ferroelectric domains. This model, initially proposed by Blinc (1960), is correct and accounts for the large isotope shift in the Curie temperature noted for deuterated specimens. The complication is that the spontaneous polarization arises along a direction perpendicular to these proton displacements, so the dipoles do not arise from proton displacements directly. Instead, the proton coupling (largely Coulombic) to the potassium and phosphorus ions causes their displacements along the polar axis. This intricate coupling between protons along hydrogen bonds, which undergo an order–disorder transition, and K and P ions, which undergo purely displacive movements in their equilibrium positions, forms the basis of the theoretical interest in the lattice dynamics of KDP. Following Strukov & Levanyuk (1998), we would say that arguments over whether this transition is displacive or order–disorder are largely semantic; the correct description of KDP is that the thermal change in occupancy of the O···H···O double wells modifies the free energy in such a way that the K and P ions undergo a displacive rearrangement.

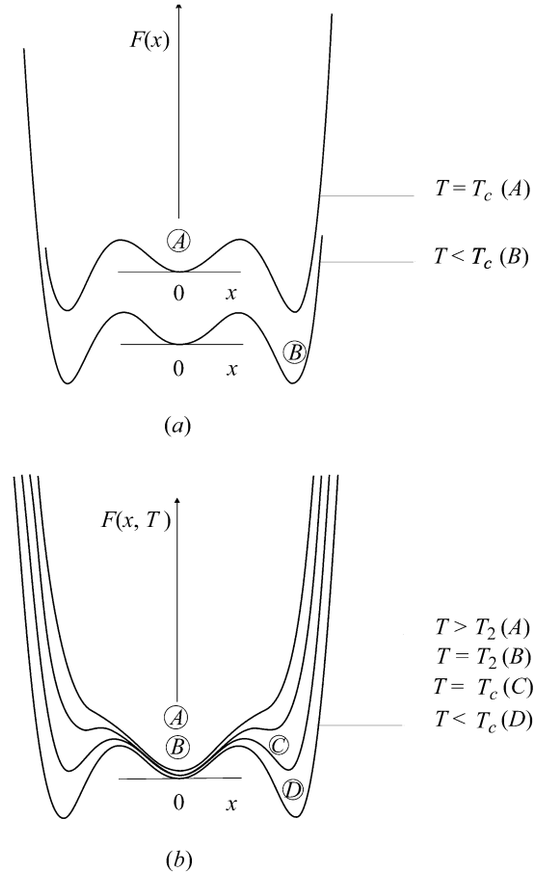

Fig. 3.1.5.17. Double-well models [circled letters show the time-averaged expectation values of the position $x(T)$ of the order parameter at each temperature]. (*a*) For purely order–disorder systems, the depth and separation of the wells is temperature-independent; only the thermal populations change, due to either true quantum-mechanical tunnelling (which only occurs for H or D ions) or thermally activated hopping (for heavier ions). (*b*) For purely displacive systems, all the temperature dependence is in the relative depths of the potential wells. [For mixed systems, such as KH_2PO_4, both well depth(s) and thermal populations change with temperature.]

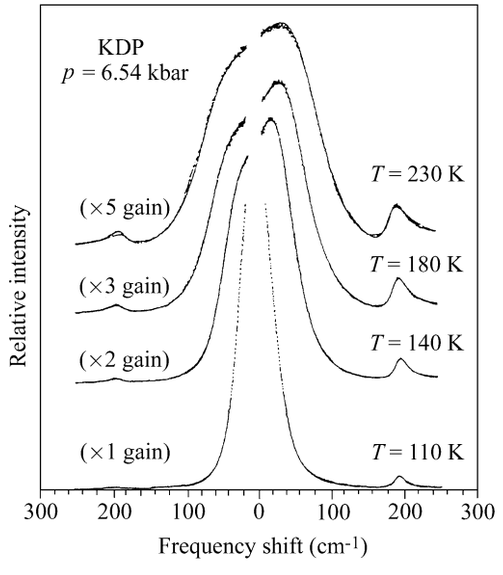

Fig. 3.1.5.18. Pressure dependence of the 'soft' optical phonon branch Raman spectra in potassium dihydrogen phosphate (after Peercy, 1975*b*), showing the displacive character of the phase transition [purely order–disorder phase transitions cannot exhibit propagating (underdamped) soft modes].

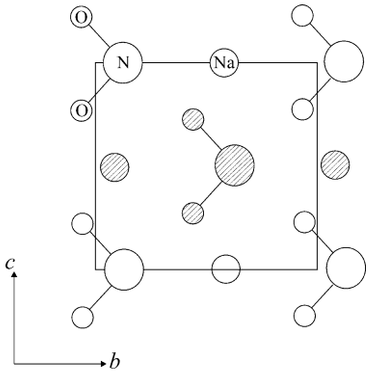

Fig. 3.1.5.19. Structure of sodium nitrite, $NaNO_2$. The molecularly bonded NO_2 ions are shaped like little boomerangs. At high temperatures they are randomly oriented, pointing up or down along the polar b axis. At low temperatures they are (almost) all pointed in the same direction ($+b$ or $-b$ domains). Over a small range of intermediate temperatures their directions have a wave-like 'incommensurate' modulation with a repeat length L that is not an integral multiple of the lattice constant b.

The difficulty comes in recognizing that the normal-mode coordinate x corresponding to the soft mode in this case involves protons (H ions) and K and P ions. Therefore, the free-energy description (as in Fig. 3.1.5.17) will have partly displacive character and partly order–disorder. If the transition were purely displacive (as in TSCC, discussed above), all the important temperature changes would be in the shape of the free energy $F(x)$ with temperature T. Whereas if the transition were purely order–disorder (as in $NaNO_2$, discussed below), the shape of the free-energy curves $F(x)$ would be quite independent of T; only the relative populations of the two sides of the double well would be T-dependent. KDP is intermediate between these descriptions. Strictly, it is 'displacive' in the sense that its normal mode is a propagating mode, shown in Fig. 3.1.5.18 by Peercy's pressure-dependence Raman studies (Peercy, 1975*a*,*b*). If it were truly order–disorder, the mode would be a Debye relaxation with a spectral peak at zero frequency, independent of pressure or temperature. Only the width and intensity would depend upon these parameters.

As a final note on KDP, this material exhibits at ambient pressure and zero applied electric field a phase transition that is very slightly discontinuous. Application of modest pressure or field produces a truly continuous transition. That is, the tricritical point is easily accessible [at a critical field of $6\,\mathrm{kV\,cm^{-1}}$, according to Western *et al.* (1978)].

3.1.5.2.11. *Sodium nitrite, $NaNO_2$*

Sodium nitrite exhibits a purely order–disorder transition and has been chosen for discussion to contrast with the systems in the sections above, which are largely displacive. The mechanism of its transition dynamics is remarkably simple and is illustrated in Fig. 3.1.5.19. There is a linear array of Na and N ions. At low temperatures, the arrow-shaped NO_2 ions (within each domain) point in the same direction; whereas above the Curie temperature they point in random directions with no long-range order. The flopping over of an NO_2 ion is a highly nonlinear response. Therefore the response function (spectrum) associated with this NO_2 flip-flop mode will consist of two parts: a high-frequency peak that looks like a conventional phonon response (lightly damped Lorentzian), plus a low-frequency Debye relaxation ('central mode' peaking at zero frequency). Most of the temperature dependence for this mode will be associated with the Debye spectrum. The spectrum of sodium nitrite is shown in Fig. 3.1.5.20.

Particularly interesting is its phase diagram, relating structure(s) to temperature and 'conjugate' field applied along the

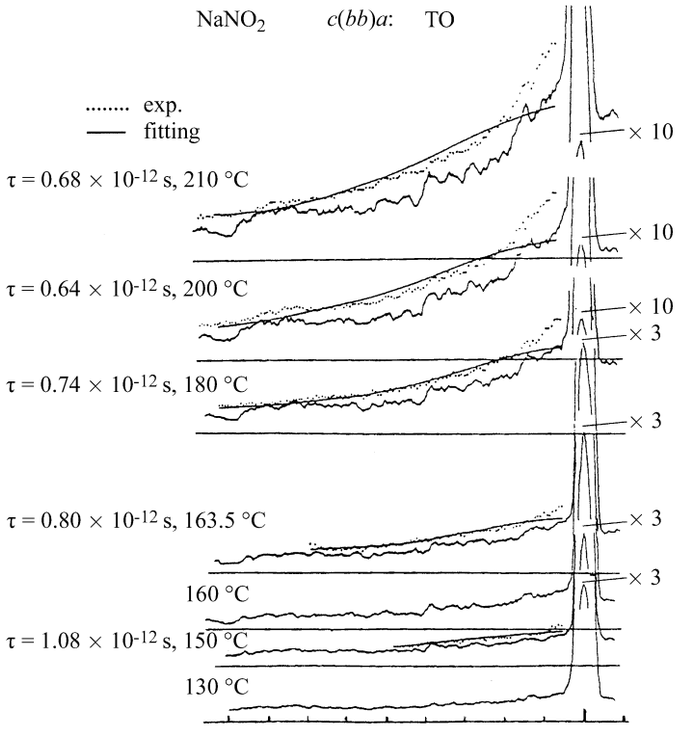

Fig. 3.1.5.20. Raman spectra of sodium nitrite, showing diffusive Debye-like response due to large-amplitude flopping over of nitrite ions [note that the high-frequency phonon-like response is due to the small-amplitude motion of this same normal mode; thus in this system N ions give rise not to $3N$ (non-degenerate) peaks in the spectral response function, but to $3N + 1$].

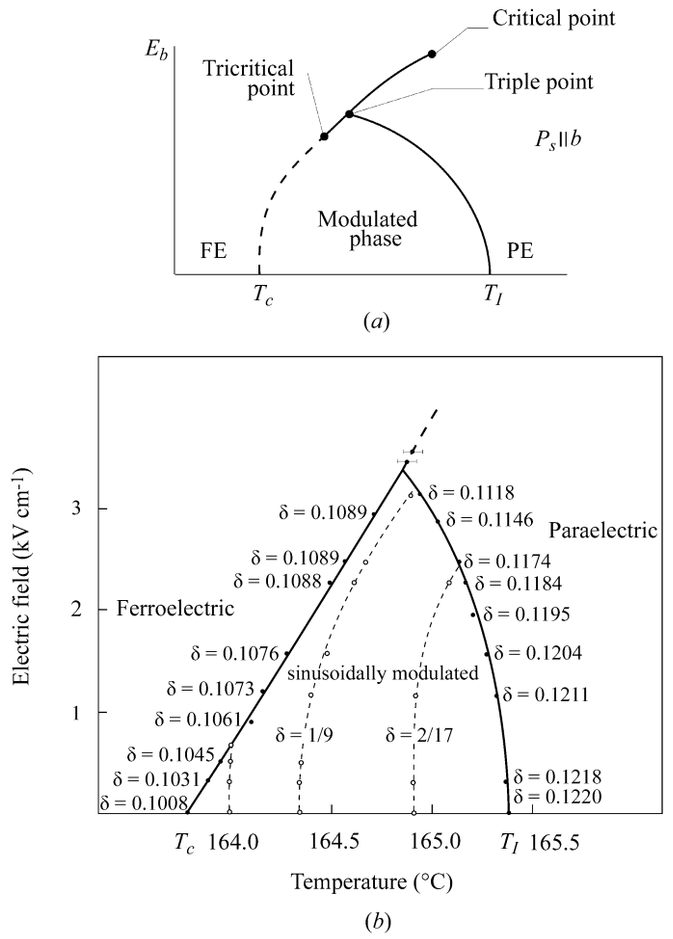

Fig. 3.1.5.21. Phase diagram for sodium nitrite for 'conjugate' electric fields applied along the polar b axis, showing triple point, tricritical point and critical end point. (*a*) Schematic; (*b*) real system.

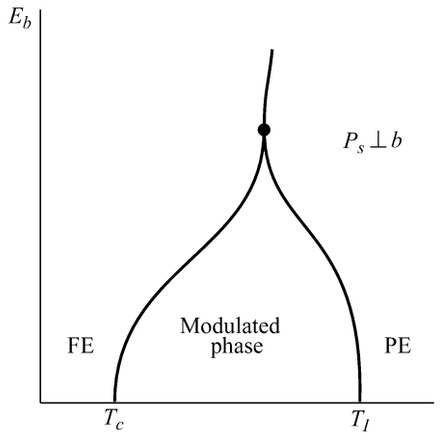

Fig. 3.1.5.22. Phase diagram for sodium nitrite for electric fields applied perpendicular to the polar b axis. In this situation, a Lifshitz point is possible where phase boundaries 'kiss' (touch tangentially).

polar axis. As Fig. 3.1.5.21 illustrates somewhat schematically, there are first-order phase boundaries, second-order phase boundaries, a tricritical point and a critical end point (as in a gas–liquid diagram). If the electric field is applied in a direction orthogonal to the polar axis, a Lifshitz point (Fig. 3.1.5.22) may be expected, in which the phase boundaries intersect tangentially. The ionic conductivity of sodium nitrite has made it difficult to make the figures in Figs. 3.1.5.21 and 3.1.5.22 precise.

3.1.5.2.12. *Fast ion conductors*

As exemplary of this class of materials, we discuss in this section the silver iodide compound $Ag_{13}I_9W_2O_8$. This material has the structure illustrated in Fig. 3.1.5.23. Conduction is *via* transport of silver ions through the channels produced by the W_4O_{16} ions (the coordination is not that of a simple tetrahedrally coordinated WO_4 tungstate lattice).

This crystal undergoes three structural phase transitions (Habbal *et al.*, 1978; Greer *et al.*, 1980; Habbal *et al.*, 1980), as illustrated in Fig. 3.1.5.24. The two at lower temperatures are first-order; that at the highest temperature appears to be perfectly continuous. Geller *et al.* (1980) tried to fit electrical data for this material ignoring the uppermost transition.

As in most of the materials discussed in this review, the phase transitions were most readily observed *via* optical techniques, Raman spectroscopy in particular. The subtle distortions involve oxygen positions primarily and are not particularly well suited to more conventional X-ray techniques. Silver-ion disorder sets in only above the uppermost phase transition, as indicated by the full spectral response (as in the discussion of sodium nitrite in the preceding section).

Infrared (Volkov *et al.*, 1985) and Raman (Shawabkeh & Scott, 1989) spectroscopy have similarly confirmed low-temperature phase transitions in $RbAg_4I_5$ at 44 and 30 K, in addition to the well studied D_3^7–D_3^2 ($R32$–$P321$) transition at 122 K. The two lower-temperature phases increase the size of the primitive cell, but their space groups cannot be determined from available optical data. The 44 K transition is signalled by the abrupt appearance of an intense phonon feature at 12 cm^{-1} in both infrared and Raman spectra.

3.1.5.2.13. *High-temperature superconductors*

It is useful to play Devil's Advocate and point out difficulties with the technique discussed, to indicate where caution might be exercised in its application. $YBa_2Cu_3O_{7-x}$ (YBaCuO) provides such a case. As in the case of $BaMnF_4$ discussed in Section 3.1.5.2.7, there was strong evidence for a structural phase transition near 235 K, first from ultrasonic attenuation (Wang, 1987;

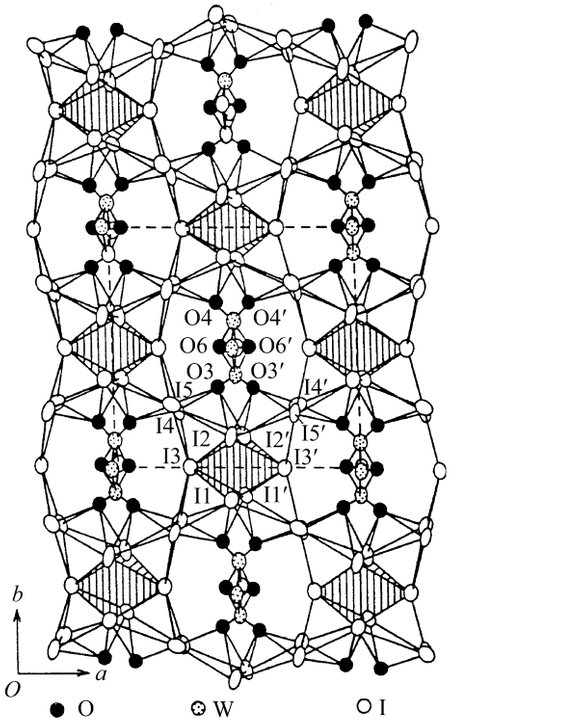

(*a*)

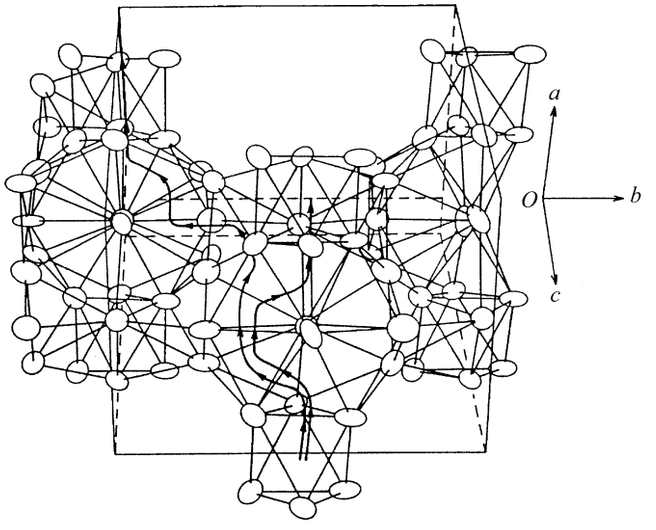

(*b*)

Fig. 3.1.5.23. (*a*) Crystal structure of silver iodide tungstate ($Ag_{13}I_9W_2O_8$); (*b*) showing conduction paths for Ag ions (after Chan & Geller, 1977).

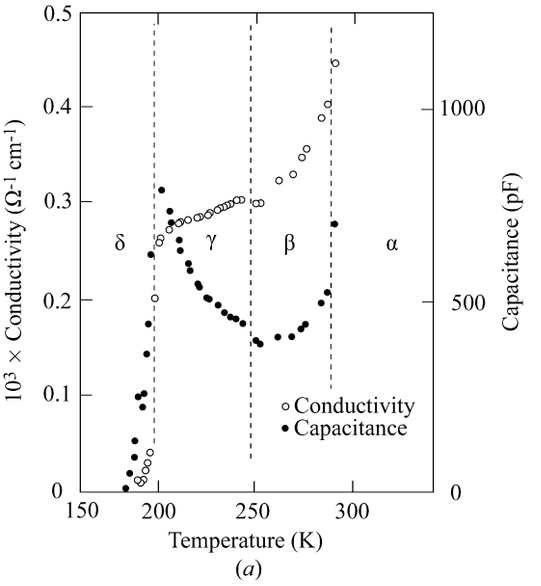

(*a*)

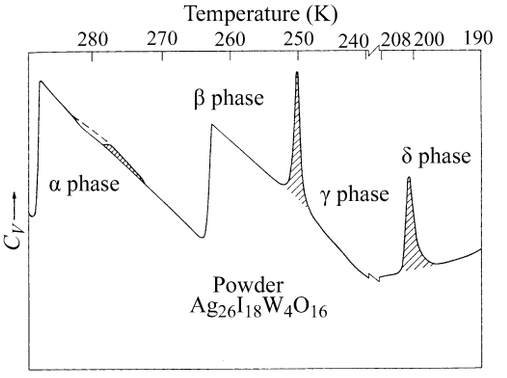

(*b*)

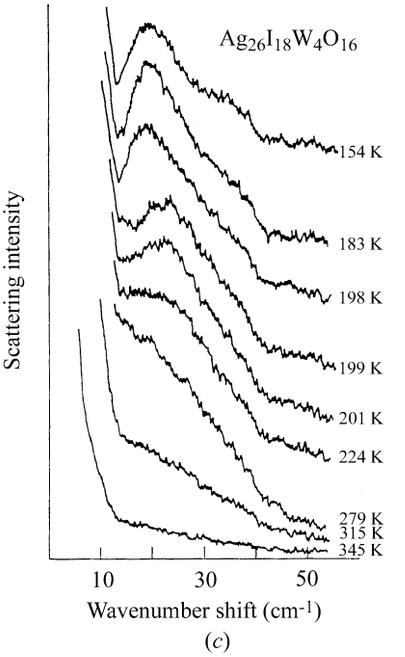

(*c*)

Fig. 3.1.5.24. Evidence for three phase transitions in silver iodide tungstate: (*a*) dielectric and conductivity data; (*b*) specific heat data; (*c*) Raman data. The lower transitions, at 199 and 250 K, are first order; the upper one, at 285 K, is second order.

Laegreid *et al.*, 1987) and then from Raman studies (Zhang *et al.*, 1988; Huang *et al.*, 1987; Rebane *et al.*, 1988). However, as years passed this was never verified *via* neutron or X-ray scattering. Researchers questioned (MacFarlane *et al.*, 1987) whether indeed a phase transition exists at such a temperature in this important material. At present it is a controversial and occasionally contentious issue. A difficulty is that light scattering in metals probes only the surface. No information is obtained on the bulk. Ultrasonic attenuation and internal friction probe the bulk, but give scanty information on mechanisms or structure.

In the specific case of YBaCuO, the 'extra' phonon line (Fig. 3.1.5.25) that emerges below 235 K is now known not to be from the superconducting $YBa_2Cu_3O_{7-x}$ material; its frequency of 644 cm^{-1} is higher than that of any bulk phonons in that material. However, this frequency closely matches that of the highest

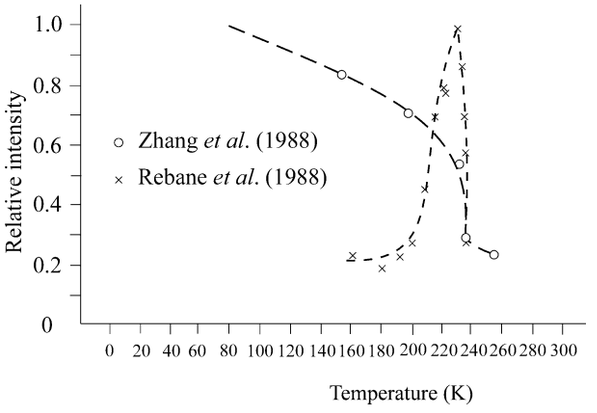

Fig. 3.1.5.25. Raman spectra of $YBa_2Cu_3O_{7-x}$ below an apparent phase transition at *ca.* 235 K (Zhang *et al.*, 1988).

LO (longitudinal optical) phonon in the semiconducting $YBa_2Cu_3O_{6+x}$ material, suggesting that the supposed phase transition at 235 K may be not a structural transition but instead a chemical transition in which oxygen is lost or gained at the surface with temperature cycling.

3.1.5.3. *Low-temperature ferroelectric transitions*

It has historically been difficult to establish the nature of ferroelectric phase transitions at cryogenic temperatures. This is simply because the coercive fields for most crystals rise as the temperature is lowered, often becoming greater than the breakdown fields below *ca.* 100 K. As a result, it is difficult to demonstrate *via* traditional macroscopic engineering techniques (switching) that a material is really ferroelectric. Some authors have proposed (*e.g.* Tokunaga, 1987) on theoretical grounds the remarkable (and erroneous) conjecture that no crystals have Curie temperatures much below 100 K. A rebuttal of this speculation is given in Table 3.1.5.1 in the form of a list of counter-examples. References may be found in the 1990 Landolt–Börnstein Encyclopedia of Physics (Vol. 28a). The original work on pure cadmium titanate and on lead pyrochlore (Hulm, 1950, 1953) did not demonstrate switching, but on the basis of more recent studies on mixed crystals $Ca_{2-2x}Pb_{2x}Nb_2O_7$ and $Ca_xCd_{1-x}TiO_3$, it is clear that the pure crystals are ferroelectric at and below the stated temperatures.

Hence, in Table 3.1.5.1 we see examples where X-ray structural studies may establish the symmetries requisite for ferroelectricity without the macroscopic switching being demonstrated. This is the converse case to that primarily emphasized in this section (*i.e.* the use of techniques complementary to X-ray scattering to determine exact crystal symmetries); it is useful to see these reverse cases to demonstrate the full complementarity of X-ray crystallography and dynamic spectroscopic techniques.

Table 3.1.5.1. *Low-temperature ferroelectrics*

Formula	Curie temperature T_c (K)	Curie constant C (K)	Entropy change ΔS (cal mol^{-1} K^{-1})
$NH_4Al(SO_4)_2{\cdot}12H_2O$	71	?	?
$NH_4Fe(SO_4)_2{\cdot}12H_2O$	88	400	0.15
$(NH_4)_2Cd(SO_4)_3$	95	?	?
$CdTiO_3$	55	4.5×10^4	?
$Pb_2Nb_2O_7$	15.3	?	?
$LiTlC_4H_4O_6{\cdot}H_2O$	10.5	?	?
$K_3Li_2Nb_5O_{15}$	7	?	?

3.1.6. Group informatics and tensor calculus

By V. Kopský and P. Boček

We shall briefly describe here the intentions and contents of the accompanying software package *GI⋆KoBo*-1 (*Group Informatics*, first two letters of authors names, release 1). A more detailed description is contained in the manual; the user may consult this file on the screen, but we recommend that it is printed out and that the printout is followed in order to become familiar with the theoretical background as well as with more detailed instructions for the use of the software.

The main purpose of this software is to describe the changes of tensor properties of crystalline materials during ferroic phase transitions, including basic information about domain states. The software provides powerful information in a standardized manner and it is based on a few advanced methodical points that are not yet available in textbooks. These points are:

(i) The introduction of *typical variables*, which was inspired by the *symbolic method* of the old invariant theory (Weitzenböck, 1923).

(ii) The method of Clebsch–Gordan products (Kopský, 1976*a*,*b*). The name stems from Clebsch–Gordan coefficients, known in quantum mechanics as coefficients of momentum addition. In this case, the coefficients are connected with the orthogonal group $\mathcal{O}(3)$; analogous coefficients were later introduced and calculated for crystal point groups (Koster *et al.*, 1963). They appear in Clebsch–Gordan products, which represent a better adaptation of results for our purposes.

(iii) Tables of *tensorial covariants* (Kopský, 1979*a*,*b*). The name covariant may sound rather unusual now, but it was originally used by Weyl (1946); it is equivalent to *symmetry-adapted bases* (*form-invariant bases* and other terms are also used). The term covariant is classical and its semantical use is easier.

(iv) Tables of *fine structures of domain states* (Kopský, 1982). These are contained in a booklet which is practically unknown though, together with tables of tensorial covariants, it contains all answers concerning changes of tensor properties at ferroic phase transitions.

Remark. The original term *fine domain structure* was amended because it is not quite accurate.

(v) *Extended integrity bases* (Patera *et al.*, 1978; Kopský, 1979*c*). These represent finite sets of polynomial invariants and covariants suitable for the calculation of all types of interactions in symmetric systems.

(vi) *Lattices of subgroups* (Ascher, 1968; Kopský, 1982). Subgroups of a group constitute a partially ordered set of special properties called a *lattice*. The unfortunate coincidence of the term (in English) with crystallographic lattices should be disregarded; it is always possible to see from the context what we mean by this term.

These methods provide good ammunition for all types of group-theoretical considerations where work with characters is insufficient and knowledge of the explicit bases of irreducible representations is necessary. This is exactly the case for the theory of structural phase transitions, and the consideration of domain states, pairs of domain states and domain walls or twin boundaries. The main results of the software are contained in tables of symmetry descents $G \Downarrow H$ and/or $G \Downarrow F_i$, where G is the parent point group, H its normal subgroup and F_i is the set of conjugate subgroups. These tables provide information about changes of tensors at ferroic phase transitions as well as basic information about interactions, and they are also supplemented by tables of equitranslational subgroups of space groups.

To make this exposition quite clear, we begin in the manual from the beginning with a brief review of elementary group-theoretical concepts used in the software. Relevant elementary tables (listed below in Section A) are followed by more advanced information proceeding towards the central goal of providing information for all symmetry descents (Section B). To achieve this goal, it was also necessary to introduce our own standard

notation for specifically oriented groups, for their elements and for irreducible representations (ireps). The reasons for the introduction of these standards are twofold: (i) There is no unique and commonly accepted notation in the literature. The recent book by Altmann & Herzig (1994) contains slight inconsistencies (different symbols for elements in a group and in its subgroup) and is also not compatible with another prominent source (Bradley & Cracknell, 1972). (ii) We need a strict specification of groups and their subgroups with reference to a Cartesian coordinate system and a strict specification of matrix ireps; neither is available in the literature. This does not mean that we introduce brand-new symbols; we simply adapt those that are already in use and we take extreme care that every symbol has a unique meaning.

It is recommended that users follow the manual when first using the software. The tabular content is as follows:

A. *General information*

On opening the program, a panel *Crystallographic* appears on the screen. In the left-hand part are listed crystallographic geometric classes in a tree form wrapped to crystallographic systems (families). A click on a system brings to the screen a list of its crystallographic geometric classes as either Hermann–Mauguin, Schoenflies or Shubnikov symbols (the latter are used only on this level).

The default choice for the notation is set in a table *Options* under the pull-down menu *File*. Hermann–Mauguin or Schoenflies symbols are offered for groups, standard or spectroscopic notation for group elements, classes of ireps and classes of conjugate elements. The temporary notation, under the pull-down menu *Notation*, also includes the choice of Shubnikov symbols.

When the user clicks on a geometric class, all specifically oriented groups of this class used in the software appear in the right-hand part of the panel. At the top appear the groups in standard orientation that are further used as the standard parent groups, all remaining groups appearing below. For some groups two or three standard orientations are available, for reasons explained in the manual. The option of using Hermann–Mauguin or Schoenflies symbols for groups is available throughout; up to a certain point there are options for using either standard symbols of group elements and of ireps (as defined here) or spectroscopic symbols. A specific group is picked using the left mouse button, then a click with the right mouse button opens a pull-down menu. The following information is available under the titles:

(1) *Basic info*: This contains information relevant to each group of the geometric class, such as the number of elements, generators, isomorphism type, normalizer, number of conjugacy classes and the standard orientations.

(2) *Group elements*: Activates the group calculator, the keys of which list elements of the group. Performs calculation of products (strings) of up to ten elements by left or right multiplication.

(3) *Correlation stnd./spectro*: Symbols of groups, elements and classes of ireps for standard and spectroscopic notation are correlated.

(4) *Class structure*: Symbols of classes of conjugate elements are defined and elements of classes are listed.

(5) *Class multiplication table*: Displays class multiplication formulae.

(6) *Character table*: Standard and spectroscopic symbols of classes of ireps are specified and kernels of ireps are presented.

(7) *Kronecker products*: Tables of Kronecker products of classes of ireps are displayed. Up to this point, both standard and spectroscopic notation are used.

(8) *Ireps and standard variables*: Irreducible matrix representations (ireps) are explicitly defined. These also define the standard symbols of typical variables.

Brief: Brief tables specify matrices of ireps for generators of the group.

Full: Full tables provide these matrices for each group element. Kernels of ireps are presented. From this point onwards only the standard notation is used.

(9) Clebsch–Gordan products: Up to orthorhombic groups, one Clebsch–Gordan product table is given. For groups of higher systems, there are two options: *complex* Clebsch–Gordan tables, where variables $(\xi_\alpha, \eta_\alpha)$ are used, and *real* Clebsch–Gordan tables, with variables (x_α, y_α) for two-dimensional real ireps.

(10) *Tensorial covariants*: Decomposition of tensors up to fourth rank into their covariant components is displayed.

B. *Ferroic phase transitions*

(11) *Subgroups*: Choice of this item displays a panel with the lattice of subgroups of the originally chosen point group G either in Schoenflies or in Hermann–Mauguin symbols. The pull-down menu *Graph* in the upper bar enables handling of the lattice: each item can be picked and moved to another place, the rearranged lattice can be fixed as default or reset, and the lattice can be sent to a printer. Notice that sets of conjugate subgroups are stacked like a pile of sheets of paper and can be unstacked. Consecutive clicks activate individual subgroups of the set. In the upper part of the panel, ireps of the parent group G in spectroscopic symbols are listed; these are followed by boxes in which it is possible to scroll for special vectors of the respective carrier space in terms of typical variables. Clicking on a vector marks its stabilizer (epikernel of the irep) in the lattice and activates it at the same time. With each irep is associated a table of the extended integrity basis; the table is called either by the option *Integrity bases* under the pull-down menu *View* or directly by using the right mouse button in the box of this irep. If the Ctrl key is pressed after the choice of one vector, another vector may be chosen; as a result, an intersection of the respective epikernels is marked in the lattice.

Each subgroup of the lattice may also be activated independently. Lattices of subgroups serve themselves as menus for consideration of specific symmetry descents. Clicking on a subgroup H or on one of the stack of conjugate subgroups F_i activates the following information about symmetry descent $G \Downarrow H$ or $G \Downarrow F_i$:

(1) *Domain*: This option brings to the screen the main table that describes changes of tensor properties in chosen ferroic descent. The option is available under the pull-down menu *View* or directly at the subgroup in the case of normal subgroups. The change of tensor properties is given with reference to the first domain state and hence to the group F_1 from the set of conjugate subgroups. It is given for all tensors listed in Section 3.1.2.3 in a slightly different manner than in Table 3.1.3.1. Namely, principal and secondary tensor parameters of the transition are distinguished. In other words, the onsetting tensor components are distinguished according to the ireps to which they belong. From this information, one can deduce the *fine structure of domain states* with all possible crossovers when some tensor properties are identical in several domains. In tables for those symmetry descents where the subgroup is not an epikernel of a certain irep, expressions of the subgroup as possible intersection of epikernels are presented.

To each table is attached information about G-invariant forms of interactions. This consists of:

Integrity basis: of invariants in the primary order parameter.

Faint interactions: These are those interactions of the primary order parameter with secondary (faint) parameters that are responsible for the occurrence of faint parameters.

Electric switching interactions: The interactions of all order parameters with an external electric field.

Elastic switching interactions: The interactions of all order parameters with an external stress field.

(2) *Integrity bases*: Needs activation of the box of ireps as explained above. Displays the *extended integrity basis* of polynomials in variables of the chosen irep. This consists of the

integrity basis of polynomial invariants and of the linear bases of polynomial covariants.

(3) *Twinning group*: This option works for the first group of the set of conjugate subgroups only. It displays a table that contains consecutive normalizers of the set of conjugate subgroups, left, right and double coset resolutions of the parent group G with respect to the subgroup F_1, and the twinning groups assigned to double cosets. This is the basic information concerning pairs of domain states.

Lattices of equitranslational subgroups of the space groups. The importance of these lattices was realized by Ascher (1968), who prepared the first tables. However, his tables do not contain full information about subgroups; neither the parent group nor the subgroups are completely specified. The current version gives the full information about subgroups including their settings and origins. The pull-down menu *Groups* contains two options: *Point* and *Space*. The choice of the second option brings to the screen another panel, in the right-hand part of which are listed space groups of the geometric class G through Hermann–Mauguin symbols corresponding to all settings and cell choices where applicable. The number of the space-group type, the Schoenflies symbol, the setting and the cell choice are shown in the left-hand part of the panel when you click on one of these Hermann–Mauguin symbols. At the same time, the symbols of the point groups in the lattice change to Schoenflies symbols of oriented space-group types. As you click on any of these subgroups, the Hermann–Mauguin symbol that specifies the subgroup completely appears in the lower bar of the panel, reserved for this information. Though the embellished lattice symbols used in this presentation are self-explanatory, consultation of the manual is recommended.

The option *Point* returns the lattice to its original form of the lattice of point groups.

The following is a list of tabular appendices contained in the manual:

Appendix A: correlation of various notations and Jones' faithful representation symbols;

Appendix B: Schoenflies and Hermann–Mauguin symbols of groups in standard orientations and of their subgroups;

Appendix C: isomorphisms used for defining irreducible representations;

Appendix D: standard polynomials;

Appendix E: labelling of covariants and conversion equations;

Appendix F: list of symmetry descents;

Appendix G: nonstandard lattice letters.

Our symbols for point-symmetry operations are compared with other sources in Appendix A. Symbols of all groups used in the software are given in Appendix B and isomorphisms in Appendix C. Standard polynomials in Appendix D are abbreviated symbols for more complicated polynomials that appear in the main tables. Appendix E is of primary importance for consideration of the relationship between tensor parameters and their contribution to Cartesian tensor components as already indicated in the text explaining Table 3.1.3.1. In Appendix F are listed and classified all symmetry descents considered in the main table. Consultation of Appendix G is strongly recommended to all users who want to use the lattices of equitranslational subgroups of the space groups.

3.1.7. Glossary

(*a*) Groups

G	point-group symmetry of the parent (prototype, high-symmetry) phase
$\mathcal{G}$	space-group symmetry of the parent (prototype, high-symmetry) phase
F	point-group symmetry of the ferroic (low-symmetry) phase (domain state not specified)
$\mathcal{F}$	space-group symmetry of the ferroic (low-symmetry) phase (domain state not specified)
F_1	point-group symmetry of the first ferroic single domain state
$\mathcal{F}_1$	space-group symmetry of the first ferroic single domain state
$G \Downarrow F$	point-group symmetry descent from G to F
$\mathcal{G} \Downarrow \mathcal{F}$	space-group symmetry descent from $\mathcal{G}$ to $\mathcal{F}$
$\mathcal{G} \Downarrow^t \mathcal{F}$	equitranslational symmetry descent from $\mathcal{G}$ to $\mathcal{F}$
Γ_η	representation of $\mathcal{G}$ (or of G) according to which η transforms
$D^{(\eta)}$	irreducible matrix representation of the order parameter η
χ_η	character of the matrix representation $D^{(\eta)}$
R-irep	physically irreducible representation
n_F	number of subgroups conjugate under G to subgroup F_1
n_f	number of ferroic single domain states
n_a	number of ferroelastic single domain states
n_e	number of ferroelectric single domain states

(*b*) Physical quantities

c	specific heat
$d_{i\mu}$	piezoelectric tensor
F, G	free energy
g_μ	optical activity
P_i	dielectric polarization
S	entropy
s_{ij}	elastic compliance
T_c	Curie temperature
u_{ij}, u_μ	strain tensor
V	cell volume
χ	dielectric susceptibility
ε	enantiomorphism, chirality
ε_{ij}	high-frequency dielectric constant or permittivity
η	order parameter (primary)
λ	order parameter (secondary)
$\omega_{\rm LO}$	longitudinal optic mode frequency
$\omega_{\rm TO}$	transverse optic mode frequency
$\pi_{\mu\nu}$	piezo-optic tensor

References

Aizu, K. (1969). *Possible species of ferroelastic crystals and of simultaneously ferroelectric and ferroelastic crystals. J. Phys. Soc. Jpn*, **27**, 387–396.

Aizu, K. (1970). *Possible species of ferromagnetic, ferroelectric, and ferroelastic crystals. Phys. Rev. B*, **2**, 754–772.

Aizu, K. (1973). *Second order ferroic states. J. Phys. Soc. Jpn*, **34**, 121–128.

Altmann, S. L. & Herzig, P. (1994). *Point-group theory tables.* Oxford: Clarendon Press.

Aroyo, M. I. & Perez-Mato, J. M. (1998). *Symmetry mode analysis of displacive phase transitions using International Tables for Crystallography. Acta Cryst.* A**54**, 19–30.

Ascher, E. (1968). *Lattices of equi-translation subgroups of the space groups.* Geneva: Battelle.

Ascher, E. & Kobayashi, J. (1977). *Symmetry and phase transitions: the inverse Landau problem. J. Phys. C: Solid State Phys.* **10**, 1349–1363.

Balkanski, M., Teng, M. K. & Nusimovici, M. (1969). *Lattice dynamics in KNO_3. Phases I, II and III*. In *Light scattering spectra of solids*, edited by G. B. Wright, pp. 731–746. Paris: Flammarion.

Blinc, R. (1960). *On the isotopic effects in the ferroelectric behaviour of crystals with short hydrogen bonds. J. Phys. Chem. Solids*, **13**, 204–211.

Blinc, R., Jamsek-Vilfan, M., Lahajnar, G. & Hajdukovic, G. (1970). *Nuclear magnetic resonance study of the ferroelectric transition in diglycine nitrate and tris-sarcosine calcium chloride. J. Chem. Phys.* **52**, 6407–6411.

Bradley, C. J. & Cracknell, A. P. (1972). *The mathematical theory of symmetry in solids. Representation theory for point groups and space groups.* Oxford: Clarendon Press.

Chan, L. Y. Y. & Geller, S. (1977). *Crystal structure and conductivity of 26-silver 18-iodine tetratungstate. J. Solid State Chem.* **21**, 331–347.

Cochran, W. (1960). *Crystal stability and the theory of ferroelectricity; Part I. Adv. Phys.* **9**, 387–402.

Cochran, W. (1961). *Crystal stability and the theory of ferroelectricity; Part II. Piezoelectric crystals. Adv. Phys.* **10**, 401–420.

Cowley, R. A. (1962). *Temperature dependence of a transverse optic mode in strontium titanate. Phys. Rev. Lett.* **9**, 159–161.

Cowley, R. A. (1964). *Lattice dynamics and phase transitions mode in strontium titanate. Phys. Rev. A*, **134**, 981–997.

Cowley, R. A. (1970). *On the dielectric properties of an anharmonic crystal. J. Phys. Soc. Jpn*, **28**, Suppl., 205–209.

Devonshire, A. F. (1954). *Theory of ferroelectrics. Adv. Phys.* **3**, 85.

Dvořák, V. (1974). *Improper ferroelectrics. Ferroelectrics*, **7**, 1–9.

Errandonea, G., Tolédano, J.-C., Litzler, A., Schneck, J., Savary, H. & Aubrée, J. (1984). *Kinetic characteristics of the thermal hysteresis in an incommensurate system. J. Phys. Lett.* **45**, L329–L334.

Fleury, P. A., Scott, J. F. & Worlock, J. M. (1968). *Soft phonon modes and the 110 K phase transition in strontium titanate. Phys. Rev. Lett.* **21**, 16–19.

Fox, D. L., Scott, J. F. & Bridenbaugh, P. M. (1976). *Soft modes in ferroelastic LaP_5O_{14} and NdP_5O_{14}. Solid State Commun.* **18**, 111–113.

Geller, S. & Bala, V. B. (1956). *Crystallographic studies of perovskite-like compounds. II. Rare earth alluminates. Acta Cryst.* **9**, 1019–1024.

Geller, S., Wilber, S. A., Ruse, G. F., Akridge, J. R. & Turkovic, A. (1980). *Anisotropic electrical conductivity and low-temperature phase transitions of the solid electrolyte $Ag_{26}I_{18}W_4O_{16}$. Phys. Rev. B*, **21**, 2506–2512.

Greer, A. L., Habbal, F., Scott, J. F. & Takahashi, T. (1980). *Specific heat anomalies and phase transitions in the solid electrolyte $Ag_{26}I_{18}W_4O_{16}$. J. Chem. Phys.* **73**, 5833–5867.

Habbal, F., Zvirgzds, J. A. & Scott, J. F. (1978). *Raman spectra of structural phase transitions in $Ag_{26}I_{18}W_4O_{16}$. J. Chem. Phys.* **69**, 4984–4989.

Habbal, F., Zvirgzds, J. A. & Scott, J. F. (1980). *Ferroelectric phase transition in the superionic conductor $Ag_{26}I_{18}W_4O_{16}$. J. Chem. Phys.* **72**, 2760–2763.

Huang, C. Y., Dries, L. T., Hor, P. H., Meng, R. I., Chu, C. W. & Frankel, R. B. (1987). *Observation of possible superconductivity at 230 K. Nature (London)*, **238**, 403–404.

Hulm, J. K. (1950). *The dielectric properties of some alkaline earth titanates at low temperatures. Proc. Phys. Soc. London Ser. A*, **63**, 1184–1185.

Hulm, J. K. (1953). *Low-temperature properties of cadmium and lead niobates. Phys. Rev.* **92**, 504.

IEEE Standard on Piezoelectricity STD 176–1987. (1987). New York: The Institute of Electrical and Electronics Engineers, Inc. This IEEE Std 176–1987 is reproduced in *IEEE Transactions on Ultrasonics, Ferroelectrics, and Frequency Control.* (1996). **43**, No. 5.

Indenbom, V. L. (1960). *Phase transitions without change in the number of atoms in the unit cell of the crystal. Sov. Phys. Crystallogr.* **5**, 105–115.

International Tables for Crystallography (2002). Vol. A. *Space-group symmetry*, edited by Th. Hahn. Dordrecht: Kluwer Academic Publishers.

International Tables for Crystallography (2003). Vol. A1. *Symmetry relations between space groups*, edited by H. Wondratschek & U. Müller. In preparation.

Izyumov, Yu. A. & Syromiatnikov, V. N. (1990). *Phase transitions and crystal symmetry.* Dordrecht: Kluwer Academic Publishers.

Janovec, V., Dvořák, V. & Petzelt, J. (1975). *Symmetry classification and properties of equi-translation structural phase transitions. Czech. J. Phys.* **B25**, 1362–1396.

Jansen, L. & Boon, M. (1967). *Theory of finite groups. Applications in physics. Symmetry groups of quantum mechanical systems.* Amsterdam: North-Holland.

Kociński, J. (1983). *Theory of symmetry changes at continuous phase transitions*. Warsaw: PWN – Polish Scientific Publishers; Amsterdam: Elsevier.

Kociński, J. (1990). *Commensurate and incommensurate phase transitions*. Warsaw: PWN – Polish Scientific Publishers; Amsterdam: Elsevier.

Kopský, V. (1976*a*). *The use of the Clebsch–Gordan reduction of the Kronecker square of the typical representation in symmetry problems of crystal physics. I. Theoretical foundations. J. Phys. C: Solid State Phys.* **9**, 3391–3405.

Kopský, V. (1976*b*). *The use of the Clebsch–Gordan reduction of the Kronecker square of the typical representation in symmetry problems of crystal physics. II. Tabulation of Clebsch–Gordan products for classical and magnetic crystal point groups. J. Phys. C: Solid State Phys.* **9**, 3405–3420.

Kopský, V. (1979*a*). *Tensorial covariants of the 32 crystal point groups. Acta Cryst.* A**35**, 83–95.

Kopský, V. (1979*b*). *A simplified calculation and tabulation of tensorial covariants for magnetic point groups belonging to the same Laue class. Acta Cryst.* A**35**, 95–101.

Kopský, V. (1979*c*). *Extended integrity bases of irreducible matrix groups. The crystal point groups. J. Phys. A: Math. Gen.* **12**, 943–957.

Kopský, V. (1979*d*). *Representation generating theorem and interaction of improper quantities with order parameter. J. Phys. A. Math. Gen.* **12**, L291–L294.

Kopský, V. (1982). *Group lattices, subduction of bases and fine domain structures for magnetic crystal point groups.* Prague: Academia.

Kopský, V. (2000). *The change of tensor properties at ferroic phase transitions. Ferroelectrics*, **237**, 127–134.

Kopský, V. (2001). *Tensor parameters of ferroic phase transitions. I. Theory and tables. Phase Transit.* **73**, No. 1–2, 1–422.

Koster, G. F., Dimmock, J. O., Wheeler, R. E. & Statz, H. (1963). *Properties of the 32 groups.* Cambridge: MIT Press.

Kozlov, G. V.., Volkov, A. A., Scott, J. F. & Petzelt, J. (1983). *Millimeter wavelength spectroscopy of the ferroelectric phase transition in tris-sarcosine calcium chloride. Phys. Rev. B*, **28**, 255–261.

Laegreid, T., Fossheim, K., Sandvold, E. & Juisrud, S. (1987). *Specific heat anomaly at 220 K connected with superconductivity at 90 K in ceramic $YBa_2Cu_3O_{7-x}$. Nature (London)*, **330**, 637–638.

Landau, L. D. (1937). *Theory of phase transitions. I. Phys. Z. Sowjun.* **11**, 26–47; *II. Phys. Z. Sowjun.* **11**, 545–555.

Landau, L. D. & Lifshitz, E. M. (1969). *Course in theoretical physics*, Vol. 5, *Statistical physics*, 2nd ed. Oxford: Pergamon Press.

Levanyuk, A. P. & Sannikov, D. G. (1974). *Improper seignetoelectrics. Uspekhi Fiz. Nauk.* **112**, 561–589. (In Russian.)

Lines, M. E. & Glass, A. M. (1977). *Principles and applications of ferroelectrics and related materials.* Oxford University Press.

Lytle, F. W. (1964). *X-ray diffractometry of low-temperature phase transformations in strontium titanate. J. Appl. Phys.* **35**, 2212–2214.

Lyubarskii, G. Ya. (1960). *The application of group theory in physics*. Oxford: Pergamon Press.

MacFarlane, R. M., Rosen, H. & Seki, H. (1987). *Temperature dependence of the Raman spectra of the high-T_c superconductor $YBa_2Cu_3O_{7-x}$. Solid State Commun.* **63**, 831–834.

Nimmo, J. K. & Lucas, D. W. (1973). *The crystal structures of γ- and β-KNO_3 and the $\alpha \leftarrow \gamma \leftarrow \beta$ phase transformations. Acta Cryst.* B**32**, 1968–1971.

Nowick, A. S. (1995). *Crystal properties via group theory.* Cambridge University Press.

Nye, J. F. (1985). *Physical properties of crystals.* Oxford: Clarendon Press.

Oliver, W. F. (1990). PhD thesis, University of Colorado.

Patera, J., Sharp, R. T. & Winternitz, P. (1978). *Polynomial irreducible tensors for point groups. J. Math. Phys.* **19**, 2362–2376.

Peercy, P. S. (1975*a*). *Soft mode and coupled modes in the ferroelectric phase of KH_2PO_4. Solid State Commun.* **16**, 439–442.

Peercy, P. S. (1975*b*). *Measurement of the soft mode and coupled modes in the paraelectric and ferroelectric phases of KH_2PO_4. Phys. Rev. B*, **12**, 2741–2746.

Pick, R. (1969). Private communication.

Prokhorova, S. D., Smolensky, G. A., Siny, I. G., Kuzminov, E. G., Mikvabia, V. D. & Arndt, H. (1980). *Light scattering study of the phase transition in tris-sarcosine calcium chloride. Ferroelectrics*, **25**, 629–632.

Rebane, L., Fimberg, T. A., Fefer, E. M., Blumberg, G. E. & Joon, E. R. (1988). *Raman scattering study of lattice instability in $YBa_2Cu_3O_{7-x}$ at 200–240 K. Solid State Commun.* **65**, 1535–1537.

Rousseau, D. L., Bauman, R. P. & Porto, S. P. S. (1981). *Normal mode determination in crystals. J. Raman Spectrosc.* **10**, 253–290.

Schneck, J. (1982). Thèse de Doctorat d'Etat ès Sciences Physiques, Université Pierre et Marie Curie (Paris).

Schneck, J., Primot, J., Von der Muhl, R. & Ravez, J. (1977). *New phase transition with increasing symmetry on cooling in barium sodium niobate. Solid State Commun.* **21**, 57–60.

Scott, J. F. (1969). *Raman study of trigonal–cubic phase transitions in rare-earth aluminates. Phys. Rev.* **183**, 823–825.

Scott, J. F. (1999). *A comparison of Ag- and proton-conducting ferroelectrics. Solid State Ionics*, **125**, 141–146.

Scott, J. F. & Pouligny, B. (1988). *Raman spectroscopic study of submicron KNO_3 films. J. Appl. Phys.* **64**, 1547–1551.

Scott, J. F. & Remeika, J. P. (1970). *High-temperature Raman study of $SmAlO_3$. Phys. Rev. B*, **1**, 4182–4185.

Shannon, R. D. & Prewitt, C. T. (1969). *Effective ionic radii in oxides and fluorides. Acta Cryst.* B**25**, 925–945.

Shapiro, S. M., Cowley, R. A., Cox, D. E., Eibschutz, M. & Guggenheim, H. J. (1976). *Neutron scattering study of incommensurate $BaMnF_4$.* In *Proc. Natl Conf. Neutron Scat.* edited by R. M. Moon, pp. 399–406. Springfield, VA: Nat. Tech. lnfo. Serv.

Shawabkeh, A. & Scott, J. F. (1989). *Raman spectra of low-temperature phase transitions in $RbAg_4I_5$. J. Raman Spectrosc.* **20**, 277–281.

Shawabkeh, A. & Scott, J. F. (1991). *Raman spectroscopy of incommensurate $Ba_2NaNb_5O_{15}$. Phys. Rev. B*, **43**, 10999–11004.

Shinnaka, Y. (1962). *X-ray study on the disordered structure above the ferroelectric Curie point in KNO_3. J. Phys. Soc. Jpn*, **17**, 820–828.

Shuvalov, L. A. (1988). Editor. *Modern crystallography IV. Physical properties of crystals.* Berlin: Springer-Verlag.

Sirotin, Yu. I. & Shaskolskaya, M. P. (1982). *Fundamentals of crystal physics.* Moscow: Mir Publishers.

Spencer, E. G., Guggenheim, H. J. & Kominiak, G. J. (1970). *$BaMnF_4$, a new crystal for microwave ultrasonics. Appl. Phys. Lett.* **17**, 300–301.

Stokes, H. T. & Hatch, D. M. (1988). *Isotropy groups of the 230 crystallographic space groups.* Singapore: World Scientific.

Strukov, B. A. & Levanyuk, A. P. (1998). *Ferroelectric phenomena in crystals.* Berlin: Springer.

Tahvonen, P. E. (1947). *X-ray structure of potassium nitrate. Ann. Acad. Sci. Fenn. Ser. A*, 44–51.

Tokunaga, M. (1987). *Two different mechanisms of the Curie–Weiss dielectric susceptibility in displacive-type ferroelectrics. J. Phys. Soc. Jpn*, **56**, 1653–1656.

Tolédano, J.-C., Schneck, J. & Errandonea, G. (1986). *Incommensurate phase of barium sodium niobate.* In *Incommensurate phases in dielectric materials*, edited by R. Blinc & A. P. Levanyuk, pp. 233–252. Amsterdam: North-Holland.

Tolédano, J.-C. & Tolédano, P. (1980). *Order parameter symmetries and free-energy expansions for purely ferroelastic transitions. Phys. Rev. B*, **21**, 1139–1172.

Tolédano, J.-C. & Tolédano, P. (1987). *The Landau theory of phase transitions.* Singapore: World Scientific.

Tolédano, P. & Dmitriev, V. (1996). *Reconstructive phase transitions.* Singapore: World Scientific.

Tolédano, P. & Tolédano, J.-C. (1976). *Order parameter symmetries for ferroelectric nonferroelastic transitions. Phys. Rev. B*, **14**, 3097–3109.

Tolédano, P. & Tolédano, J.-C. (1977). *Order parameter symmetries for the phase transitions of nonmagnetic secondary and higher order ferroics. Phys. Rev. B*, **16**, 386–407.

Tolédano, P. & Tolédano, J.-C. (1982). *Non-ferroic phase transitions. Phys. Rev. B*, **25**, 1946–1964.

Unoki, H. & Sakudo, T. (1967). *Electron spin resonance of Fe^{+3} in strontium titanate with specific reference to the 110 K phase transition. J. Phys. Soc. Jpn*, **23**, 546–552.

Van der Waals, J. D. (1873). PhD thesis, University of Leiden.

Volkov, A. A., Kozlov, G. V., Mirzoyants, G. I. & Petzelt, J. (1985). *Submicron dielectric spectroscopy of superionic conductors. Jpn. J. Appl. Phys.* **24**, Suppl. 24-2, 531–533.

Wadhawan, V. K. (2000) *Introduction to ferroic materials.* Australia: Gordon and Breach Science Publishers.

Wang, Y., Shen, H., Zhu, J., Xu, Z., Gu, M., Niu, Z. & Zhang, Z. (1987). *Ultrasonic anomaly in $YBa_2Cu_3O_{7-x}$ at 235 K. J. Phys. Condens. Mat.* **20**, L665.

Weiss, P. (1907). *L'hypothèse du champ moléculaire et la propriété ferromagnétique. J. Phys. Radium*, **6**, 661–690.

Weitzenböck, R. (1923). *Invariantentheorie.* Groningen: Noordhof.

Western, A. B., Baker, A. G., Bacon, C. R. & Schmidt, V. H. (1978). *Pressure-induced critical point in the ferroelectric phase transition in KH_2PO_4. Phys. Rev. B*, **17**, 4461–4473.

Weyl, H. (1946). *The classical groups.* Princeton: UP.

Windsch, W. & Volkel, G. (1980). *EPR investigation of the dynamics of ferroelectric tris-sarcosine calcium chloride. Ferroelectrics*, **24**, 195–202.

Wondre, F. R. (1977). Unpublished. Cited in Scott, J. F. (1978). *Spectroscopy of magnetoelectric $BaMnF_4$ and ferroelastic NdP_5O_{14}. Ferroelectrics*, **20**, 69–74.

Worlock, J. M. (1971). *Light scattering studies of structural phase transitions*. In *Structural phase transitions and soft modes*, edited by E. Samuelsen, E. Andersen & Z. Feder, pp. 329–370. Oslo: Universitetsforlaget.

Zhang, M.-S., Chen, Q., Sun, D., Ji, R.-F., Qin, Z.-K., Yu, Z. & Scott, J. F. (1988). *Raman studies of phonon anomalies at 235 K in $YBa_2Cu_3O_{7-x}$. Solid State Commun.* **65**, 487–490; see also Huang *et al.* (1987).